P-07-79

Oskarshamn site investigation

Method evaluation of single hole hydraulic injection tests at site investigations Oskarshamn

Cristian Enachescu, Golder Associates GmbH

Nils Rahm, Golder Associates AB

April 2007

Svensk Kärnbränslehantering AB
Swedish Nuclear Fuel
and Waste Management Co
Box 5864
SE-102 40 Stockholm Sweden
Tel 08-459 84 00
+46 8 459 84 00
Fax 08-661 57 19
+46 8 661 57 19

ISSN 1651-4416
SKB P-07-79

Oskarshamn site investigation

Method evaluation of single hole hydraulic injection tests at site investigations Oskarshamn

Cristian Enachescu, Golder Associates GmbH

Nils Rahm, Golder Associates AB

April 2007

Keywords: Site/project, Hydrogeology, Hydraulic tests, Injection test, Hydraulic parameters, Transmissivity, Methodology.

Abstract

In the frame of the site characterization programs for the Oskarshamn and Forsmark sites, SKB has conducted a large number of injection tests with the aim of deriving the hydraulic properties of the granite formations at the two sites. The present report describes the methodology used for the measurement and analysis of the tests conducted by Golder Associates in years 2003 and 2004 at the Oskarshamn site.

The objective of the present report is to describe the methodology used during the past two years for the measurement and analysis of the injection tests conducted at the Oskarshamn site. The report presents both technical and practical details of the work with reference to actual field cases in order to exemplify the individual aspects. References to test analysis theory are made to the extent necessary, in order to clarify the interpretation procedures applied.

The analysis of the tests was conducted in accordance with the technical standards applicable to hydraulic measurements in boreholes. All aspects of the analysis, including handling of non-ideal data conditions were described such that the reader can trace and reconstruct the work done. In addition, statistics of the tests conducted with respect to different aspects of non-ideal test behavior are presented. Non-ideal test behavior was mainly identified in conjunction with very fast pressure recovery observed in several cases. The hypothesis is stated, that this behavior is related with the occurrence of turbulent flow in fractures near the test section.

The testing and analysis procedures applied by Golder Associates for the measurements at the Oskarshamn site and by Geosigma at the Forsmark site are shown to be largely similar and to lead to consistent results.

Based on the findings of the report recommendations for improvement are suggested. These mainly concern the conduction of specialized tests conducted with the aim of clarifying the presence of turbulent flow and improvements in pressure gauge resolution which are expected to mitigate the problem of fast pressure recovery.

Sammanfattning

Inom ramen för platsundersökningarna i Oskarshamn och Forsmark har Svensk Kärnbränslehantering (SKB) utfört ett stort antal injektionstester i syfte att ta fram bergets hydrauliska egenskaper på respektive plats. Föreliggande rapport beskriver den metod som använts för mätning och analys av testerna utförda av Golder Associates (Golder) mellan åren 2003 och 2004 vid Oskarshamn.

Syftet med föreliggande rapport är att beskriva metoderna som använts för mätning och analys av injektionstesterna utförda i Oskarshamn. Rapporten presenterar både tekniska och praktiska detaljer från fallstudier i fält i syfte att exemplifiera individuella aspekter av testet. Referenser till teoretisk testanalys görs i den mån det är nödvändigt för att klargöra tolknings arbetet.

Testanalysen utfördes i linje med standardiserade förfaranden tillämpliga vid hydrauliska mätningar i borrhål. Alla aspekter av analysen, även hantering av icke-ideala responser var beskrivna så att läsaren kan spåra och återge det utförda arbetet. Utöver det utfördes statistik på de utförda testerna med avseende på olika typer av icke-ideala responser. Dessa data var i huvudsak identifierade i kombination med mycket snabba återhämtningsresponser observerade i flera fall. En hypotes som framlagts utgör att denna respons är relaterad till turbulent flöde i sprickor nära test sektionen.

Testningarna och analysmetoderna utförda av Golder vid Oskarshamn och av Geosigma i Forsmark visar i stora drag likheter i resultaten.

Baserat på resultaten har rekommendationer föreslagits för förbättringar av metoderna. Dessa berör huvudsakligen utförandet av specialtester utförda i syfte att klargöra förekomsten av turbulent flöde och förbättringar i tryckgivarnas upplösning vilka förväntas mildra osäkerheterna av resultaten kring snabba tryckåterhämtningar.

Contents

1 Introduction

In the frame of the site characterization programs for the Oskarshamn and Forsmark sites, SKB has conducted a large number of injection tests with the aim of deriving the hydraulic properties of the granite formations at the two sites. The present report describes the methodology used for the measurement and analysis of the tests conducted in years 2003 and 2004 at the Oskarshamn site.

During this period, following boreholes were tested using the PSS2 equipment and the injection test design:

1.1 Structure of the document

The present document was structured as follows:

- The Introduction (Chapter 1) describes the context of the report, the work done so far at the Oskarshamn site and lists the related documents relevant to the report.
- Chapter 2 describes the objectives of the report.
- Chapter 3 describes the test design and decision procedures used during the work as well as the equipment used.
- Chapter 4 describes the analysis methodology applied for the tests. Individual sections describe the analysis of constant pressure injection tests (CHi phases), of pressure recovery tests (CHir phases) and of pulse and slug injection tests (PI and SI phases). A final section describes the derivation of recommended values and confidence ranges for the hydraulic parameters.
- Chapter 5 describes uncertainties which occur during testing, such as packer compliance and background pressure gradients.
- Chapter 6 presents the statistics of the tests conducted so far.
- Chapter 7 highlights differences in the analysis methodology between the two SKB contractors who conducted the work (Geosigma and Golder Associates).
- Chapter 8 summarizes conclusions and recommendations, based on the experience gained from past work.
- Chapters 9 and 10 present the literature references, the nomenclature, and a glossary of abbreviations.

The location of the boreholes is presented in the following map.

Table 1-1. Testing work conducted at the Oskarshamn site till April 2005.

Borehole	Testing period	Number of tests
KLX02	July 2003	80
KSH01A	Dec 2003–Jan 2004	135
KSH03A	February 2004	9
KAV04A	July–August 2004	51
KLX04	August–October 2004	126

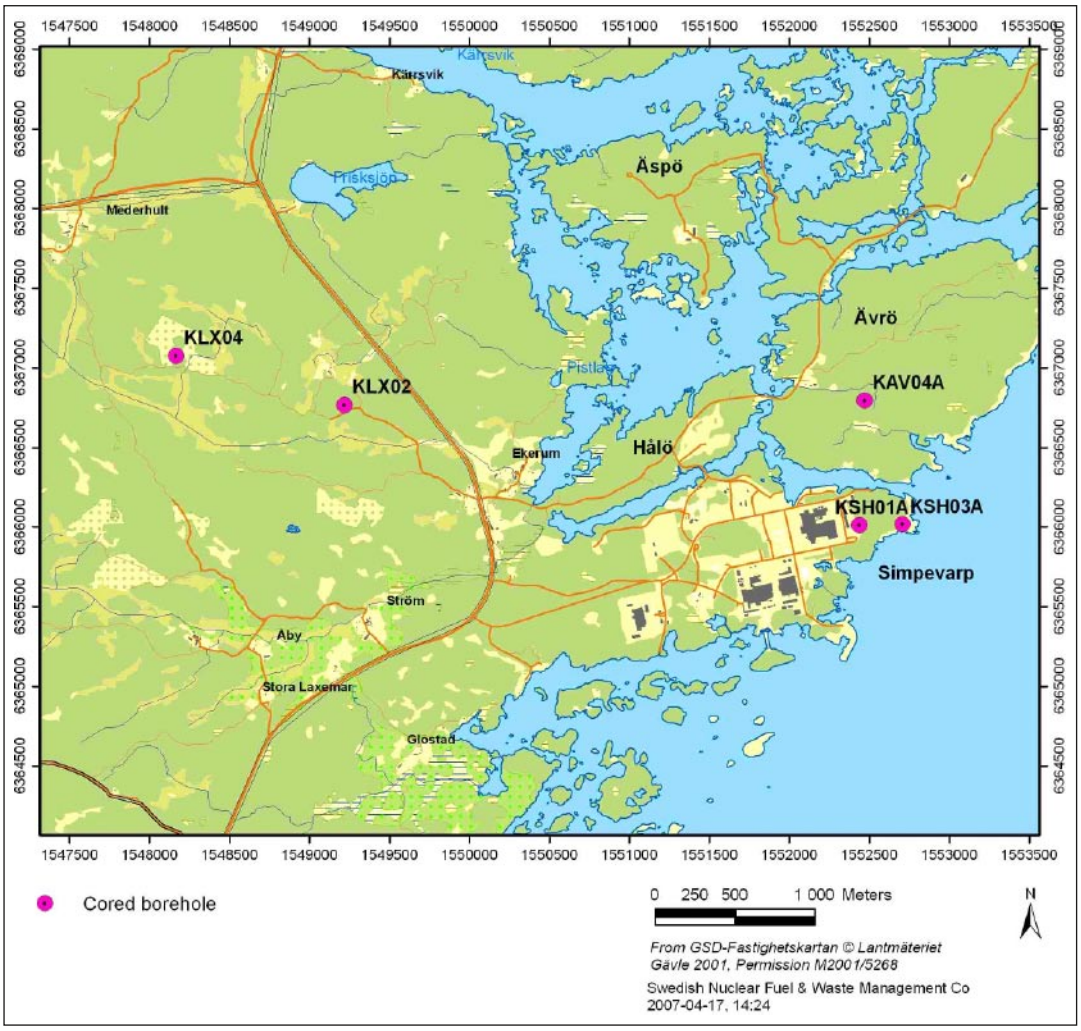

Figure 1-1. *The Oskarshamn investigation site with borehole locations.*

1.2 Related documents

The methods and procedures which govern the testing work conducted at the Oskarshamn site were defined by SKB and presented in the following SKB internal controlling documents:

- SKB 320-004e: Analysis and data delivery.
- SKB MD 323.001: Performance and recording.
- SKB MD 345.100-124: Users manual PSS.
- Activity plan Specified for each borehole.
- SKB MD 600.004: Cleaning descriptions.
- SKB MD 620.010: Length calibration.
- SKBSDPO-0: Site and safety regulations.
- SKB SDP-301: Conduction of environmental control.
- SKB SDP-508: Data handling of primary data.

The documents listed above were edited before the start of the site operation. In the course of the testing work some of the procedures and analysis techniques were changed with the aim of optimizing and improving the workflow and/or the interpretation results. Therefore, the current document should be seen as an updated description of these procedures.

The description and analysis of the tests conducted at the Oskarshamn site are presented in the following documents:

- SKB P-04-288: Oskarshamn site investigation, Hydraulic injection tests in borehole KLX02, 2004, subarea Laxemar.
- SKB P-04-289: Oskarshamn site investigation, Hydraulic injection tests in borehole KSH01A, 2004, subarea Simpervarp.
- SKB P-04-290: Oskarshamn site investigation, Hydraulic injection tests in borehole KSH03A, 2004, subarea Simpervarp.
- SKB P-04-291: Oskarshamn site investigation, Hydraulic injection tests in borehole KAV04A, 2004, subarea Simpervarp.
- SKB P-04-292: Oskarshamn site investigation, Hydraulic injection tests in borehole KLX04, 2004, subarea Laxemar.

2 Objective and scope

The objective of the present report is to describe the methodology used during the past two years for the measurement and analysis of the injection tests conducted at the Oskarshamn site.

The report presents both technical and practical details of the work with reference to actual field cases in order to exemplify the individual aspects. References to test analysis theory are made to the extent necessary, in order to clarify the interpretation procedures applied.

Apart from the conclusions and recommendations presented in Chapter 8, the document strictly describes the procedures that were actually applied as opposed to making recommendations about alternative or improved techniques.

3 Test design and equipment

The present chapter describes the test design applied to the tests conducted at the Oskarshamn site. A separate section describes the testing equipment used (i.e. SKB's PSS2 equipment).

3.1 Test design

Injection tests were conducted according to the method description for hydraulic injection tests, SKB MD 323.001 (SKB internal documents). Tests were conducted in 100 m, 20 m and 5 m test sections. The initial criteria for performing injection tests in 20 m and 5 m test sections was a measurable flow of Q > 0.001 L/min in the previously measured tests covering the smaller sections (see Figure 3-1). The measurements were performed with SKB's custom made equipment for hydraulic testing called PSS2.

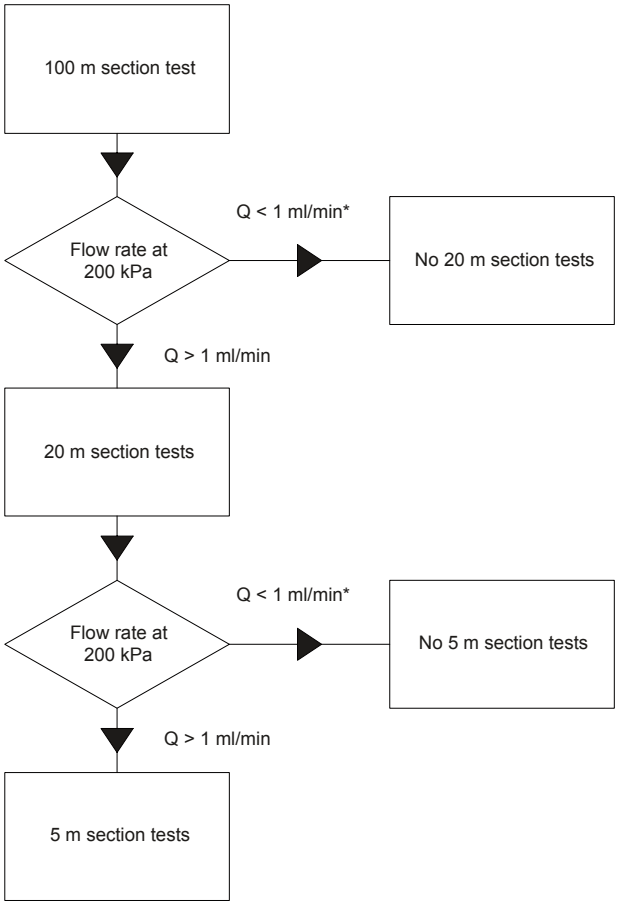

* eventually tests performed after specific discussion with SKB

Figure 3-1. *Flow chart for test sections.*

The tests were conducted as constant pressure injection (CHi phase) followed by a shut-in pressure recovery (CHir phase). In some cases, when the test section transmissivity was too low (typically lower than 10^{-9} m²/s) no measurable flow could be registered during the CHi phase (Q < 1 mL/min). In such cases, Pulse or Slug tests were conducted as active tests[1] (Figure 3-2).

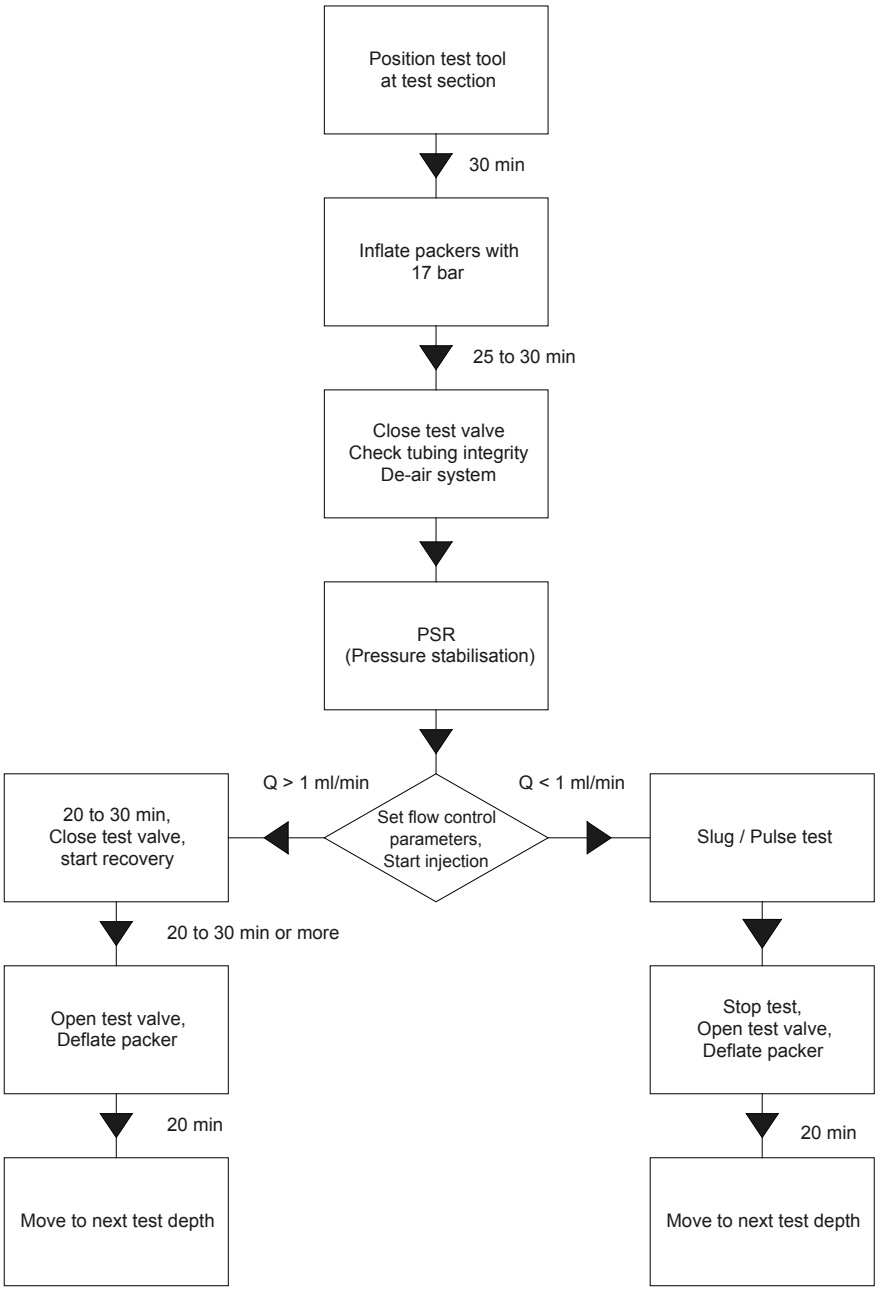

Figure 3-2. *Flow chart for test performance.*

[1] Beginning with 2005 the test design was changed to include a pre-test pulse in every test section. The pre-test pulse was than used to estimate the flow rate for the subsequent injection phase. In cases of very low transmissivity of the test section the pulse test was measured longer and was the only test phase conducted in the respective test section.

A test cycle includes the following phases: 1) Transfer of down-hole equipment to the next section. 2) Packer inflation. 3) Pressure stabilization. 4) Constant head injection. 5) Pressure recovery. 6) Packer deflation. The injection tests have been carried out by applying a constant injection pressure of ca 200 kPa (20 m water column) above the static formation pressure in the test section. Before start of the injection tests, approximately stable pressure conditions prevailed in the test section. After the injection period, the pressure recovery in the section was measured. In some cases, if small flow rates were expected, the automatic regulation unit was switched off and the test was performed manually. In other cases, where small flow rates ($Q < 1$ mL/min) were observed, the test procedure was switched to a pulse test. For the conduction of a pulse test the shut-in tool has been closed immediately after starting the injection. The duration for each phase is presented in Table 3-1.

3.2 PSS equipment

The equipment called PSS2 (Pipe String System 2) is a highly integrated tool for testing boreholes at great depth (see conceptual drawing in Figure 3-3). The system is built inside a container suitable for testing at any weather. Briefly, the components consist of a hydraulic rig, down-hole equipment including packers, pressure gauges, shut-in tool and level indicator, racks for pump, gauge carriers, break-pins, etc shelf and drawers for tools and spare parts.

There are three spools for a multi-signal cable, a test valve hose and a packer inflation hose. There is a water tank for injection purposes, pressure vessels for inflation of packers, to open test valve and for low flow injection. The PSS2 has been upgraded with a computerized flow regulation system. The office part of the container consists of a computer, regulation valves for the nitrogen system, a 24 V back-up system in case of power shut-offs and a flow regulation board.

The down-hole equipment consists from bottom to top of the following components:

- Level indicator – SS 630 mm pipe with OD 73 mm with 3 plastic wheels connected to a Hallswitch.
- Gauge carrier – SS 1.5 m carrying bottom section pressure transducer and connections from positioner.
- Lower packer – SS and PUR 1.5 m with OD 72 mm, fixed ends, seal length 1.0 m, maximum pressure 6.5 MPa, working pressure 1.6 MPa.

Table 3-1. Durations for packer inflation, pressure stabilization, injection and recovery phase and packer deflation.

• Position test tool to new test section (correct position using the borehole markers)	Approx. 30 min
• Inflate packers with 1,700 kPa	25 min
• Close test valve.	10 min
• Check tubing integrity with 800 kPa	5 min
• De-air system.	2 min
• Set automatic flow control parameters	5 min
• Start injection	20 to 45 min*
• Close test valve, start recovery	20 min. or more
• Open test valve	10 min
• Deflate packers	25 min
• Move to next test depth	…

* In case of a Pulse Injection the injection time is shorter than 1 min.

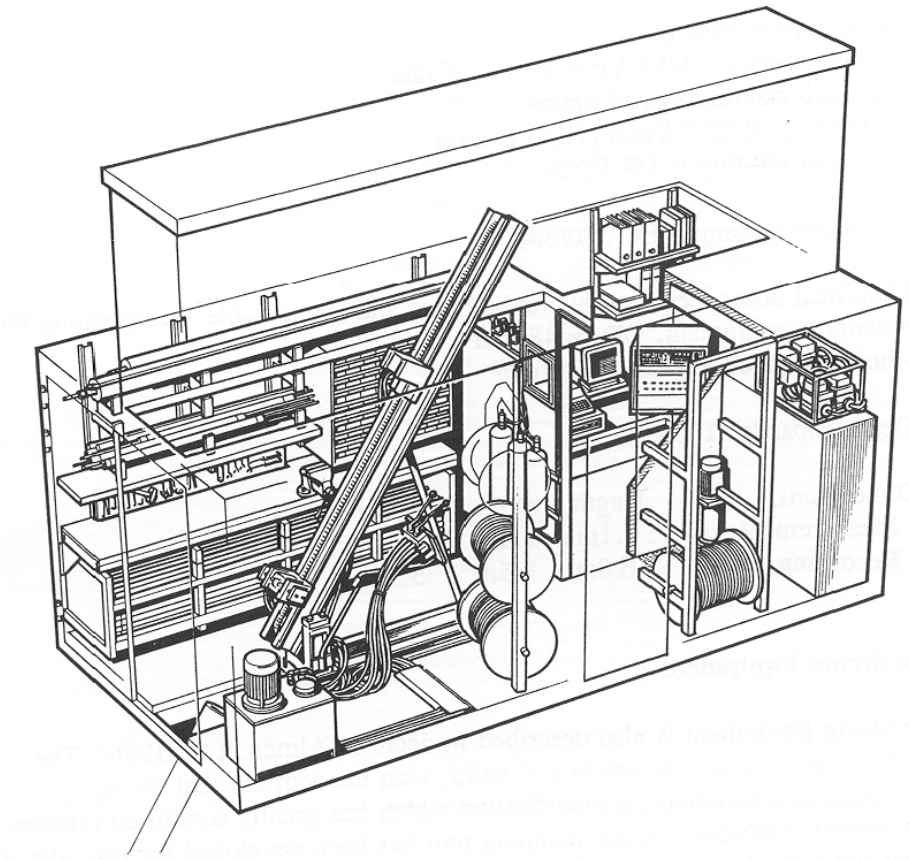

Figure 3-3. *A view of the layout and equipment of PSS2.*

- Gauge carrier with break-pin – SS 1.75 m carrying test section pressure transducer, temperature sensor and connections for sensors below. Break-pin with maximum load of 47.3 (± 1.0) kN. The gauge carrier is covered by split pipes and connected to a stone catcher on the top.
- Pup joint – SS 1.0 or 0.5 m with OD 33 mm and ID 21 mm, double O-ring fittings, trapezoid thread, friction loss of 3 kPa/m at 50 L/min.
- Pipe string – SS 3.0 m with OD 33 mm and ID 21 mm, double O-ring fittings, trapezoid thread, friction loss of 3 kPa/m at 50 L/min.
- Connector carrier – SS 1.0 m carrying connectors for sensors below.
- Upper packer – SS and PUR 1.5 m with OD 72 mm, fixed ends, seal length 1.0 m, maximum pressure 6.5 MPa, working pressure 1.6 MPa.
- Break-pin – SS 250 mm with OD 33.7 mm. Maximum load of 47.3 (± 1.0) kN.
- Gauge carrier – SS 1.5 m carrying top section pressure transducer, connectors from sensors below. Flow pipe is double bent at both ends to give room for sensor equipment. The pipe gauge carrier is covered by split pipes.
- Shut-in tool (test valve) – SS 1.0 m with a OD of 48 mm, Teflon coated valve piston, friction loss of 11 kPa at 10 L/min (260 kPa–50 L/min). Working pressure 2.8–4.0 MPa. Break-pipe with maximum load of 47.3 (± 1.0) kN. The shut-in tool is covered by split pipes and connected to a stone catcher on the top.

The tool scheme is presented in Figure 3-4.

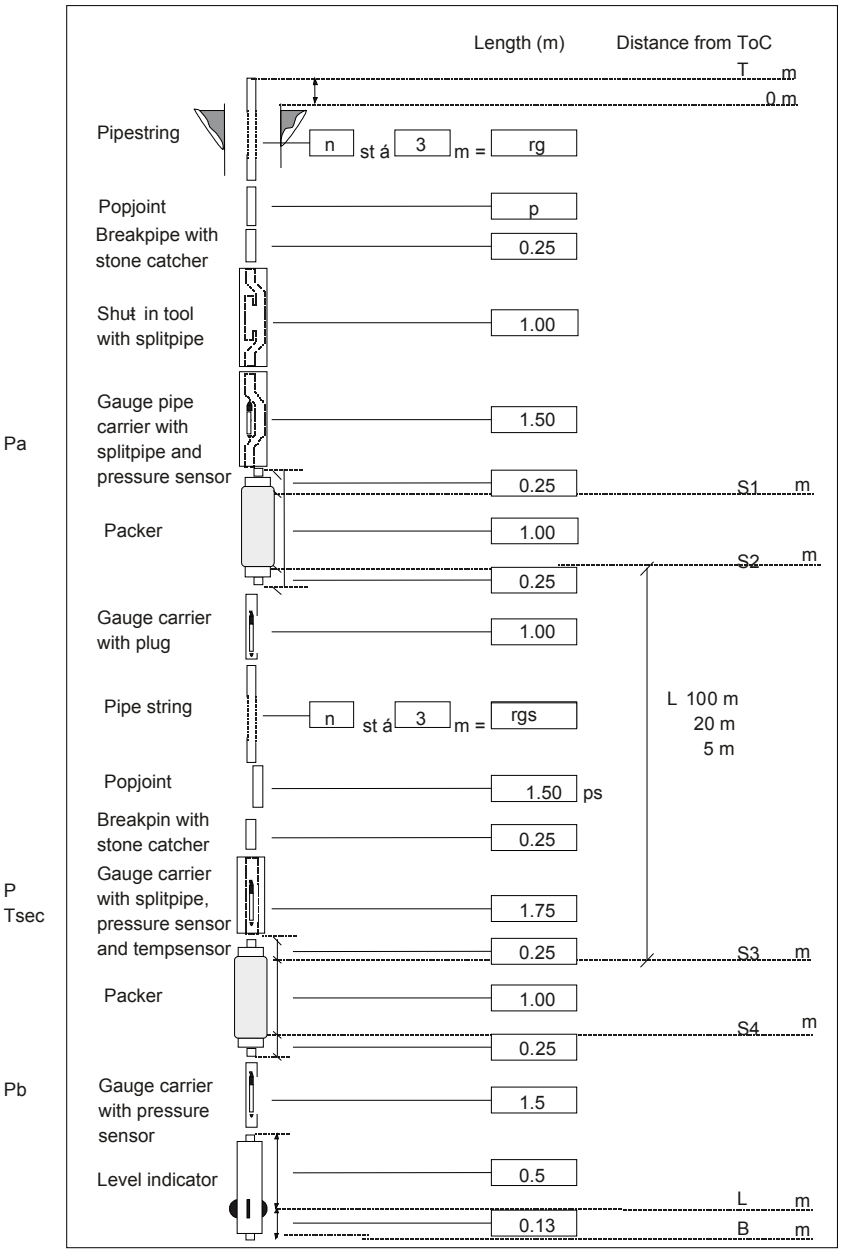

Figure 3-4. *Schematic drawing of the down-hole equipment in the PSS2 system.*

The data acquisition system in the PSS2 container contains a stationary PC with the software Orchestrator. Pump- and injection test parameters such as pressure, temperature and flow are monitored and sensor data collected. A second laptop PC is connected to the stationary PC through a network containing the evaluation software, FlowDim.

The data acquisition system controls the test automatically or can be disengaged for manual operation of magnetic and regulation valves within the injection/pumping system. An outline of the data acquisition system is outlined in Figure 3-5.

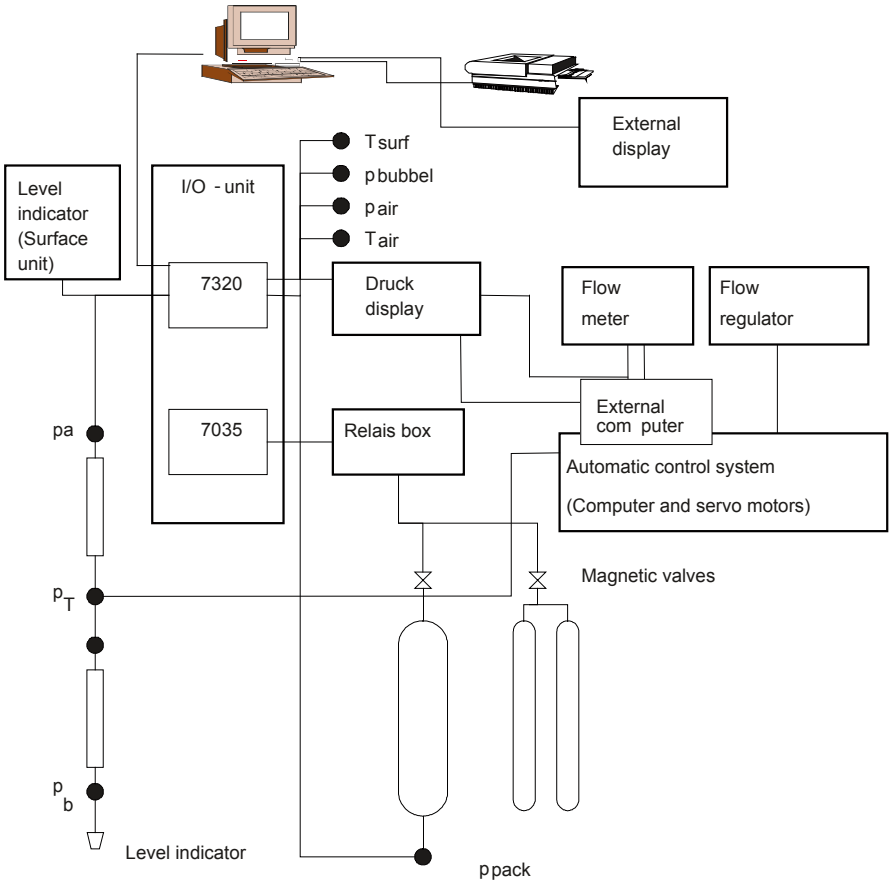

Figure 3-5. *Schematic drawing of the data acquisition system and the flow regulation control system in PSS2.*

4 Analysis of hydraulic tests

The present chapter describes the analysis theory and procedures, as applied for the injection tests conducted in boreholes KLX02, KSH01A, KSH03A, KAV04A and KLX04 at the Oskarshamn site. In these boreholes a total of 401 injection tests was conducted.

All tests were analyzed using a type curve matching method. The analysis was performed using Golder's test analysis program FlowDim. FlowDim is an interactive analysis environment allowing the user to interpret constant pressure, constant rate and slug/pulse tests in source as well as observation boreholes. The program allows the calculation of type-curves for homogeneous, dual porosity and composite flow models in variable flow geometries from linear to spherical.

In the following, the analysis of the individual test types is described together with the relevant theory and specific practical aspects encountered during the operations.

4.1 Analysis of constant pressure injection tests (the CHi phase)

Constant pressure tests were analyzed using a rate inverse approach. The method initially known as the /Jacob and Lohman 1952/ method was further improved for the use of type curve derivatives and for different flow models. In addition a steady state analysis was conducted.

4.1.1 Brief theoretical background

In their paper from 1952 Jacob C. E. and Lohman S. W. describe the analysis of flowing artesian wells under constant pressure conditions. The solution presented by the authors assumes a radially flowing well in a homogeneous confined formation of constant transmissivity and storativity. Any transmissivity changes at the wellbore (typically described as skin) are described in the model by using the concept of effective wellbore radius.

The authors propose a straight line analysis method. The inverse flow rate (1/q) is plotted against the logarithm of time. At middle and late times, the flow model has a logarithmic approximation. Therefore, if the formation flow fulfils the assumptions listed above, the data will plot as a straight line. The formation transmissivity is calculated from the slope of the straight line ($M = d(1/q)/dlog(t)$):

$$T = \frac{1}{M}\frac{\rho g}{4\pi\Delta p} \qquad (4\text{-}1)$$

The flow model expressed in dimensionless flow rate and time plotted as proposed by Jacob and Lohman (i.e. semi-logarithmically) together with the linear approximation at late times in presented in Figure 4-1.

The analysis method applied to the tests conducted at the Oskarshamn site is an extension of the theory developed by Jacob and Lohman by using type curves and type curve derivatives.

4.1.1.1 Type curve analysis

The type curve analysis method makes use of dimensionless variables, which allow calculating the flow model (i.e. the type curve) independently of the primary formation flow parameters (i.e. transmissivity and storativity) and of the applied pressure difference (Δp) at the well. The dimensionless flow rate and dimensionless time are defined as follows:

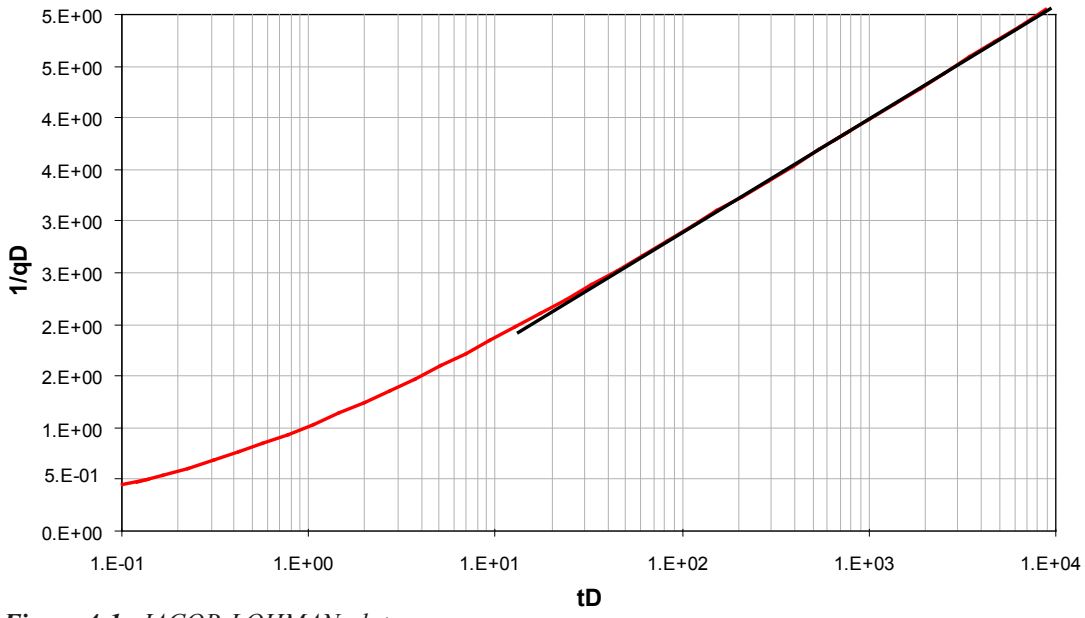

Figure 4-1. *JACOB-LOHMAN plot.*

$$\frac{1}{q_D} = \frac{1}{q}\frac{2\pi T \Delta p}{\rho g} \tag{4-2}$$

$$t_D = \frac{T}{S}\frac{\Delta t}{r_w^2} \tag{4-3}$$

Since, by definition, dimensionless rate and time are linear functions of actual flow rate and time, the logarithm of inverse rate (log(*1/q*)) will differ from the logarithm of the dimensionless inverse rate (log($1/q_D$); i.e. the type curve) by a constant amount:

$$\log(1/q) = \log(1/q_D) - \log\left(\frac{2\pi T \Delta p}{\rho g}\right) \tag{4-4}$$

similarly:

$$\log(\Delta t) = \log(t_D) - \log\left(\frac{T}{S}\frac{1}{r_w^2}\right) \tag{4-5}$$

Hence a log-log graph of *1/q* vs. Δt will have the same shape to the graph of $1/q_D$ vs. t_D and the curves will be shifted vertically by $\log(2\pi T\Delta p/\rho g)$ and horizontally by $\log(T/Sr_w^2)$. Matching the two curves (data and type curve) will provide estimates of Transmissivity (*T*) and Storativity (*S*).

A type curve calculated for a well flowing radially in a confined and homogeneous formation (the Jacob-Lohman assumption) is presented in Figure 4-2.

For the analysis of constant pressure tests using the type curve method, further flow models other than the radial homogeneous model have been developed. As a first extension, models are available for flow geometries other than radial (flow dimension = n=2). Flow models are developed for any dimension between linear flow (n=1), radial flow (n=2) and spherical flow (n=3). Figure 4-3 presents type curves for different flow dimensions.

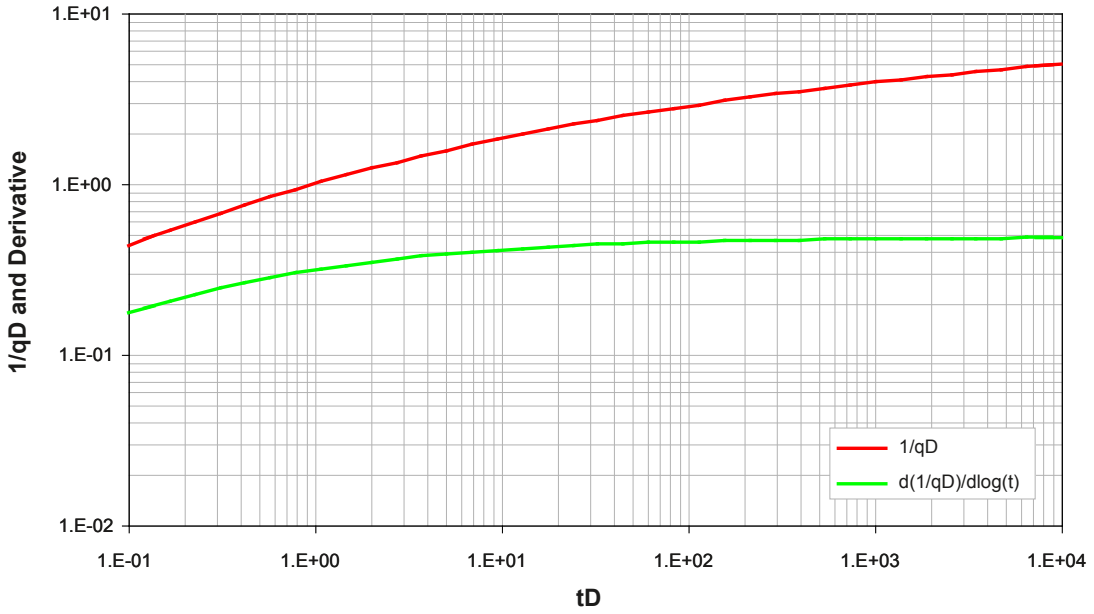

Figure 4-2. *Type curve for a well flowing radially in a confined, homogeneous formation.*

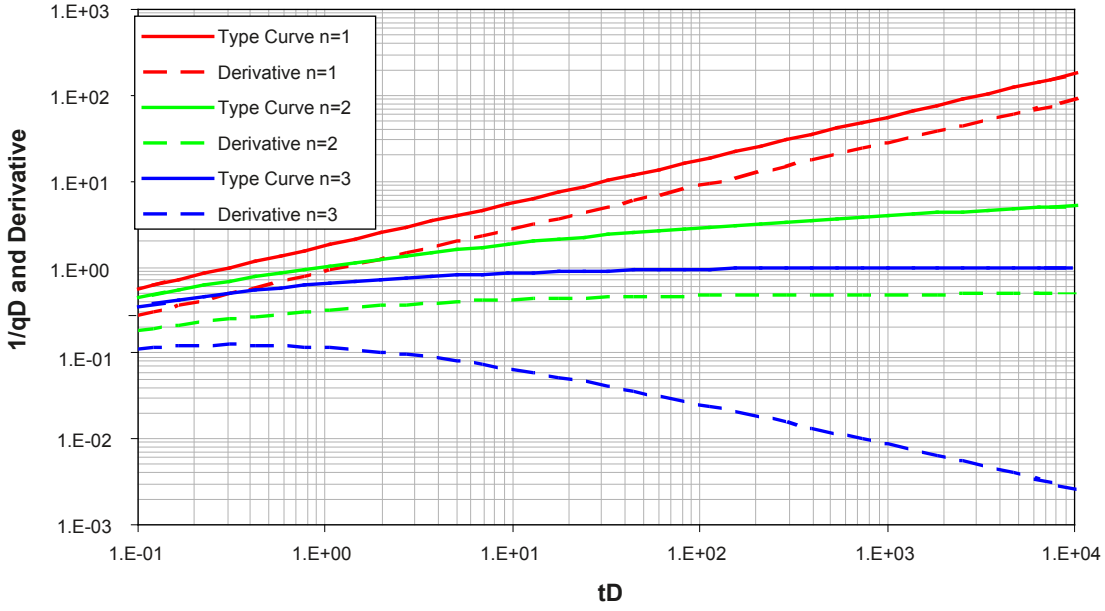

Figure 4-3. *Type curves for flow dimension of 1, 2 and 3.*

A further flow model extension is the development of type curves for heterogeneous formations, where the transmissivity and/or the storativity of the formation changes at some distance from the borehole. This so called composite flow model provides the both transmissivities in the vicinity of the borehole and further away. Figure 4-4 presents a comparison showing how the type curves change when the transmissivity increases at some distance away from the wellbore.

Composite flow models can be calculated for any given flow dimension, as shown in Figure 4-5.

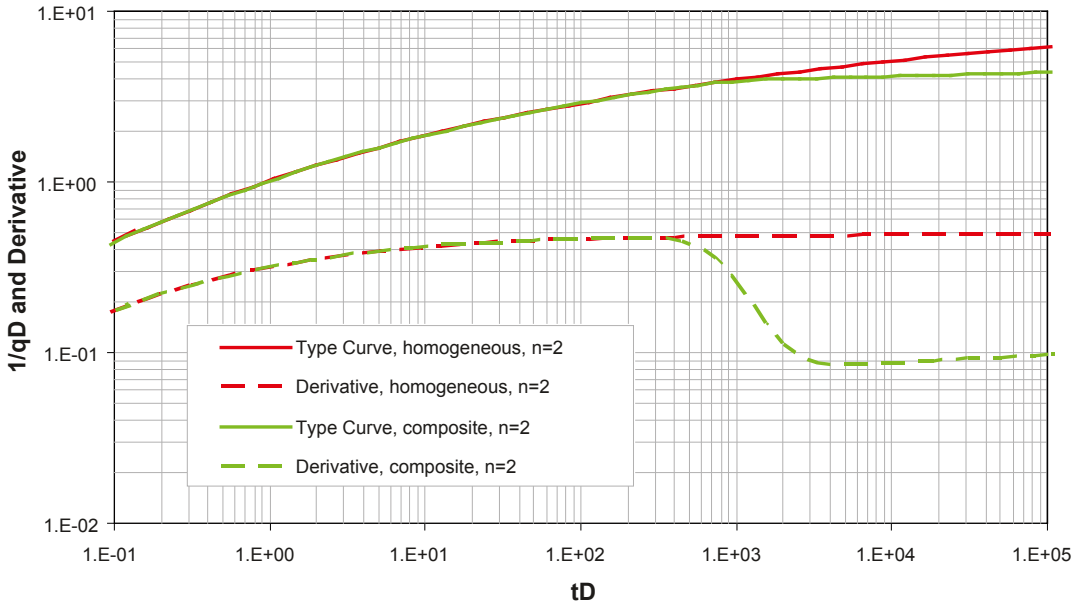

Figure 4-4. *Comparison of type curves for a homogeneous and composite flow model with increasing transmissivity away from the borehole (n=2).*

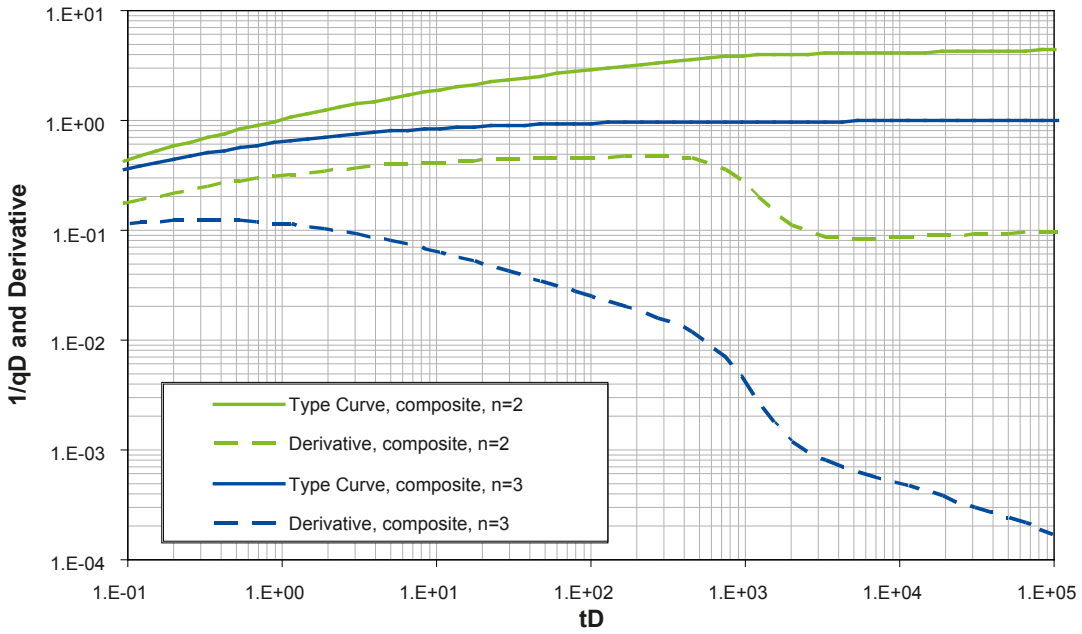

Figure 4-5. *Comparison of composite type curves for radial (n=2) and spherical flow (n=3).*

In addition, type curves accounting for transmissivity change at the wellbore face (described as skin) have been developed. Figure 4-6 presents type curves for radial flow and different skin factors at the wellbore.

Based on the transformation equations presented above and on the type curve describing the appropriate flow model, tests with constant injection pressure can be analyzed for transmissivity, storativity, skin factor, flow dimension and any transmissivity changes away from the borehole (i.e. by using composite flow models). In cases when the early time test data is not available or too noisy due to poor test control, the storativity and the skin factor become correlated, which means that they cannot be solved independently any more. In this case as a result of the analysis

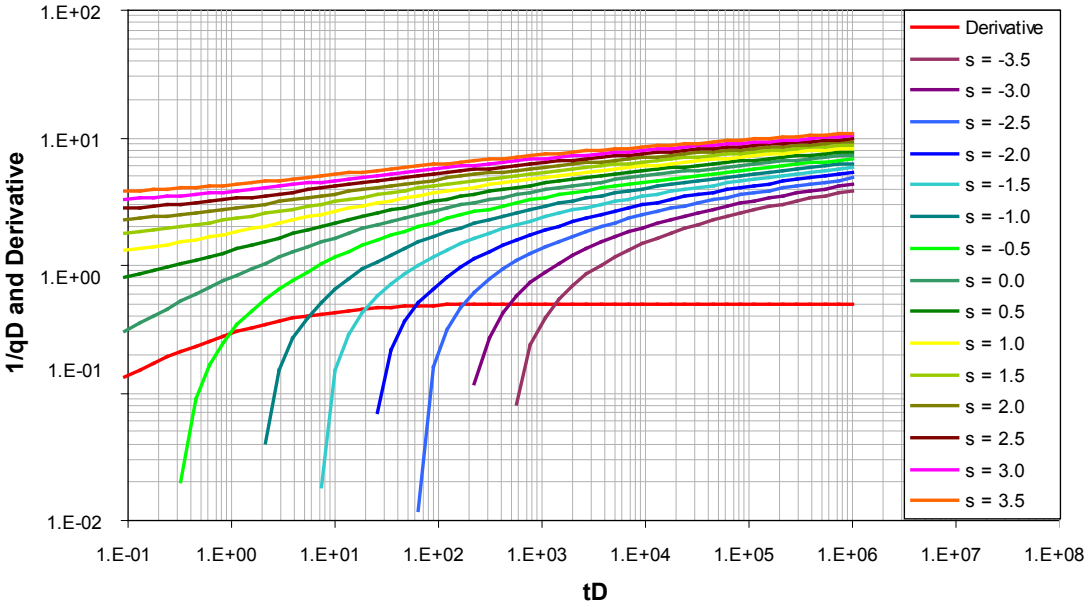

Figure 4-6. *Type curves for radial flow and different skin factors.*

one determines the correlation group $e^{2\xi}/S$. This means that in such cases the skin (ξ) can only be calculated when assuming the storativity (S) as known. In the case of the tests conducted at the Oskarshamn site the storativity was assumed to be 10^{-6} for all tests conducted below the depth of 100 m.

4.1.1.2 Steady state analysis

In addition to the type curve analysis, an interpretation based on the assumption of stationary conditions was performed as described by /Moye 1967/.

The test zone transmissivity according to /Moye 1967/ was denoted as T_M. For a delimited section T_M is calculated as:

$$T_M = \frac{Q_p \cdot \rho_w \cdot g}{dp_p} \cdot C1 \qquad (4\text{-}6)$$

For an open section T_M is calculated as:

$$T_M = \frac{Q_p}{dh_p} \cdot C1 = \frac{Q_p}{s} \cdot C1 \qquad (4\text{-}7)$$

With:

T_M	=	Transmissivity after /Moye 1967/	[m^2/s]
Q_p	=	Flow in test section immediately before stop of flow	[m^3/s]
dp_p	=	Maximal change in pressure during the perturbation phase	[Pa]
ρ_w	=	Density of water in test section	[kg/m^3]
g	=	Constant of gravitation (9.81)	[m/s^2]
s	=	Maximal drawdown in open section during the perturbation phase	[m]

and

$$C1 = \frac{1 + \ln\left(\frac{L_w}{2r_w}\right)}{2\pi} \quad (4\text{-}8)$$

with

L_w = Length of test section [m]
r_w = Nominal radius of borehole in test section [m]

In addition, the specific capacity (*Q/s*) of each of the test zones was calculated from:

for delimited section

$$Q/s = \frac{Q_p \cdot \rho_w \cdot g}{dp_p} \quad (4\text{-}9)$$

for open section

$$Q/s = \frac{Q_p}{dh_p} \quad (4\text{-}10)$$

4.1.2 Determination of the flow model

The granite formation at the Oskarshamn site can be described from a hydraulic point of view as a sparsely connected fracture network. The matrix is expected to have extremely low conductivity and storativity, such that hydraulic interaction between fractures and matrix is not expected. Therefore, the tests conducted at Oskarshamn are expected to reveal fracture transmissivities. The derived transmissivities will reflect the properties of fractures intersecting the test zone. Also, the transmissivity may vary with the distance from the borehole to the extent further fractures are intersected. Conceptually, the flow dimension displayed by the tests can vary between linear and spherical. However, as the experience of the tests conducted so far shows, the majority of the tests display radial flow geometry.

The flow models used in analysis were derived from the shape of the inverse rate (*1/q*) derivative calculated with respect to log time (also called the semi-log derivative) and plotted in log-log coordinates. Figure 4-7 presents the case of the test 205.34–305.34 conducted in borehole KLX04 where the semi-log derivative shows a clear stabilization indicating radial flow in a homogeneous formation.

In several cases the pressure derivative suggests a change of transmissivity with the distance from the borehole. In such cases a composite flow model was used in the analysis. Figure 4-8 presents the case of test 225.35–245.35 conducted in borehole KLX04 where the semi-log derivative of the constant pressure injection phase indicates radial flow and decreasing transmissivity at some distance from the borehole:

The flow dimension displayed by the test can be diagnosed from the slope of the pressure derivative. A slope of 0.5 indicates linear flow, a slope of 0 (horizontal derivative) indicates radial flow and a slope of –0.5 indicates spherical flow. The flow dimension diagnosis was commented for each of the tests. At tests where a flow regime could not clearly identified from the test data, a radial flow regime was assumed in the analysis.

In cases were different flow models were matching the data in comparable quality, the simplest model was preferred.

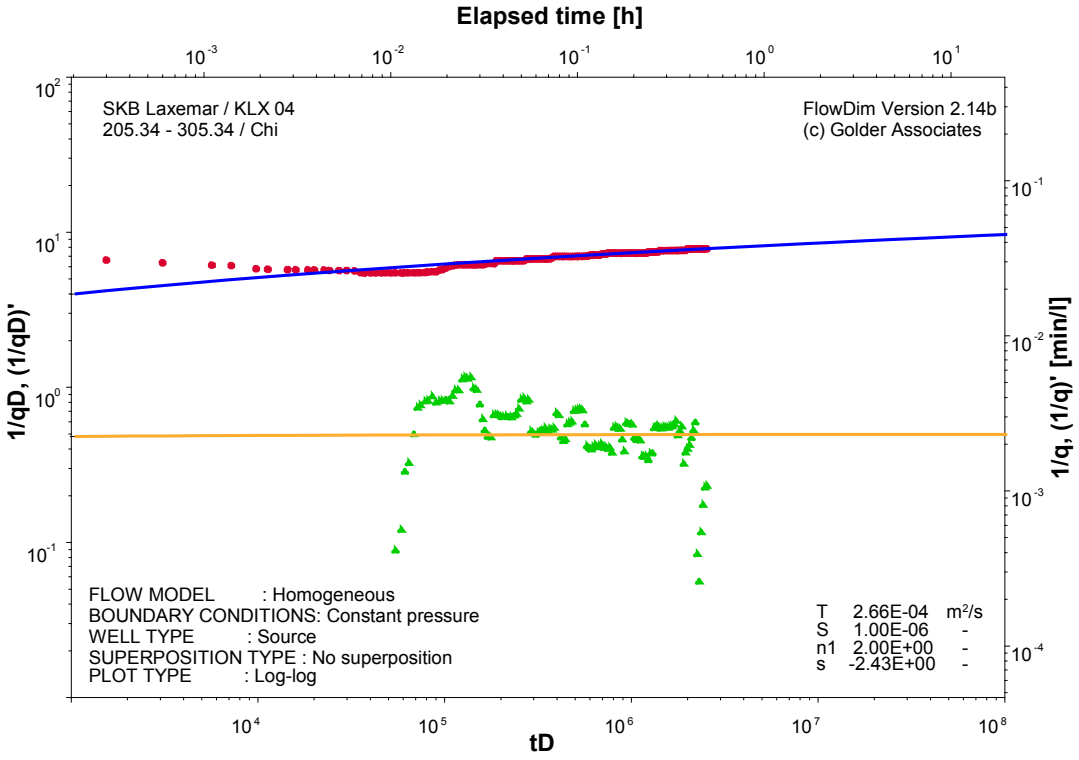

Figure 4-7. *Flow model identification; example of typical homogeneous radial flow behavior.*

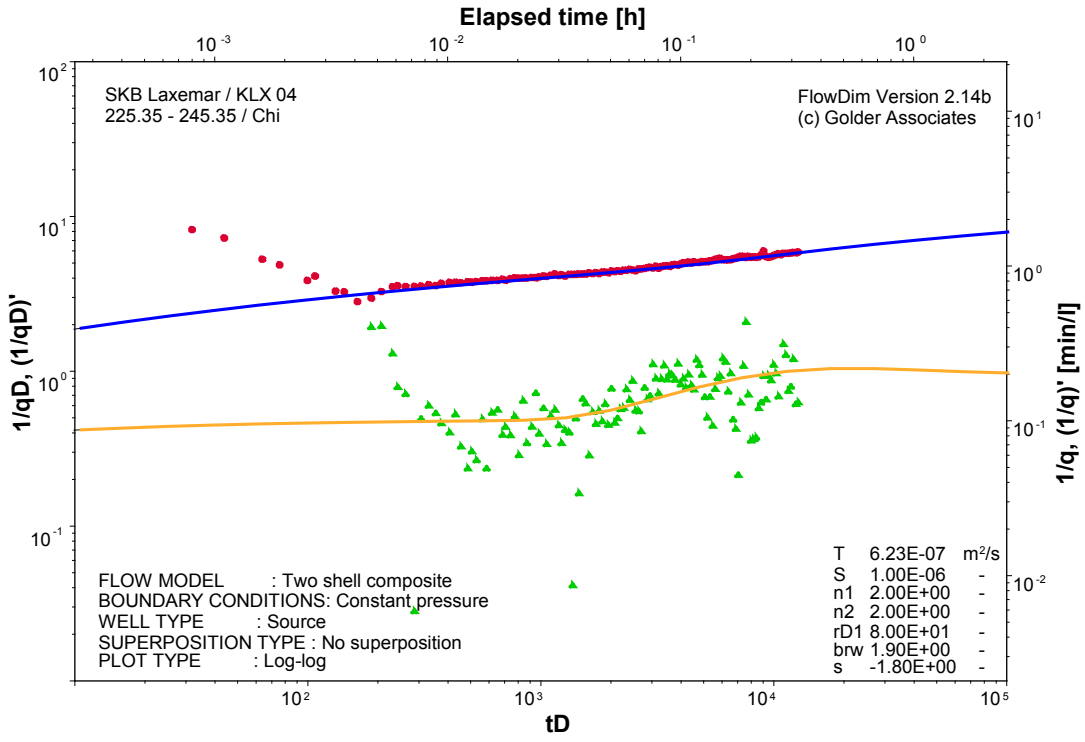

Figure 4-8. *Flow model identification; example of typical radial flow behavior with decreasing transmissivity away from the borehole (composite flow model).*

4.1.3 Conducting the analysis using a prescribed storativity, deriving the skin factor

As presented above, the type curve analysis of constant pressure injection tests allows the determination of:

- Transmissivity: from the vertical shift of the data in the log-log plot to match the type curve.
- Storativity: from the horizontal shift of the data in the log-log plot to match the type curve.
- Skin factor: from parameter of the type curve that matches the data best.

In cases when the early time test data is not available or too noisy due to poor test control, the storativity and the skin factor become correlated, which means that they cannot be solved independently any more. In this case as a result of the analysis one determines the correlation group $e^{2\xi}/S$. This means that in such cases the skin (ξ) can only be calculated when assuming the storativity (S) as known. Figure 4-9 uses the test 465.52–485.52 conducted in borehole KLX04 to illustrate the issue of correlation between skin and storativity.

In Figure 4-9 we see that the data can be matched equally well with type curves of different skin factors (ξ=0, –1 and –2) just by shifting the data horizontally, thus changing the storativity ($S = 7.6\ 10^{-6}$, 10^{-6} and $1.4\ 10^{-7}$). Note that in all three cases the correlation group $e^{2\xi}/S$ is equal to $1.3\ 10^{5}$. This is equivalent to exchanging skin for storativity in the solution, hence the two parameters are correlated. Skin and storativity are uncorrelated only at early test times ($t_D < 10$) when the horizontal shift of the data is fixed by the curvature of the derivative (t_D as defined in equation 4-3).

In the case of the tests conducted at the Oskarshamn site the storativity was assumed to be 10^{-6} for all tests conducted below the depth of 100 m.

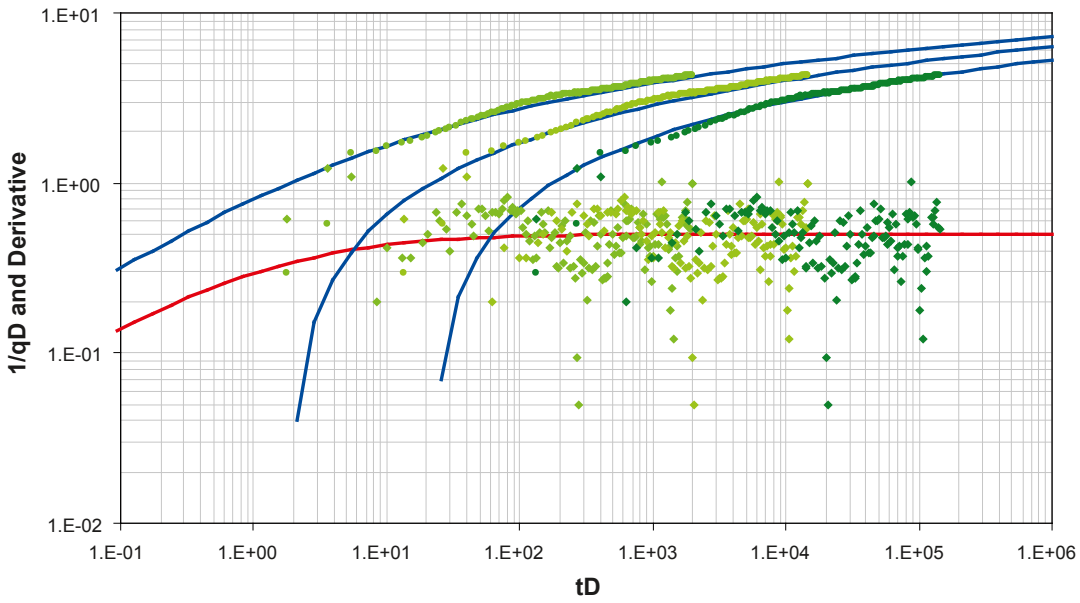

Figure 4-9. *The skin-storativity correlation.*

4.1.4 Analysis example – Constant pressure injection test, 245.38–265.38 m in borehole KLX04

The test 245.38–265.38 was conducted on August 25th 2004 in borehole KLX04. Figure 4-10 presents a Cartesian plot of the pressure measured in the test section and the injection rate recorded at the surface during the constant pressure injection phase (CHi).

The analysis of the CHi phase starts with the construction of the rate inverse and derivative log-log plot (Figure 4-11). As we can see, the derivative shows an initial stabilization at early times which indicated radial flow in the borehole vicinity. At middle times the derivative shows a downward slope and stabilizes at late times at a lower level. This behavior indicates increasing transmissivity at some distance away from the borehole. Based on these observations, the test can be matched using a radial flow composite flow model with increasing transmissivity away from the borehole.

In a second step, an initial estimate of the transmissivity is obtained using the steady state calculations presented in Section 4.1.1.2. Table 4-1 presents the input parameters and results of these calculations conducted using the equations 4-6 to 4-10. The Table 4-1 presents the calculation of transmissivity and Q/s for two different system assumptions: (1) for the case when the test section is delimited by packers and (2) for the case when the measurement was conducted without packers (i.e. open section).

The results of the T_M and Q/s calculations indicate that the formation transmissivity near the borehole is approx. $1.4 \cdot 10^{-5}$ m^2/s.

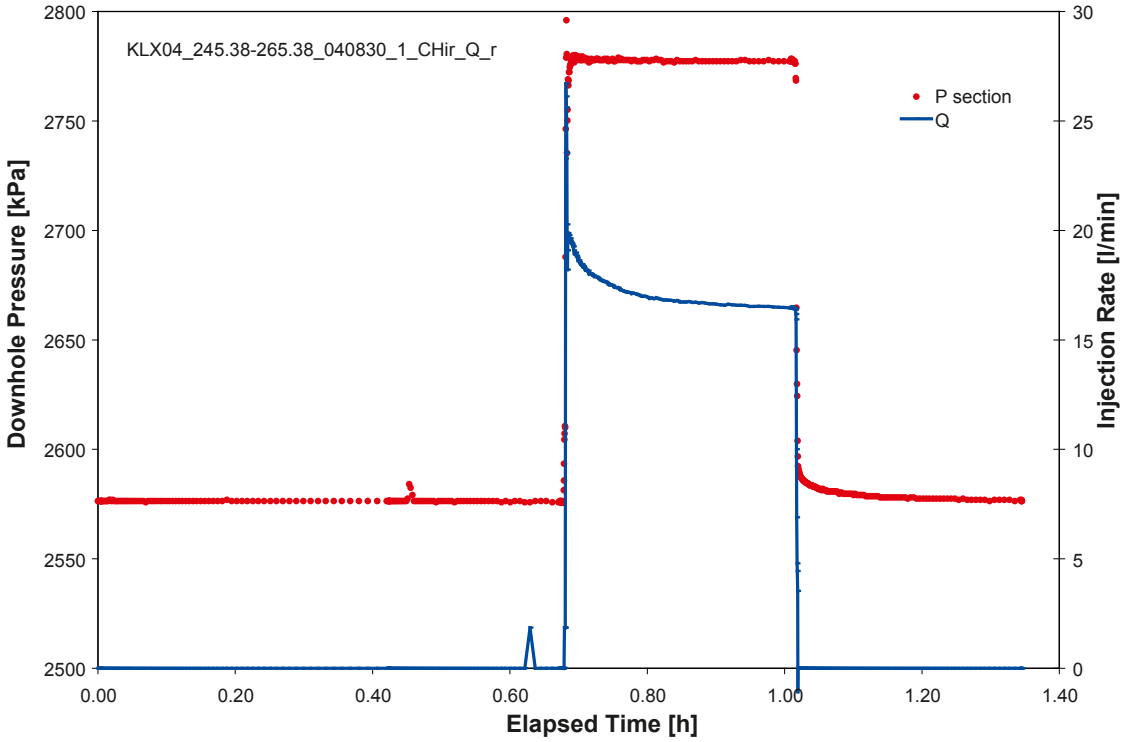

Figure 4-10. *Test 245.38–265.38 m in borehole KLX04; pressure and rate plot.*

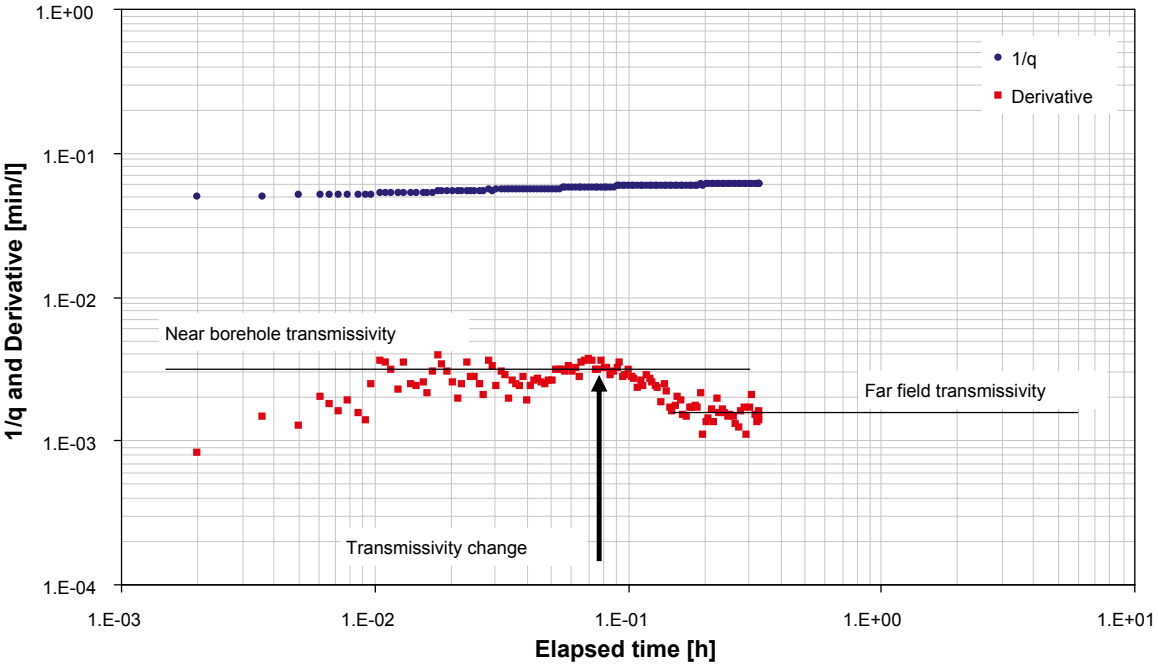

Figure 4-11. *Test 245.38–265.38 m in borehole KLX04; log-log diagnostic plot of the CHi phase.*

Table 4-1. Test 245.38–265.38 m in borehole KLX04; steady state calculations.

Inputs Description	Symbol	Unit	Value	SI Unit	SI Value
Flow in test section immediately before stop of flow	Qp	L/min	16.39	m^3/s	273E–04
Maximal change in pressure during perturbation phase	dpp	kPa	201	pA	200,100
Water density in test section	rhow	kg/m^3	1,000	Kg/m^3	1,000
Constant of graviation	gr	m/s^2	9.81	m/s^2	9.81
Lengt of test section	Lw	m	20	m	20
Nominal radius of borehole in test section	rw	m	0.038	m	0.038
Maximal drawdown in open section during perturbation phase	sd	m	20	m	20
Constant	C	–			1.0461
Outputs					
T delimited section	TM(d)			m^2/s	1.39E–05
T open section	TM (o)			m^2/s	1.43E–05
Q/s delimited section	Q/s(d)			m^2/s	1.33E–05
Q/s open section	Q"/s(o)			m^2/s	1.37E–05

The third step is to analyze the test using type curve matching. Figure 4-12 shows the type curve match and the analysis results. The near borehole transmissivity was matched to $2.1 \cdot 10^{-5}$ m^2/s, which is similar to the T_M value of $1.4 \cdot 10^{-5}$ m^2/s derived from the steady state analysis. The transmissivity further away from the borehole was calculated to $5.5 \cdot 10^{-5}$ m^2/s. The test was matched using a storativity of $3.7 \cdot 10^{-8}$ and a skin of zero. Assuming that the true storativity is 10^{-6}, the equivalent skin is 1.6.

4.1.5 Uncertainties

The present section describes sources of uncertainty related to the conduction and analysis of constant pressure injections tests and how these uncertainties were treated in the analysis. Examples of real test data are given whenever appropriate.

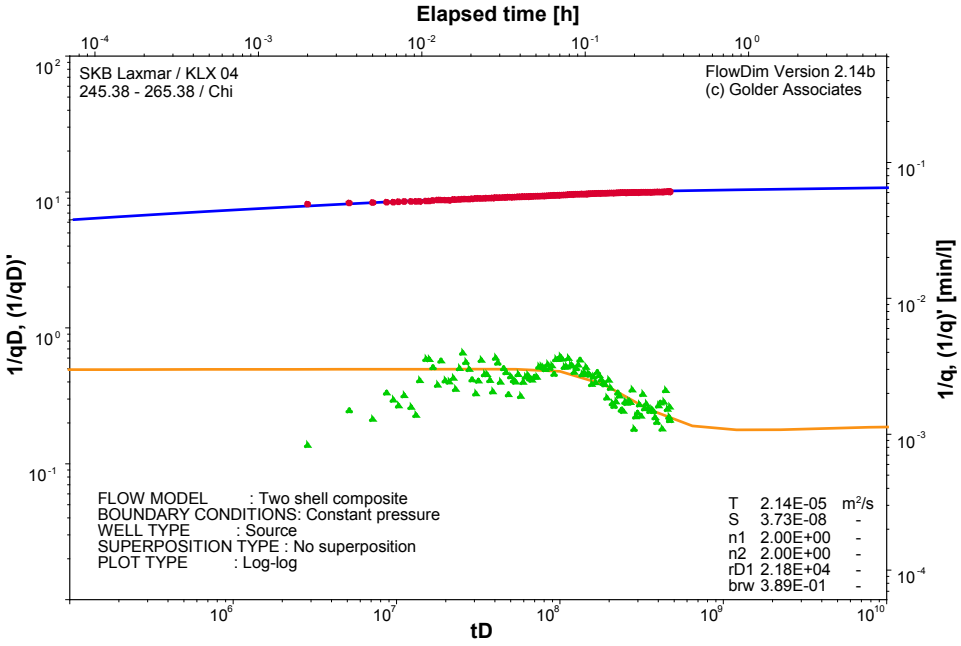

Figure 4-12. *Test 245.38–265.38 m in borehole KLX04; log-log type curve match of the CHi phase using a composite flow model.*

4.1.5.1 Poor pressure control

The pressure control of the constant pressure injection tests was handled by an automated system using magnetic valves controlled by a computer. In cases when the flow rate was expected to fall below the control limits of the system (0.001 L/min), the injection was conducted using a pressure vessel with Nitrogen buffer. In most of the cases, the pressure couldbe controlled within 10% of the target value within the first 45 seconds of the test. In cases when the pressure control did not work fast enough or was not precise enough, the injection test was repeated. Figure 4-13 and Figure 4-14 present the case of test 505.55–605.55 m conducted in borehole KLX04. In Figure 4-14 we see that the pressure control system needed approx. 100 seconds to bring the pressure to the target level. In the same time the flow rate deviates from the expected shape due to the ongoing pressure fluctuations.

Figure 4-15 shows the rate inverse data and derivative in a log-log plot. The rate data is disturbed at early times due to the pressure fluctuations. However, the middle and late test times are analyzable and a reliable test zone transmissivity can be derived. The only disadvantage of the poor pressure control at early times is the fact that the hydraulic response of the formation in the immediate vicinity of the borehole cannot be characterized due to the disturbance.

4.1.5.2 Noise in the flow rate data

Because of reasons related to measurement technology, it is much more difficult to measure flow rate with a relatively low level of noise than it is the case for pressure. Although the PSS2 equipment is very well suited to measure flow rates with high accuracy, for low flow rates ($q < 0.01$ L/min) the level of noise increases. In addition, the noise is magnified when calculating the derivative. Figure 4-16 presents the case of test 445.50–465.50 m conducted in borehole KLX04. As presented in the figure the noise level is approx. 0.001 L/min at a measured flow rate of approx. 0.003 L/min (i.e. approx. 30%). This noise influences negatively the calculation of the inverse rate derivative (see Figure 4-17). Algorithms are available (and used) to smooth the derivative, however, increasing the smoothing of the derivative introduces numerical effects which distort the response. In the example presented below, the derivative quality does not

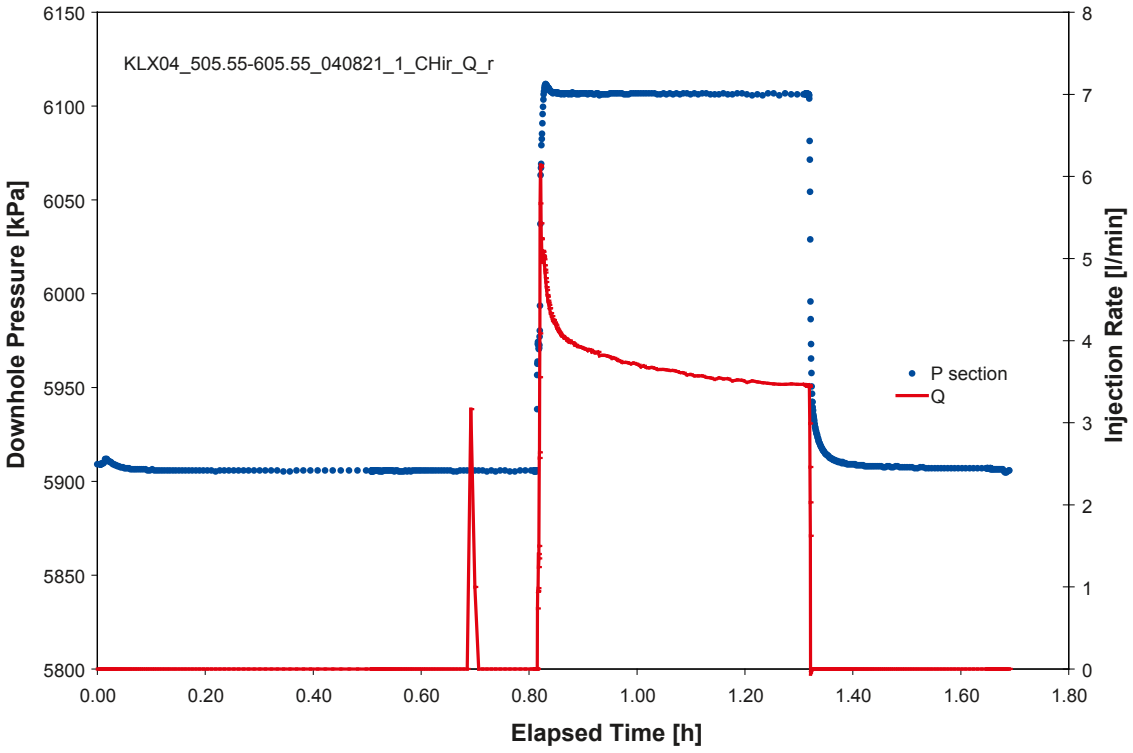

Figure 4-13. *Test 505.55–605.55 in borehole KLX04; effect of poor pressure control at early times; Cartesian plot.*

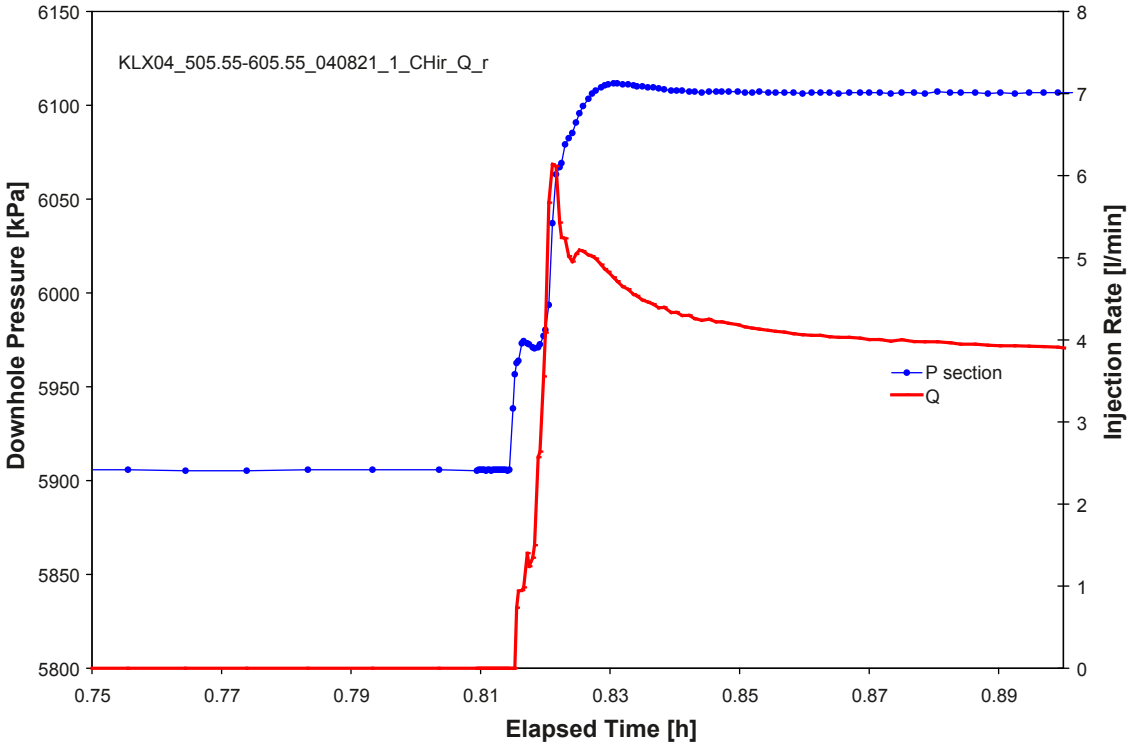

Figure 4-14. *Test 505.55–605.55 in borehole KLX04; effect of poor pressure control at early times; Cartesian plot (zoomed).*

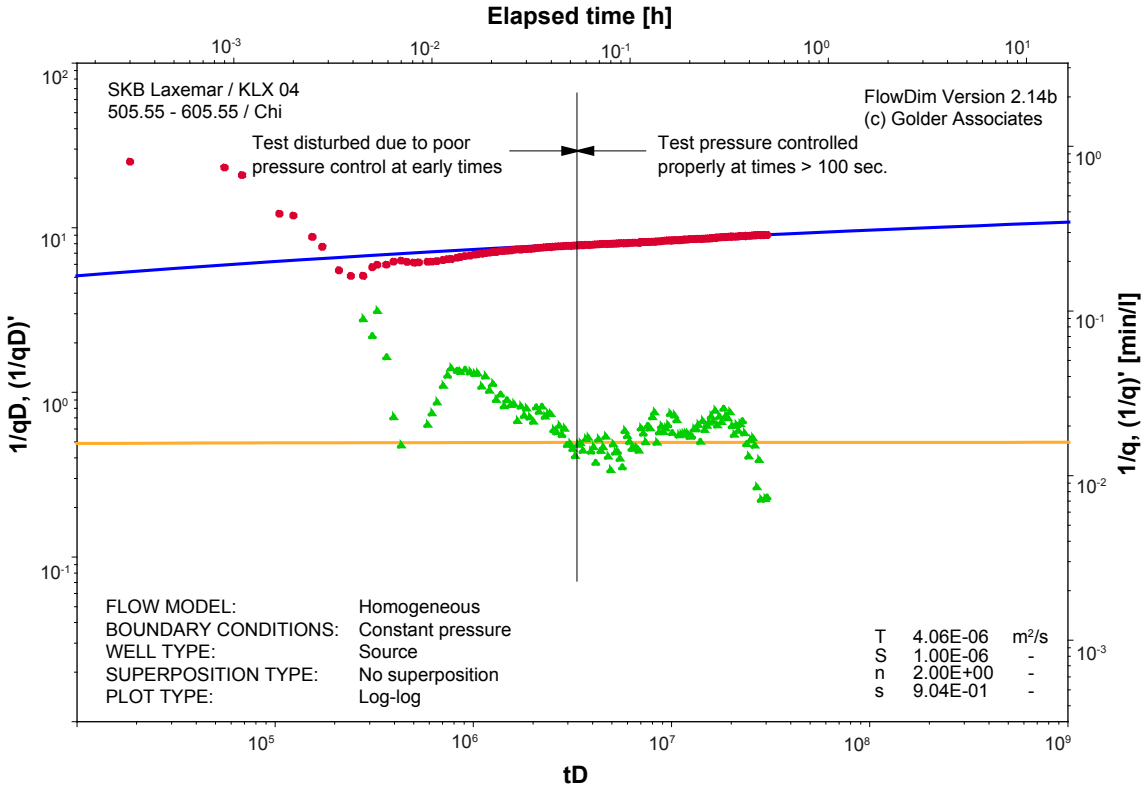

Figure 4-15. *Test 505.55–605.55 in borehole KLX04; effect of poor pressure control at early times; Log-log match.*

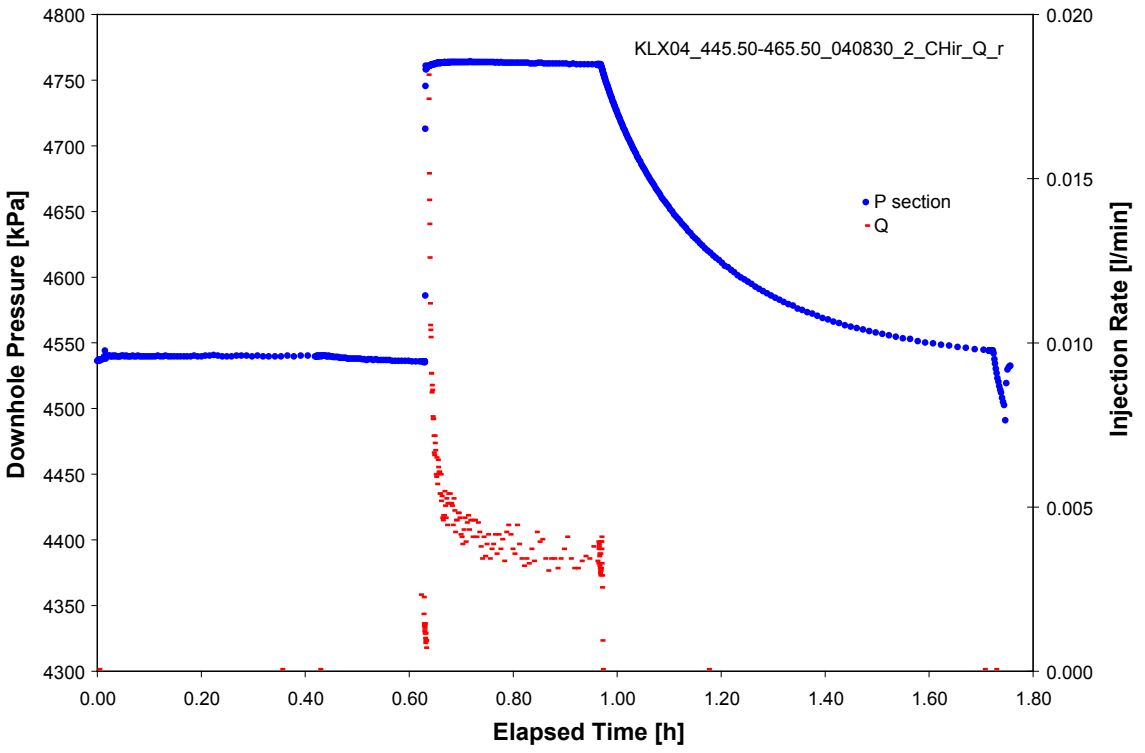

Figure 4-16. *Test 445.50–465.50 in borehole KLX04; noise in the flow rate measurement; Cartesian plot.*

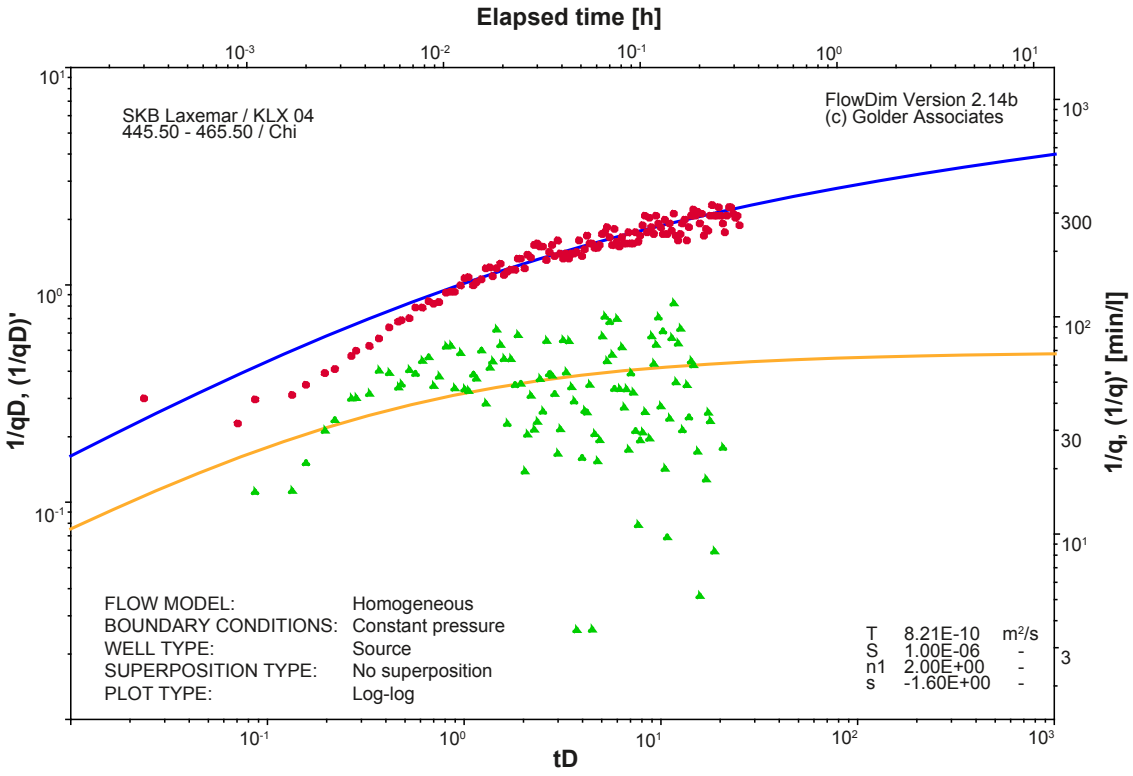

Figure 4-17. *Test 445.50–465.50 in borehole KLX04; noise in the flow rate measurement; Log-log derivative plot.*

allow a clear flow model identification. In addition, considering the fact that the level of the radial flow stabilization of the derivative is a direct measure for the test zone transmissivity, the high level of noise in the derivative also introduces uncertainty in the derived transmissivity (in the case presented here approx. half order of magnitude). The uncertainty in transmissivity is subsequently reconciled with the result of the analysis of the pressure recovery phase with the aim of achieving maximum consistency of results between the two test phases.

4.1.6 Flow rates below measurement limit

The PSS2 system allows the measurement of flow rates with a lower limit of 0.001 L/min. Two different cases exist, when the flow rates during a constant pressure injection test fall below the measurement limit:

1. The flow rate falls below the measurement limit during the injection phase (Figure 4-18 and Figure 4-19). In such cases the analysis is conducted using the normal derivative type curve matching procedure. However, the early test data is emphasized in the analysis, which accounts for the fact that the late time data may not be as accurate due to the measurement limit.
2. The flow rate drops below measurement limit (virtually zero) from the beginning of the test (see Figure 4-20). In such cases the injection phase is not analyzable. The subsequent pressure recovery phase was analyzed as a pulse injection test. The wellbore storage coefficient was calculated from the total volume of water injected into the test zone (as calculated from the flowmeter readings).

In cases when the test section transmissivity was expected to be very low ($< 2 \cdot 10^{-10}$ m^2/s) the test was conducted as a pulse injection.

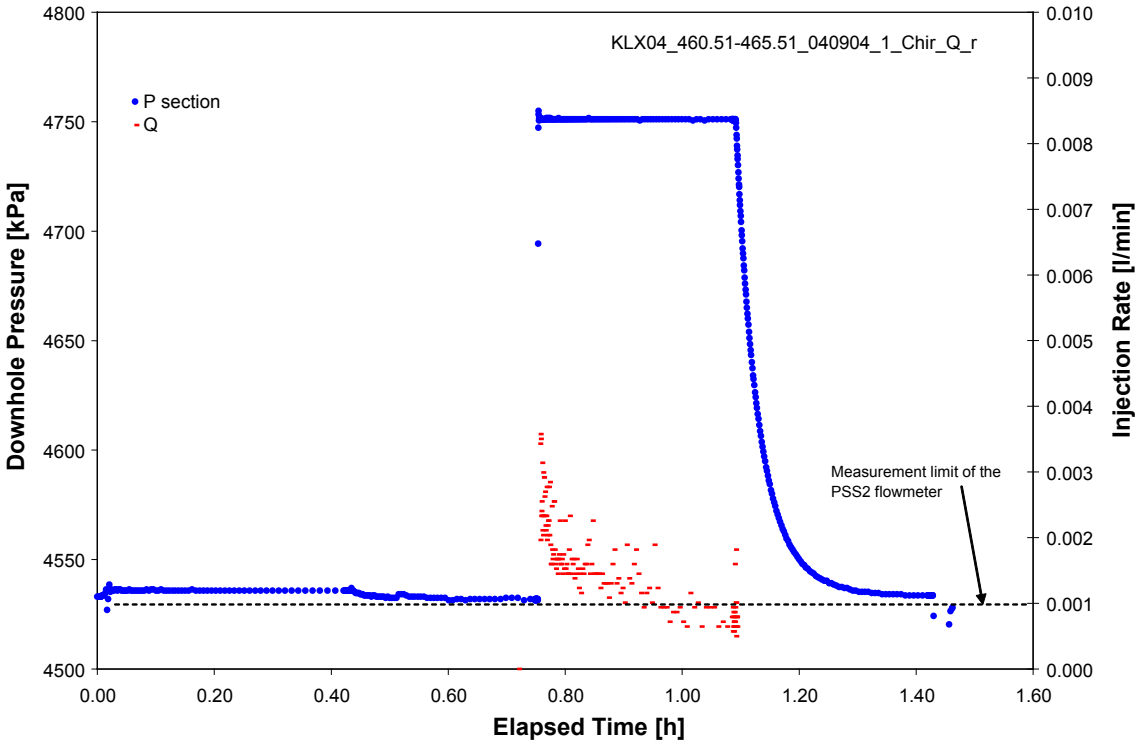

Figure 4-18. *Test 460.51–465.51 in borehole KLX04; flow rate below measurement limit (case 1); Cartesian plot.*

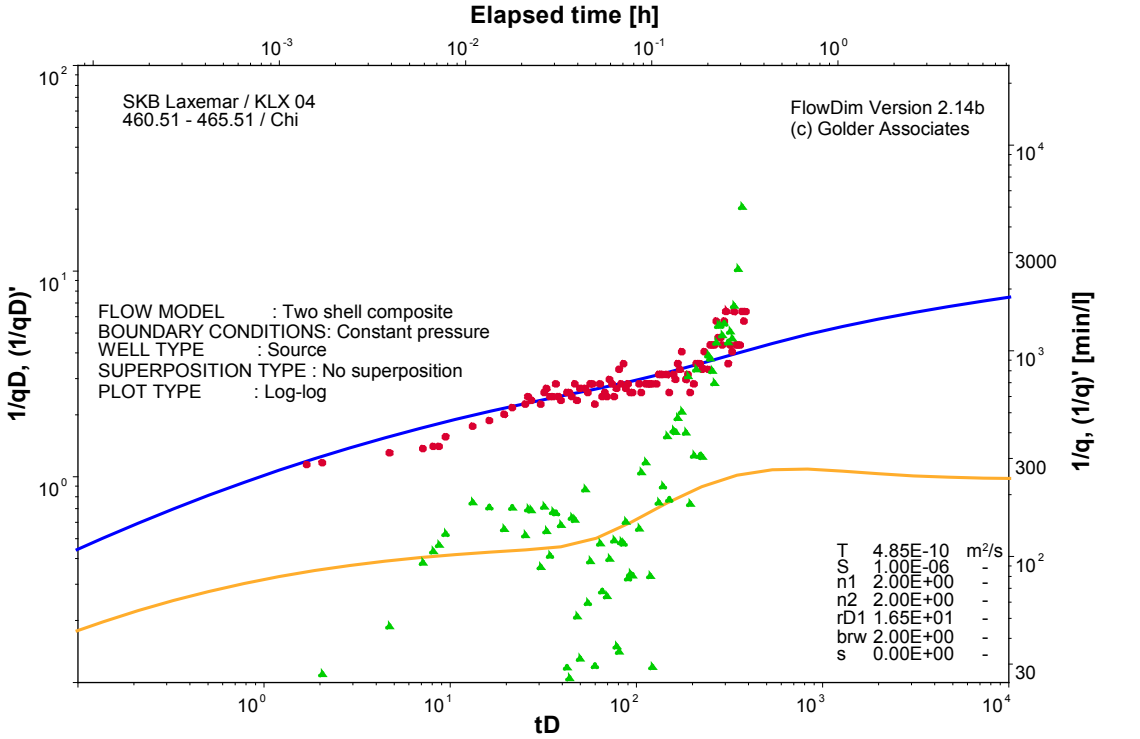

Figure 4-19. *Test 460.51–465.51 in borehole KLX04; flow rate below measurement limit (case 1); Log-log derivative plot.*

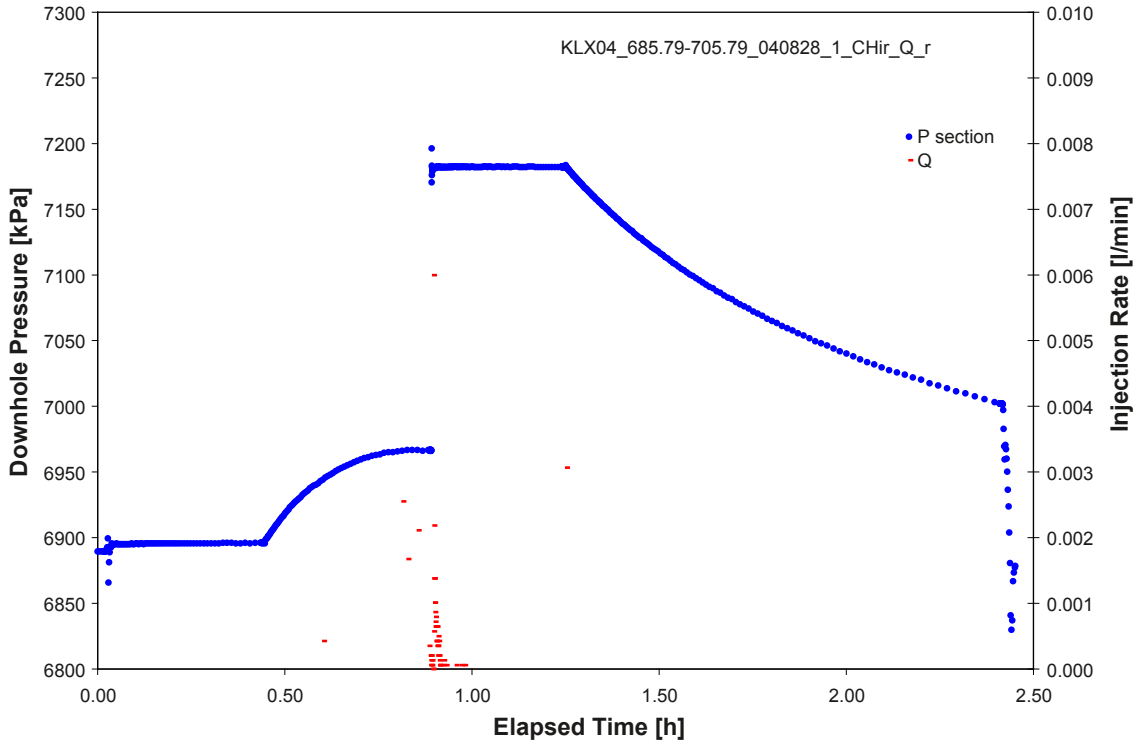

Figure 4-20. *Test 460.51–465.51 in borehole KLX04; flow rate below measurement limit (case 2); Cartesian plot.*

4.2 Analysis of pressure recovery tests (the CHir phase)

Constant pressure recovery tests were analyzed using the method described by /Gringarten 1986/ and /Bourdet et al. 1989/ by using type curve derivatives calculated for different flow models. In addition, the recovery phase was analyzed using the /Horner 1951/ method to derive a second estimation of transmissivity and to extrapolate the static formation pressure.

4.2.1 Brief theoretical background

The analysis of constant rate and pressure recovery tests is best described in /Horne 1990/. Type curve analysis and the use of pressure derivative in log-log coordinates currently is the standard analysis method both in hydrogeology and petroleum industry. The present section describes the type curve analysis method, as applied for the pressure recovery tests conducted at the Oskarshamn site.

4.2.1.1 Type Curve Analysis

The type curve analysis method makes use of dimensionless variables, which allow calculating the flow model (i.e. the type curve) independently of the primary formation flow parameters (i.e. transmissivity and storativity) and of the applied flow rate. The dimensionless pressure and time groups are defined as:

$$p_D = \frac{2\pi T \Delta p}{q \rho g} \tag{4-11}$$

$$t_D = \frac{T \Delta t}{S r_w^2} \tag{4-12}$$

Since, by definition, dimensionless pressure and time are linear functions of actual pressure and time, then the logarithm of the pressure difference will differ from the logarithm of the dimensionless pressure (i.e. the type curve) by a constant amount.

$$\log \Delta p = \log p_D - \log \frac{2\pi T}{q\rho g} \tag{4-13}$$

similarly

$$\log \Delta t = \log t_D - \log \frac{T}{S r_w^2} \tag{4-14}$$

Hence a log-log graph of Δp vs. Δt will have the same shape to a graph of p_D vs. t_D and the curves will be shifted vertically by $\log(2\pi T/q\rho g$ and horizontally by $\log(T/Sr_w^2)$. Matching the two curves provides estimates of Transmissivity (T) and Storativity (S).

Constant rate and pressure recovery tests differ from constant pressure tests through the fact that they are influenced by wellbore storage. The wellbore storage is characterized by the wellbore storage coefficient (C) which quantifies the volume of fluid the wellbore (or test section) can store when the pressure changes by one unit:

$$C = \frac{dV}{dP} \tag{4-15}$$

For the type curve analysis the dimensionless wellbore storage coefficient is defined as:

$$C_D = \frac{C\rho g}{2\pi r_w^2 S} \tag{4-16}$$

For analysis purposes, the type curves are plotted as p_D vs. t_D/C_D in log-log coordinates:

$$\frac{t_D}{C_D} = \frac{2\pi T t}{C\rho g} \tag{4-17}$$

The individual type curves for a well with wellbore storage (C) and skin (ξ) flowing radially (n=2) at a constant rate (q) in a confined homogeneous formation of constant transmissivity (T) and storativity (S) are characterized by the type curve parameter $C_D e^{2\xi}$ (see Figure 4-21). When matching the test pressure data (Δp vs. Δt) with the type curve (p_D vs. t_D/C_D) in log-log coordinates following parameters are derived:

- The shift needed to match the data vertically; also called pressure match (*PM*).
- The shift needed to match the data horizontally; also called time match (*TM*).
- The parameter of the type curve that fits the data best; $(C_D e^{2\xi})_M$.

As shown above:

$$PM = \frac{\Delta p}{p_D} = \frac{q\rho g}{2\pi T} \tag{4-18}$$

and

$$TM = \frac{\Delta t}{\frac{t_D}{C_D}} = \frac{C\rho g}{2\pi T} \tag{4-19}$$

From the *PM* definition the transmissivity can be derived as:

$$T = \frac{q\rho g}{2\pi} \frac{1}{PM} \tag{4-20}$$

Further, using the *TM* definition and the transmissivity calculated from the pressure match, the wellbore storage coefficient can be calculated as:

$$C = \frac{2\pi T}{\rho g} TM \tag{4-21}$$

At this stage the derived wellbore storage coefficient (C) is introduced in the equation of the type curve parameter:

$$(C_D e^{2\xi})_M = \frac{C \rho g}{2\pi r_w^2 S} e^{2\xi} \tag{4-22}$$

The equation above has two unknowns, the storativity (S) and the skin factor (ξ). Therefore it can only be either solved for skin by assuming that the storativity is known or solved for storativity by assuming the skin as known (typically zero). For the tests conducted at the Oskarshamn site at depths of more than 100 m the tests were analyzed by using a prescribed storativity of 10^{-6}.

For the analysis of pressure recovery (also known as **B**uild-**U**p) tests the type curves ($p_{D\,BU}$) must be calculated by superimposing constant rate type curves (p_D) in order to account for the change in flow rate which occurs when the pressure recovery is started (q=0 L/min). If the test interval has being flowing (injection or production) at a constant rate (q) for a dimensionless time t_{pD} and is then shut-in, the subsequent pressure build-up after the shut-in time (t_D) is calculated as:

$$p_{D\,BU} = p_D(t_{pD} + t_D) - p_D(t_D) \tag{4-23}$$

A type curve calculated for a well with wellbore storage and skin flowing radially in a confined and homogeneous formation (the simplest flow model used in the analysis of the tests conducted at the Oskarshamn site) is presented in Figure 4-21.

For the analysis of pressure recovery tests using the type curve method, further flow models other than the radial homogeneous model are available. As a first extension, models are available for flow geometries other than radial (flow dimension = n=2). Flow models are developed for any dimension between linear flow (n=1), radial flow (n=2) and spherical flow (n=3). Figure 4-22 presents type curves for different flow dimensions.

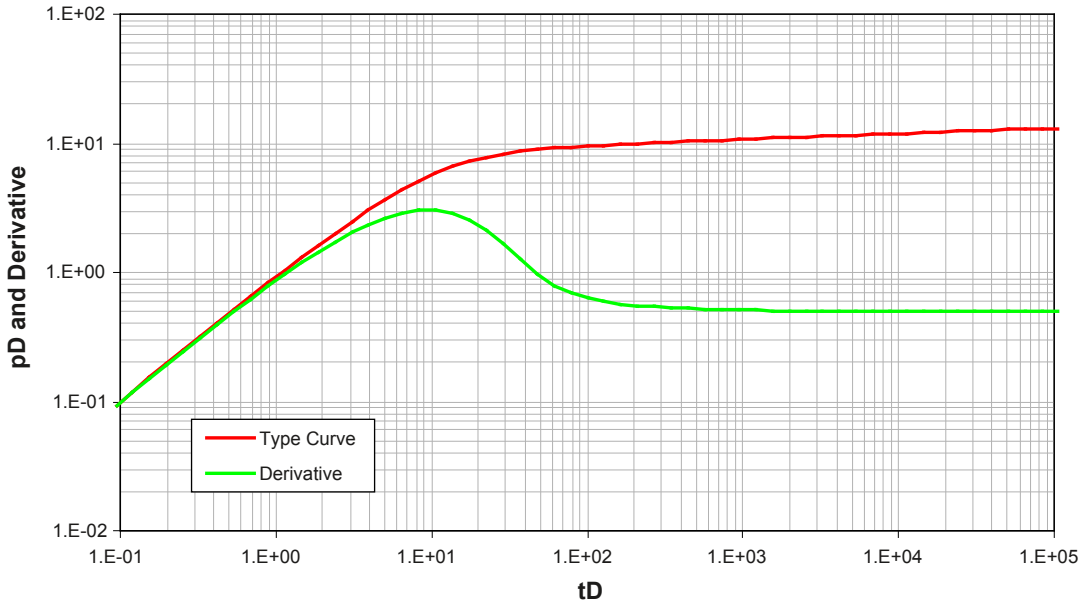

Figure 4-21. *Type curve for a well with wellbore storage and skin flowing radially in a confined, homogeneous formation.*

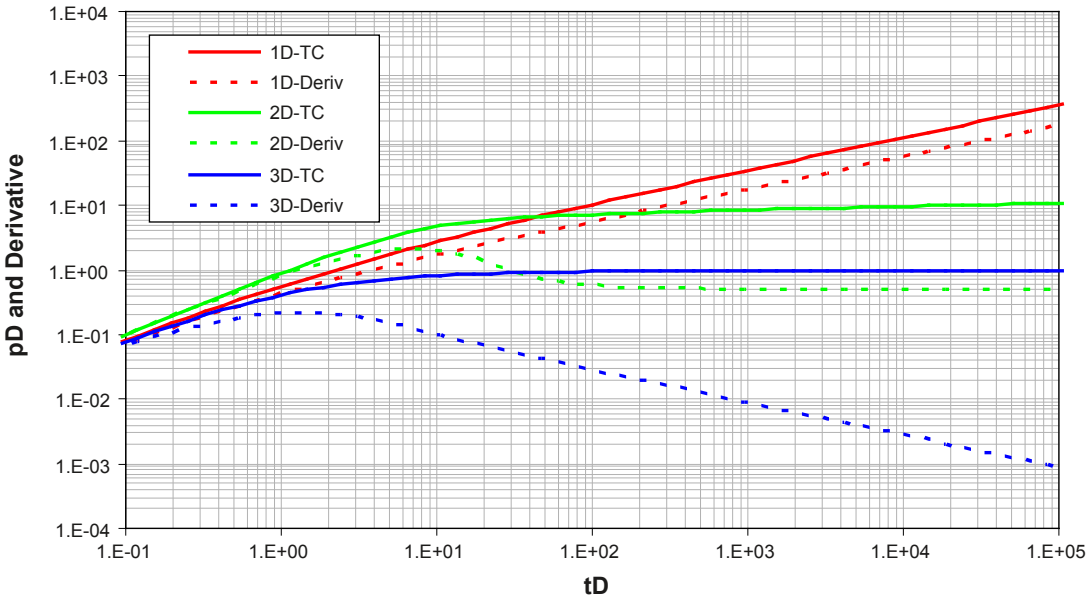

Figure 4-22. *Type curves with wellbore storage and skin for flow dimension of 1, 2 and 3.*

A further flow model extension is the development of type curves for heterogeneous formations, where the transmissivity and/or the storativity of the formation changes at some distance from the borehole. This so called composite flow model provides the both transmissivities in the vicinity of the borehole and further away. Figure 4-23 presents a comparison showing how the wellbore storage and skin type curves change when the transmissivity increases or decreases at some distance away from the wellbore. Composite flow models can be calculated for any given flow dimension. Also, changes of flow dimension with the distance from the borehole can be calculated as well.

All type curves used for constant pressure and recovery tests account for wellbore storage and skin effects.

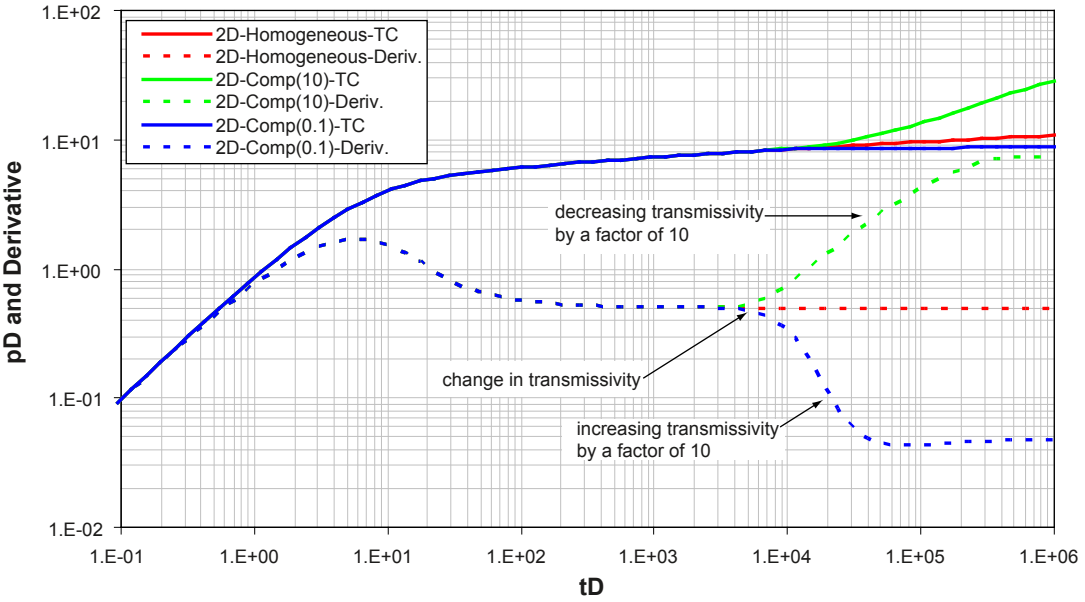

Figure 4-23. *Comparison of wellbore storage type curves for a homogeneous and two composite flow models with increasing and decreasing transmissivity away from the borehole (n=2).*

4.2.1.2 HORNER analysis

The HORNER analysis method is used for the analysis of pressure recovery test phases following a production or injection test phase conducted at a constant rate. In the case of the tests conducted at the Oskarshamn site, the recovery phase was following a phase of constant pressure (i.e. variable rate) injection. Therefore, the method cannot be correctly applied in a strict theoretical sense. However, it was found to deliver results which were consistent with the type curve analysis method and with the analysis of the preceding constant pressure injection phase. Therefore the HORNER method was used as a crosscheck for the formation transmissivity and for the extrapolation of the static formation pressure of the respective test zone.

The HORNER method involves plotting the test pressure (p) vs. the logarithm of HORNER time (also called superposition time) defined as:

$$t_{HORNER} = \frac{t_p + \Delta t}{\Delta t} \tag{4-24}$$

Provided that the test reached the infinite acting radial flow period (horizontal derivative in log-log coordinates and data plotting alon a straight line in the HORNER plot) the test zone transmissivity can be derived from the slope of the straight line (M) which approximates the late time data in the HORNER plot:

$$T = \frac{1}{M}\frac{q\rho g}{4\pi} \tag{4-25}$$

A further useful feature of the HORNER plot is that the test data can be extrapolated to infinite times to derive the static formation pressure because:

$$\begin{aligned} &\lim\left(\frac{t_p + \Delta t}{\Delta t}\right)_{\Delta t \to \infty} = 1 \\ &\log(t_{HORNER}) = 0 \end{aligned} \tag{4-26}$$

Figure 4-24 shows a HORNER plot of the pressure recovery phase of test 405.49–505.49 m conducted in borehole KLX04. In cases when the infinite acting radial flow phase of the test was achieved (data plots on a straight line on the HORNER plot), the data can be extrapolated to infinite times by using the straight line (as shown in Figure 4-24). In cases when the data does not display the infinite acting radial flow, the type curve matched in log-log coordinates can be used in the HORNER plot to extrapolate the test to infinite times and derive the static pressure (see Figure 4-25).

4.2.2 Determination of the flow model

The granite formation at the Oskarshamn site can be described from a hydraulic point of view as a sparsely connected fracture network. The matrix is expected to have extremely low conductivity and storativity, such that hydraulic interaction between fractures and matrix is not expected. Therefore, the tests conducted at Oskarshamn are expected to reveal fracture transmissivities. The derived transmissivities will reflect the properties of fractures intersecting the test zone. Also, the transmissivity may vary with the distance from the borehole to the extent further fractures are intersected. Conceptually, the flow dimension displayed by the tests can vary between linear and spherical. However, as the experience of the tests conducted so far shows, the majority of the tests display radial flow geometry.

The flow models used in analysis were derived from the shape of the pressure derivative calculated with respect to log time (also called the semi-log derivative) and plotted in log-log coordinates. The flow models used for the analysis of the pressure recovery phase are similar with the models used for the analysis of the constant pressure injection tests described in

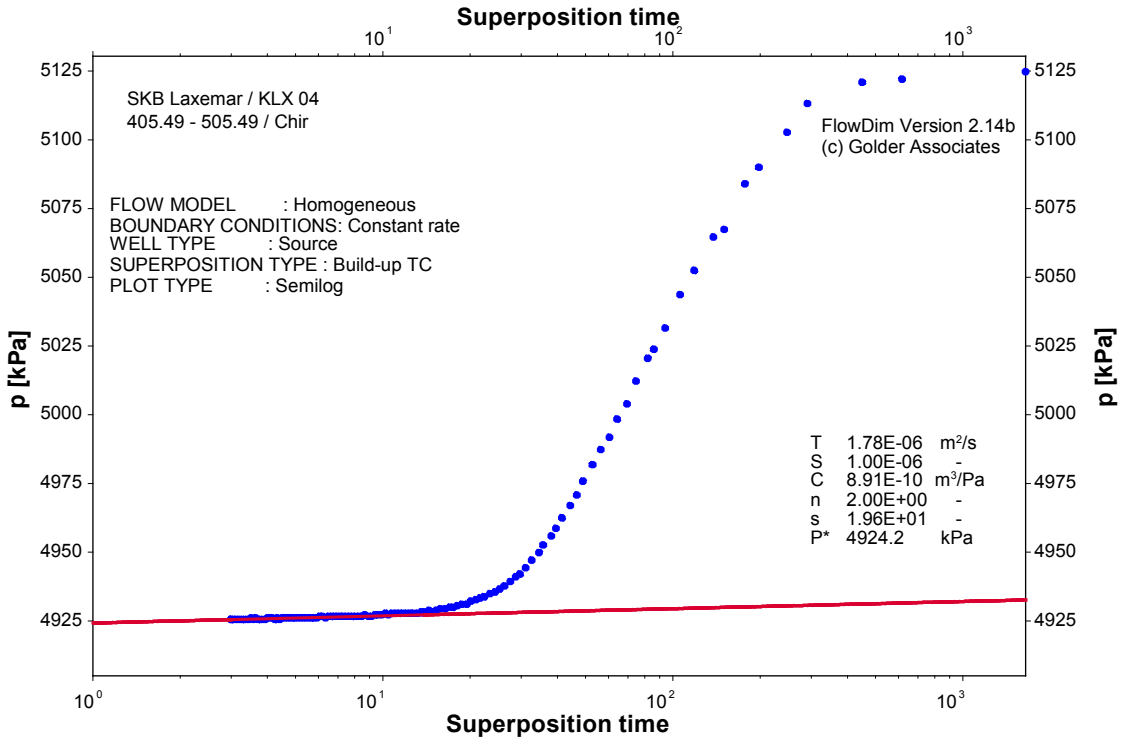

Figure 4-24. *Test 405.49–505.49 m conducted in borehole KLX04; HORNER plot with HORNER straight line of the pressure recovery phase.*

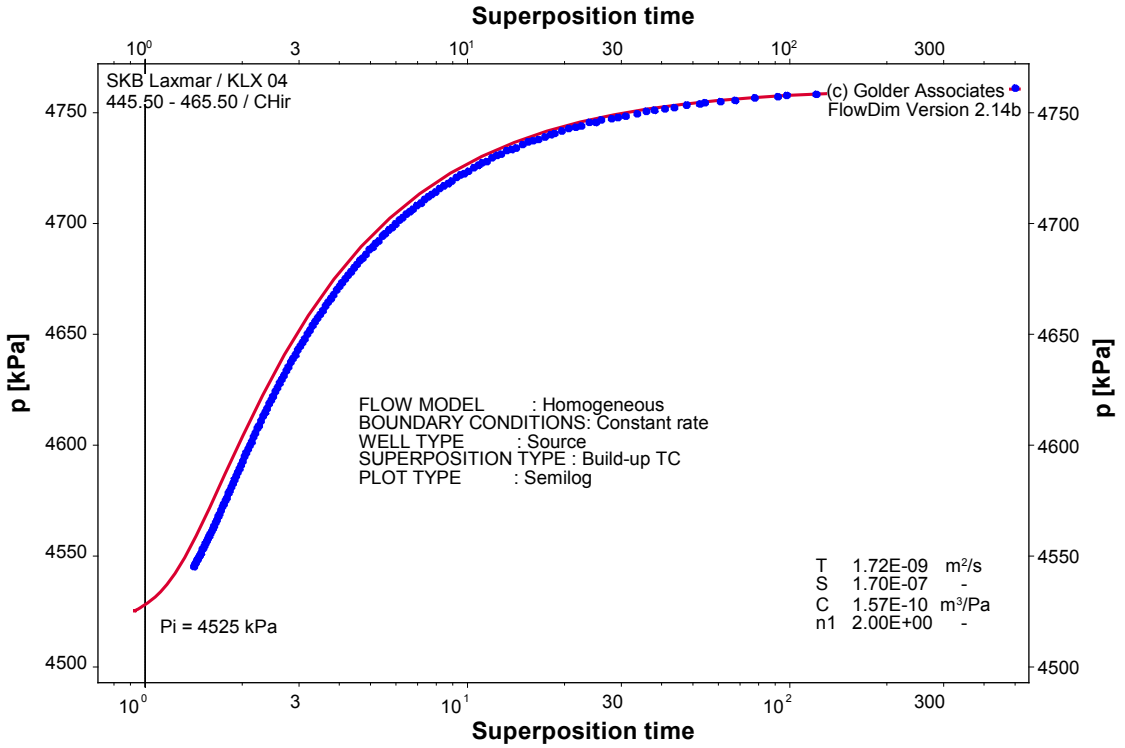

Figure 4-25. *Test 445.50–465.50 m conducted in borehole KLX04; HORNER plot with HORNER type curve of the pressure recovery phase.*

Section 4.1.2, with the difference that the pressure recovery tests are influenced by wellbore storage at early times. The wellbore storage is identified as a unit slope line in the data and derivative in the log-log plot. Figure 4-26 shows an annotated log-log diagnostic plot of test 943.05–963.05 m conducted in borehole KLX04.

Based on the diagnostic features described above, the transient response in Figure 4-26 can be described as follows:

1. During early times (elapsed time < 10^{-3} hours) a closed system behavior is indicated by the unit slope which is consistent with the wellbore storage period.
2. The transition period (10^{-3} hours < t < 10^{-2} hours) reflects the near wellbore properties and shows a decrease of storage capacity (from the wellbore storage dominated system to the formation storativity dominated system) and possibly a zone of lower transmissivity around the borehole (also known as positive skin).
3. At middle times (10^{-2} hours < t < 10^{-1} hours) the semi-log derivative is flat, indicating radial flow geometry. This is the portion of the test data that is used to derive the inner composite zone transmissivity.
4. At late times (t > 10^{-1} hours) the derivative shows an upward unit slope followed by a new stabilization, indicating the presence of a zone of lower transmissivity at some distance from the borehole. This is the portion of the test data that is used to derive the outer composite zone transmissivity.

Depending on the formation properties ”seen” by the test some of the 4 zones described above may not be present or very short, thus overlapping with other zones.

Figure 4-27 presents the case of the test 305.41–405.41 m conducted in borehole KLX04 where the semi-log derivative shows a clear stabilization indicating radial flow in a homogeneous formation.

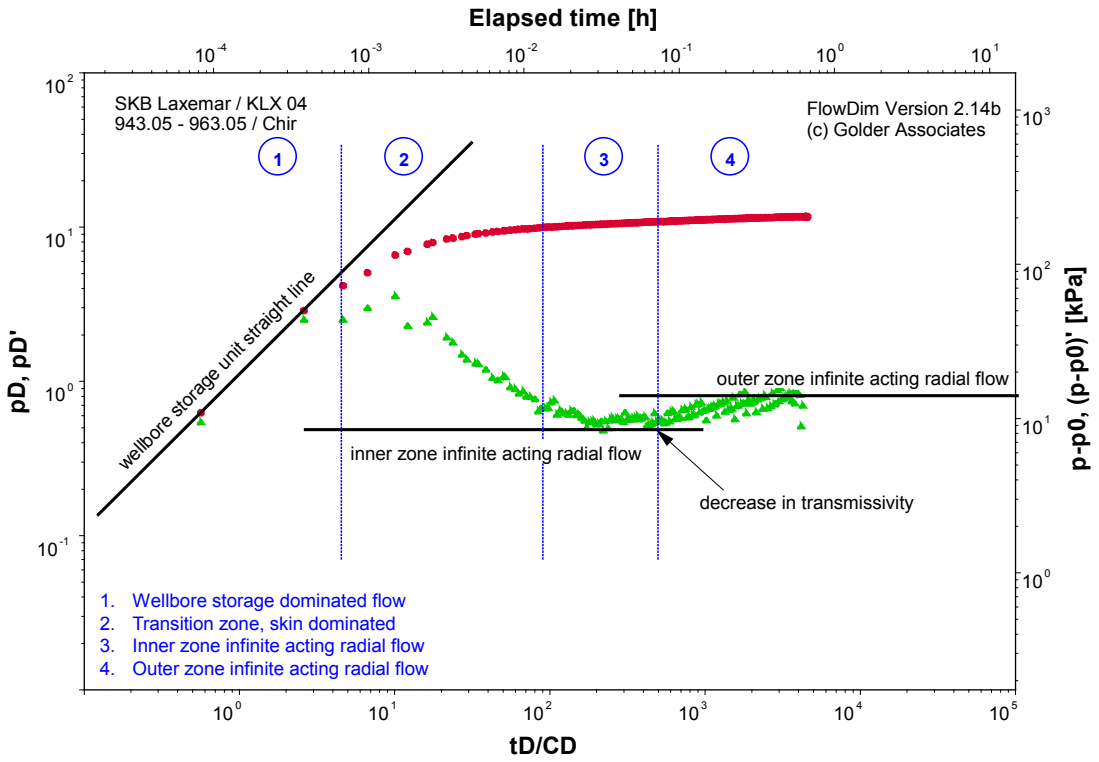

Figure 4-26. *Test 943.05–963.05 conducted in borehole KLX04; diagnostic plot of the pressure recovery phase; typical radial composite flow model with decreasing transmissivity away from the borehole.*

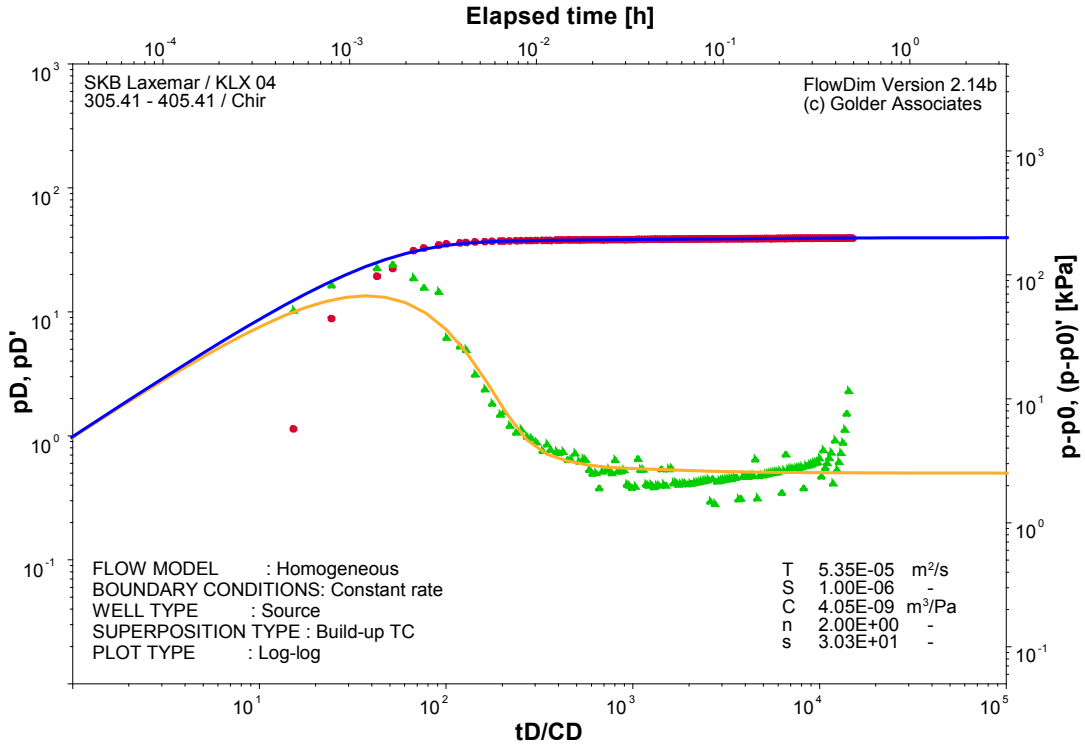

Figure 4-27. *Test 305.41–405.41 conducted in borehole KLX04; example of typical homogeneous radial flow behavior with wellbore storage and skin.*

In several cases the pressure derivative suggests a change of transmissivity with the distance from the borehole. In such cases a composite flow model was used in the analysis. Figure 4-28 presents the case of test 505.55–605.55 m conducted in borehole KLX04 where the semi-log derivative of the pressure recovery phase indicates radial flow and increasing transmissivity at some distance from the borehole.

The flow dimension displayed by the test can be diagnosed from the slope of the pressure derivative. A slope of 0.5 indicates linear flow, a slope of 0 (horizontal derivative) indicates radial flow and a slope of –0.5 indicates spherical flow. The flow dimension diagnosis was commented for each of the tests. Figure 4-29 presents an example of linear flow in the outer composite zone.

In several cases, when the transmissivity was relatively low, the tests were stopped in the skin transition phase, hence they did not achieve the infinite acting radial flow period. In such cases the derivation of formation transmissivity becomes more uncertain. As presented in Figure 4-30, in such cases the visually most probable type curve match was chosen, which inherently bares a certain degree of subjectivity.

In many cases the pressure recovered very fast indicating a large pressure loss in the vicinity of the borehole wall. This behavior is consistent with the presence of a large positive skin and could be caused by turbulent flow in fractures near the borehole. In such cases the infinite acting radial flow phase was not achieved. At late times the derivative was sloping downwards indicating a large transmissivity or the presence of a constant pressure boundary. In addition, due to the small pressure differences at late times and the relatively poor resolution of the pressure gauge (approx. 0.5 kPa) the late time derivative becomes numerically unstable, its shape being strongly sensitive to the smoothing factor. Therefore both flow model identification and the derivation of transmissivity become uncertain (see Figure 4-31).

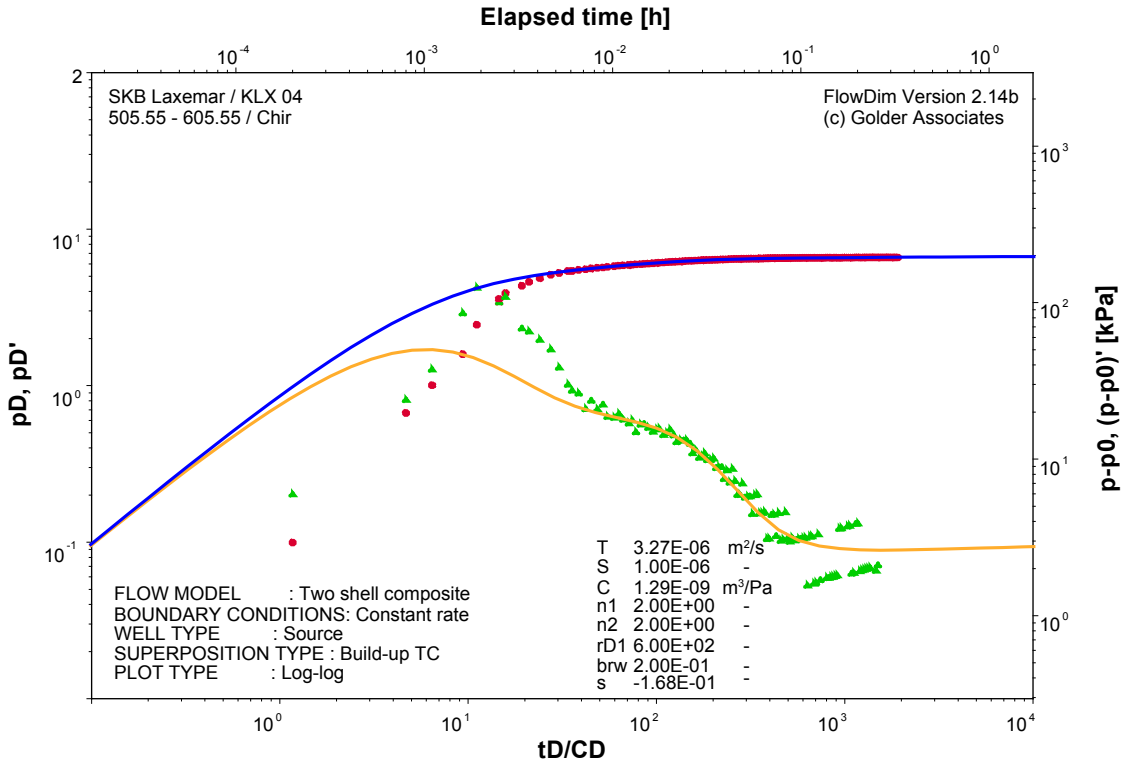

Figure 4-28. *Test 505.55–605.55 m conducted in borehole KLX04; example of typical radial flow behavior with increasing transmissivity away from the borehole (composite flow model).*

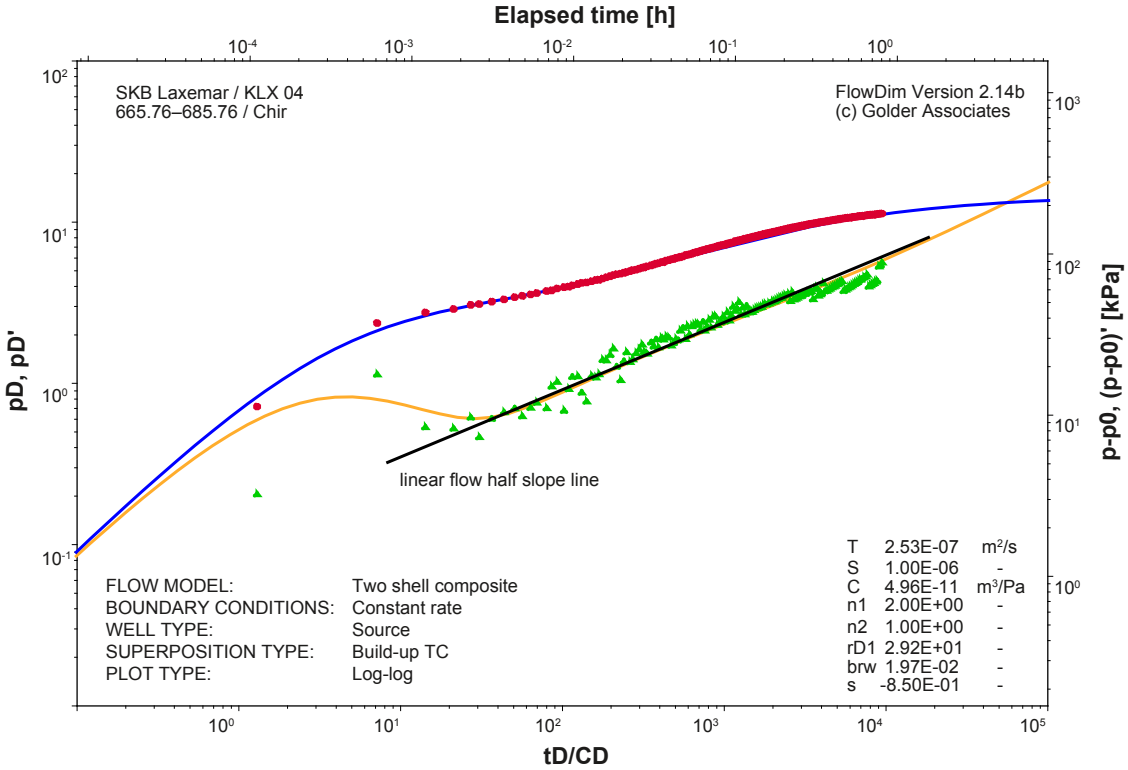

Figure 4-29. *Test 665.76–685.76 m conducted in borehole KLX04; example of linear flow in the outer composite zone.*

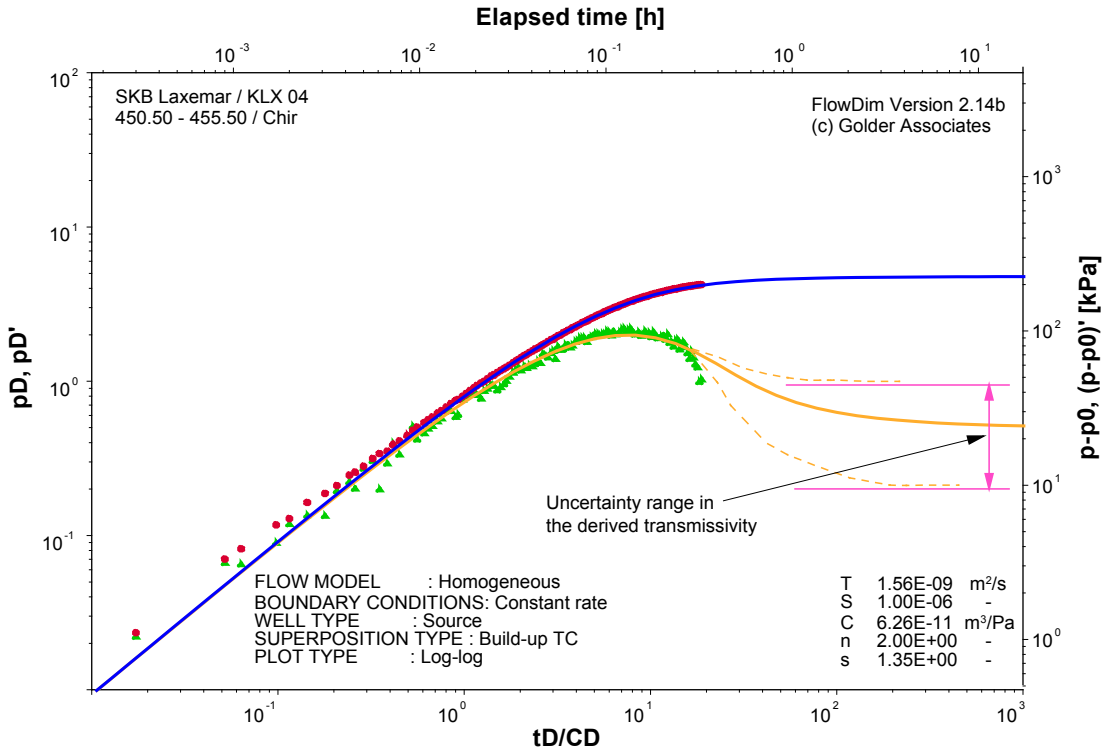

Figure 4-30. *Test 450.50–455.50 m conducted in borehole KLX04; example of uncertain flow model identification and transmissivity calculation due to short test duration.*

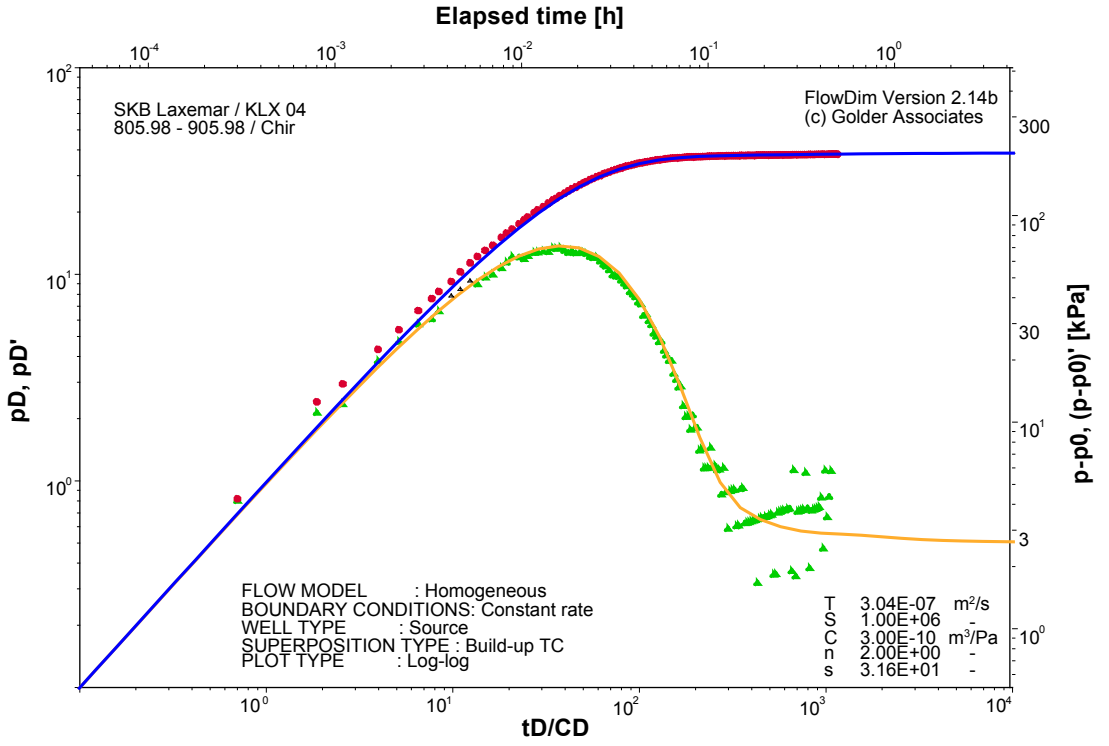

Figure 4-31. *Test 805.98–905.98 m conducted in borehole KLX04; example of fast recovery test indicating large skin; formation transmissivity uncertain.*

Finally, in cases when the test zone transmissivity was very low, the test could only detect the skin zone transmissivity and ended with an upwards sloping derivative indicating the transition to a zone of much lower transmissivity which could also be interpreted as a closed no flow boundary (see Figure 4-32).

In cases were different flow models were matching the data in comparable quality, the simplest model was preferred. For tests where a flow regime could not clearly identified from the test data, a radial flow regime was assumed in the analysis.

4.2.3 Determination of the wellbore storage coefficient

The wellbore storage coefficient quantifies the volume of fluid that the borehole (or test zone) can store when changing the pressure by one unit. This parameter is not of big interest for the characterization of the formation but it is used as a control parameter to assess how realistic the analysis is. There are several methods to derive the wellbore storage coefficient. In the following sections these methods are presented.

4.2.3.1 Determination of the wellbore storage coefficient from the type curve match

The wellbore storage coefficient is one of the parameters derived from the type curve analysis (as presented in Section 4.2.1.1, equation 4-21). As shown in this section the wellbore storage coefficient is determined from the horizontal shift of the data needed to match the model (i.e. the type curve). The wellbore storage coefficient derived from the type curve match was reported in the analysis reports as well as on the analysis plots of the pressure recovery tests.

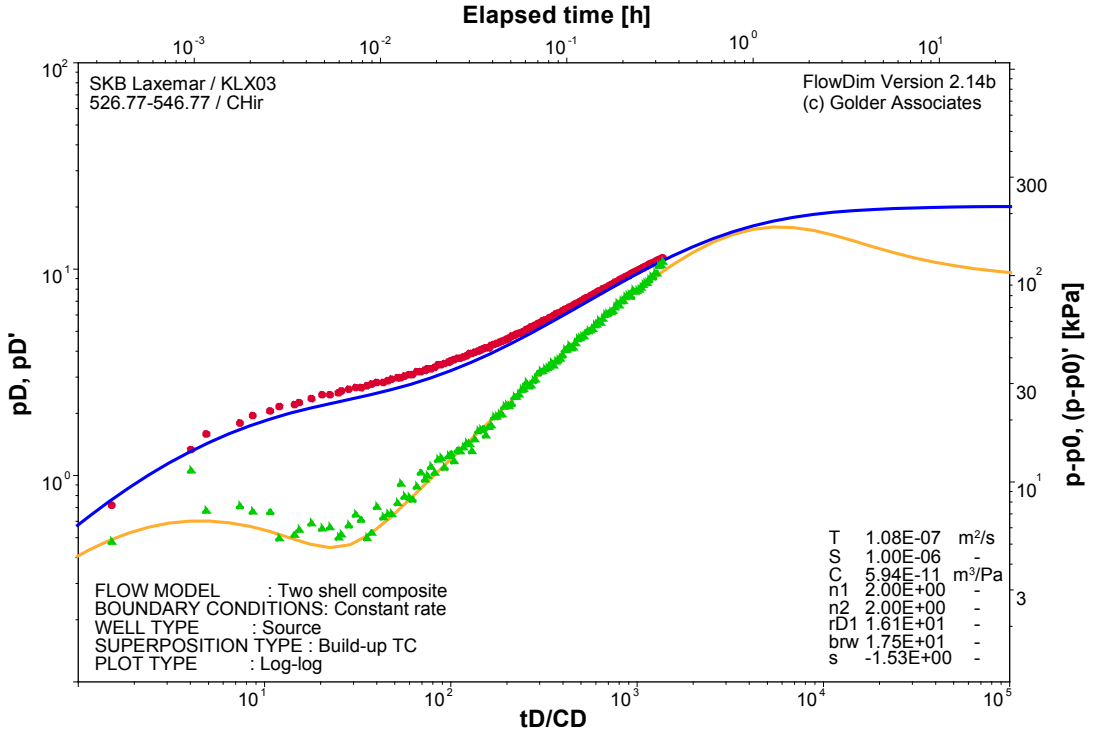

Figure 4-32. *Test 526.77–546.77 m conducted in borehole KLX03; example of closed system behavior; outer zone transmissivity uncertain.*

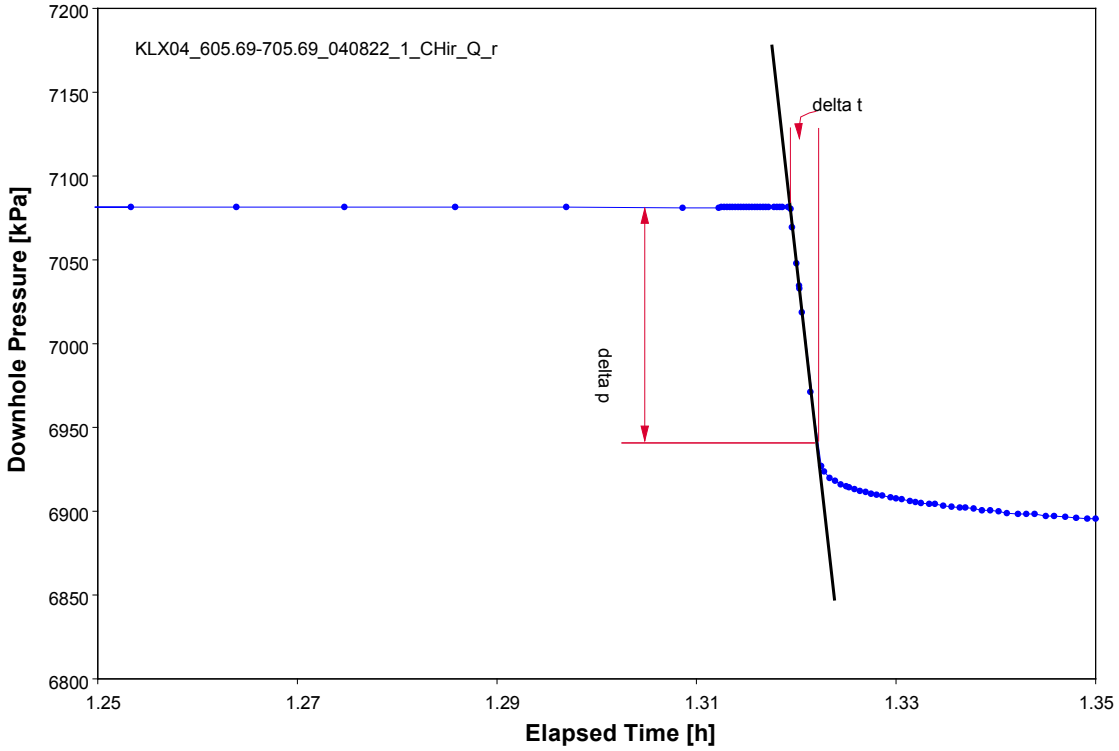

Figure 4-33. *Parameters used for the calculation of the wellbore storage coefficient from the early time pressure recovery data*

4.2.3.2 Determination of the wellbore storage coefficient from the early time recovery data

Alternatively, the wellbore storage coefficient can be calculated from the slope of the early time pressure recovery data:

$$C = \frac{q}{\frac{\Delta p}{\Delta t}} \qquad (4\text{-}27)$$

The wellbore storage coefficient was calculated for all tests conducted at the Oskarshamn site using this method as well.

4.2.3.3 Comparison with the theoretical value

The theoretical value of the wellbore storage coefficient in a closed system (i.e. downhole test valve closed) is given by the volume of the test section (V_i) and the test zone compressibility (c_{tz}):

$$C = V_i c_{tz} \qquad (4\text{-}28)$$

The test zone compressibility is calculated as the sum of the compressibilities of the individual system components: (a) water compressibility (approx. equal to 5 10^{-10} 1/Pa), (b) rock compressibility (estimated to approx. 10^{-10} 1/Pa) and (c) packer compressibility (derived from laboratory measurements to an average value of 5 10^{-11} 1/Pa). The sum of the three compressibility components is approx. 7 10^{-10} 1/Pa with the largest component being the water compressibility. The test zone volume is calculated from the test zone length and the borehole radius.

Figure 4-34 shows a comparison of for all tests conducted at the Oskarshamn site between the theoretical wellbore storage coefficient and the one determined from the type curve match and the one calculated from the early time data. We can see that the wellbore storage coefficient derived from the analysis is typically larger (by up to 3 orders of magnitude) than the theoretical value.

Figure 4-35 compares the wellbore storage coefficient derived from the type curve match with the one calculated from the early time data. We see that there is a very good correlation between the values derived using the two methods.

In conclusion, the two calculation methods for the wellbore storage coefficient show consistent results, however, these results are typically much larger than the theoretical value. The reason for this phenomenon is not clear. The hypothesis exists that the apparent large wellbore storage coefficients (i.e. test zone compressibilities) are induced by turbulent flow in fractures. This observation would be consistent with the turbulent flow model published by /Spivey et al. 2002/. Another possibility is that the increased test zone compressibility is caused by the presence of a free gas phase in the test section. However, on the one side the presence of gas was never observed during testing and on the other side relatively large gas saturations (larger than 10%) would be needed to increase the test zone compressibility by two orders of magnitude. Because of this argument we believe that the increased test zone compressibilities are not caused by gas.

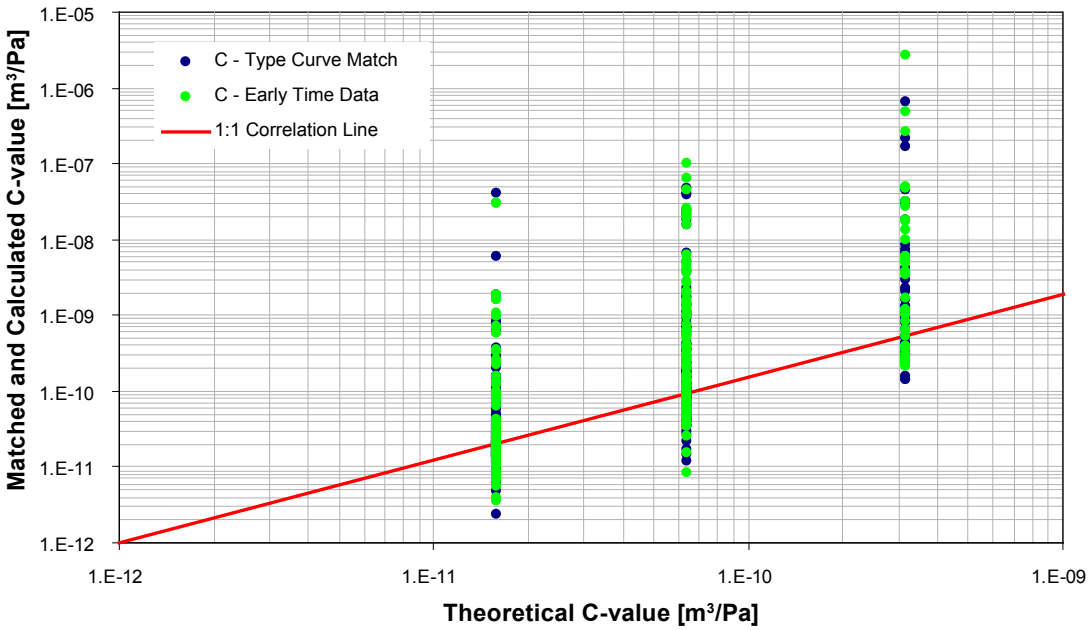

Figure 4-34. *Comparison between the theoretical wellbore storage coefficient and the one derived from the type curve match and from the early time data.*

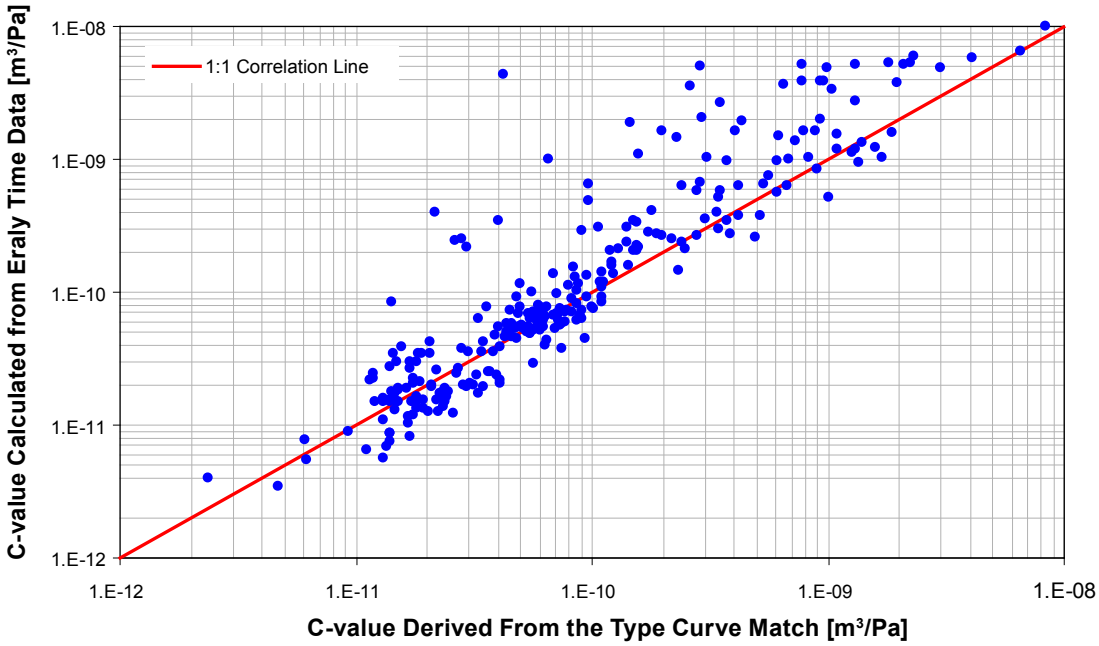

Figure 4-35. *Comparison between the wellbore storage coefficient derived from the type curve match and the one calculated from the early time data.*

4.2.4 Determination of the static formation pressure and of the equivalent freshwater head

The determination of the static formation pressure was discussed in Section 4.2.1.2 (the HORNER analysis method). As shown there, the static formation pressure (as measured at transducer depth) is derived from the HORNER plot by extrapolating the pressure recovery to infinite time:

$$\lim\left(\frac{t_p+\Delta t}{\Delta t}\right)_{\Delta t\to\infty}=1 \qquad \log(t_{HORNER})=0 \tag{4-29}$$

The extrapolation can be conducted either by using a straight line (in case the pressure recovery reached infinite acting radial flow at late times) or by using the type curve matched in log-log coordinates.

The static formation pressure (p^*) is derived from the intersection of the straight line (or type curve) with the pressure axis at the point $t_{HORNER} = 1$ or $\log(t_{HORNER}) = 0$ (for examples refer to Figure 4-24 and Figure 4-25).

The equivalent freshwater head (h_{iwf}) is defined as the position of the water table with respect to the sea level (NN), which would be equivalent with the static formation pressure derived for the respective test zone, if a body of freshwater only would be situated above the gauge. For the calculation of the equivalent freshwater head (see Figure 4-36) we define:

- The gauge depth corrected for borehole inclination – (Gd; measured in mbRP).
- The elevation of the reference point (RP), typically the top of casing (TOC) – (RP_{elev}; measured in metres above sea level).
- The atmospheric pressure - (p_{atm}; measured in Pa).
- The height of freshwater column equivalent to the extrapolated static pressure – (h_w; measured in m above corrected transducer depth).

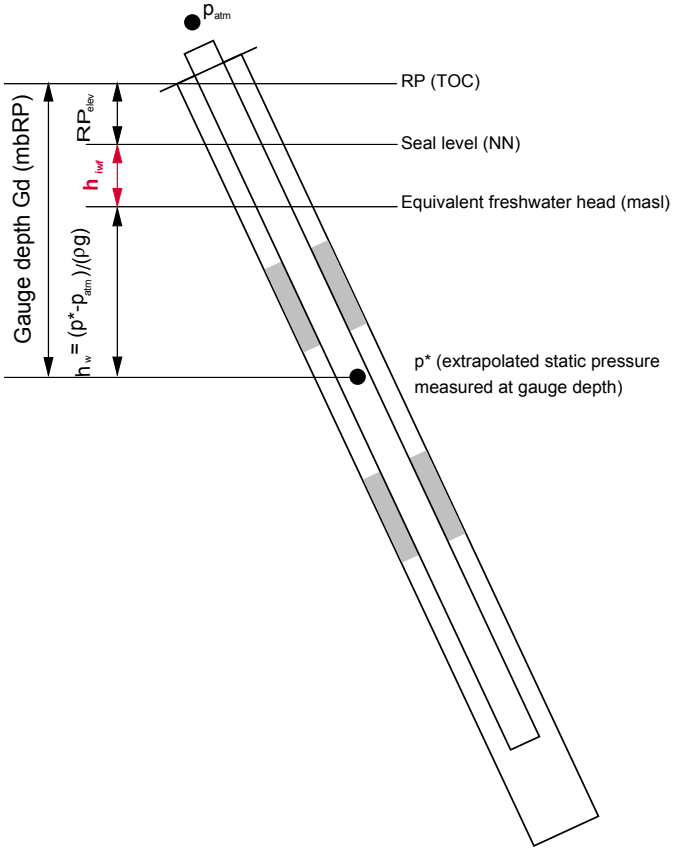

Figure 4-36. *Calculation procedure for the equivalent freshwater head.*

The height of freshwater column equivalent to the extrapolated static pressure (p^* measured in Pa) is calculated as:

$$h_w = \frac{p^* - p_{atm}}{\rho_w g} \tag{4-30}$$

The equivalent freshwater head (measured in metres above sea level) is calculated as:

$$h_{iwf} = RP_{elev} - Gd + h_w \tag{4-31}$$

4.2.5 Conducting the analysis using a prescribed storativity, deriving the skin factor

As presented in Section 4.2.1.1, the type curve analysis of pressure recovery tests allows the determination of:

- Transmissivity: from the vertical shift of the data in the log-log plot to match the type curve (Equation 4-20) and
- Wellbore storage coefficient: from the horizontal shift of the data in the log-log plot to match the type curve (Equation 4-21).

The derived wellbore storage coefficient (C) is introduced in the equation of the type curve parameter:

$$(C_D e^{2\xi})_M = \frac{C\,\rho\,g}{2\pi r_w^2\,S} e^{2\xi} \tag{4-32}$$

The equation above has two unknowns, the storativity (S) and the skin factor (ζ) which expresses the fact that for the case of constant rate and pressure recovery tests the storativity and the skin factor are 100% correlated. Therefore, the equation can only be either solved for skin by assuming that the storativity is known or solved for storativity by assuming the skin as known (typically zero).

For the tests conducted at the Oskarshamn site the storativity was assumed to be 10^{-6} for all tests conducted below the depth of 100 m.

4.2.6 Analysis example – Pressure recovery test, 943.05–963.05 m in borehole KLX04

The test 943.05–963.05 was conducted on August 31st 2004 in borehole KLX04. Figure 4-37 presents a Cartesian plot of the pressure measured in the test section and the injection rate recorded at the surface during the constant pressure injection phase preceding the pressure recovery (CHir).

The analysis of the CHir phase starts with the construction of the pressure and derivative log-log plot (Figure 4-38). The derivative starts at early times with a unit slope line indicating the influence of wellbore storage. After a transition period influenced by the dissipating wellbore storage and by the skin effect the derivatives stabilizes at approx. $2 \cdot 10^{-2}$ hours. The derivative stabilization indicates radial flow in the borehole vicinity. At middle times the derivative shows an upward slope and stabilizes at late times at a higher level. This behavior indicates decreasing transmissivity at some distance away from the borehole. Based on these observations, the test can be matched using a radial flow composite flow model with decreasing transmissivity away from the borehole.

In a second step the CHir phase is matched in log-log coordinates using a composite flow model (see Figure 4-39). The flow rate used for analysis is the last rate measured during the constant pressure injection phase (0.16 L/min). The analysis shows that the transmissivity in the borehole vicinity is $2.7 \cdot 10^{-7}$ m²/s and it decreases to $1.9 \cdot 10^{-7}$ m²/s at approx. 18 m. The skin factor was calculated to 5.2 assuming a storativity of 10^{-6}. The wellbore storage coefficient was matched to $9 \cdot 10^{-11}$ m³/Pa.

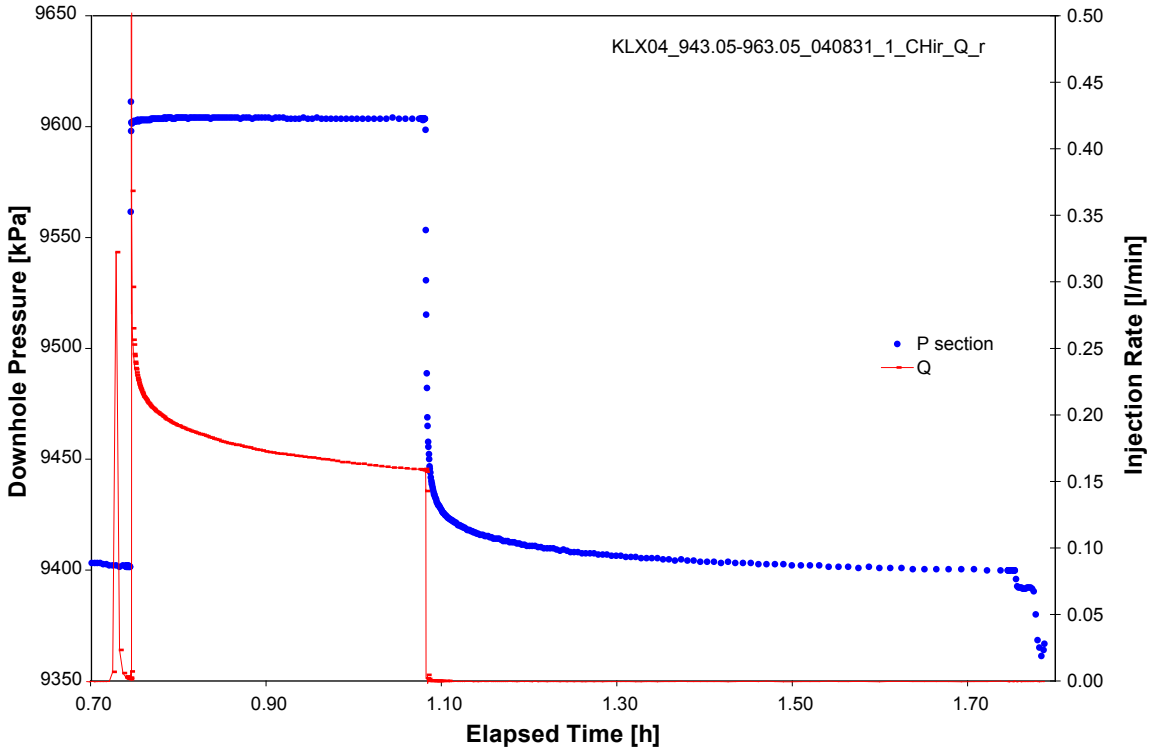

Figure 4-37. *Test 943.05–963.05 m conducted in borehole KLX04; Cartesian plot of test zone pressure and injection rate.*

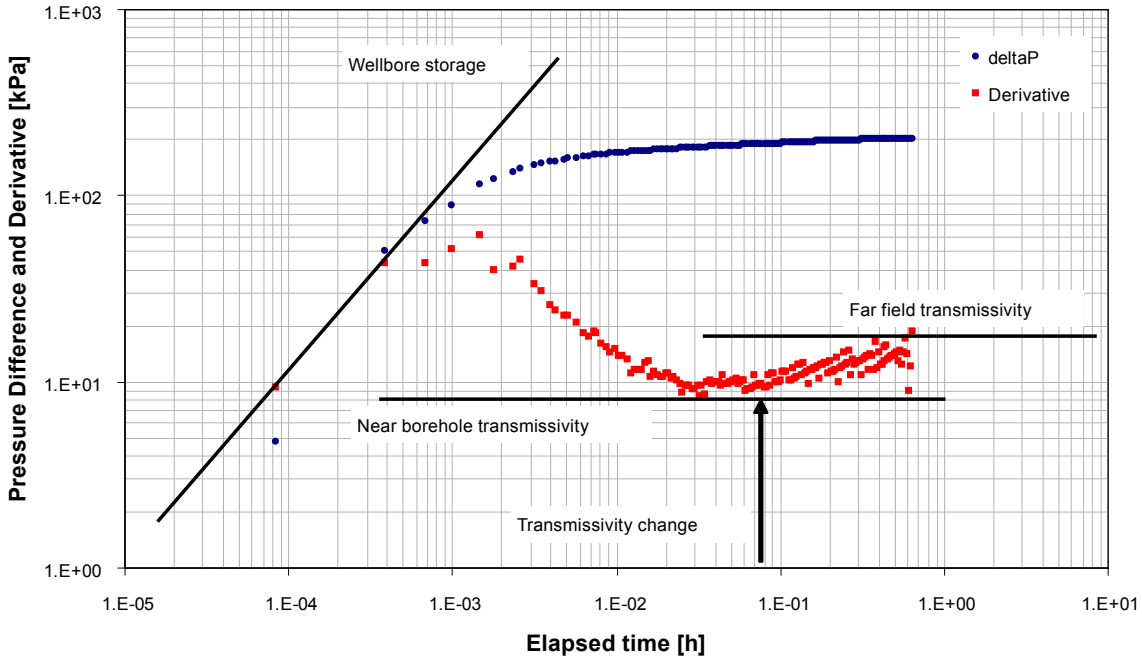

Figure 4-38. *Test 943.05–963.05 m conducted in borehole KLX04; Log-log diagnostic plot of the pressure recovery phase.*

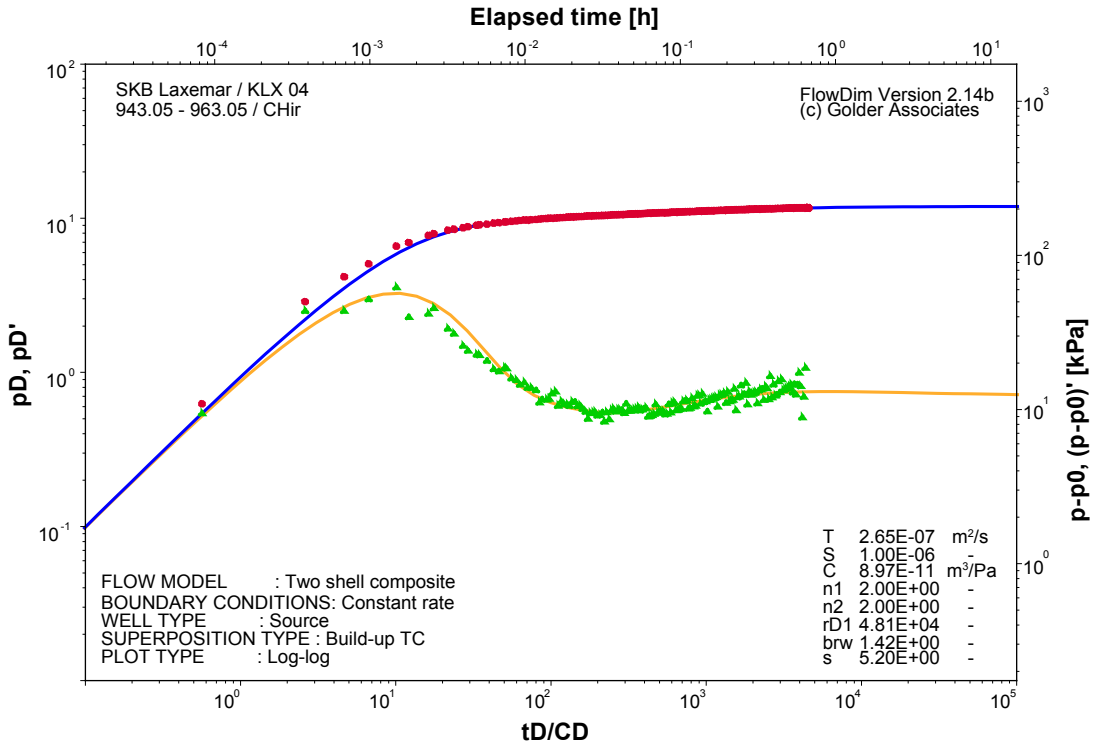

Figure 4-39. *Test 943.05–963.05 m conducted in borehole KLX04; Log-log match of the pressure recovery phase.*

The HORNER analysis is presented in Figure 4-40. Because the infinite acting radial flow period was achieved at late times, the HORNER analysis is conducted using the straight line method. From the slope of the straight line a transmissivity of $1.7 \cdot 10^{-7}$ m²/s is derived, which is consistent with the outer zone transmissivity derived from the type curve match. The static formation pressure (p^*) was extrapolated to 9,396 kPa.

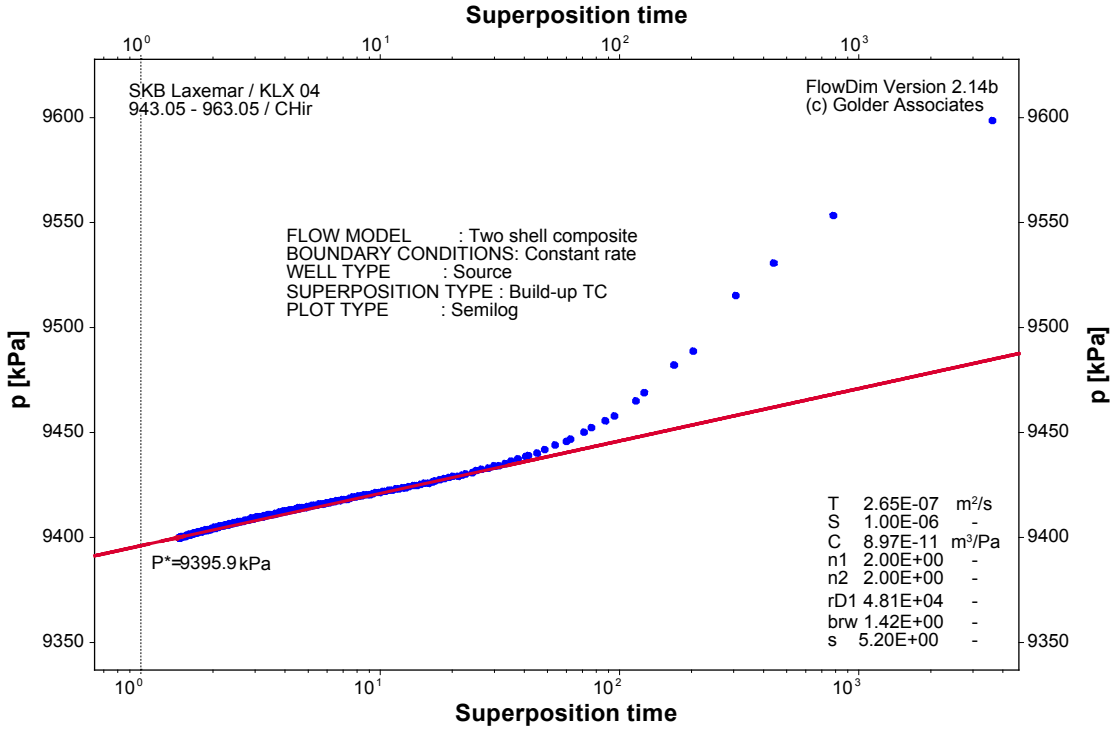

Figure 4-40. *Test 943.05–963.05 m conducted in borehole KLX04; HORNER plot of the pressure recovery phase.*

For the calculation of the equivalent freshwater head we use following input parameters:

- Reference Point elevation (RP_{elev}) = 24.09 metres above sea level.
- Gauge depth corrected for borehole inclination (Gd) = 965.71 m bRP.
- Atmospheric pressure (p_{atm}) = 100 kPa.
- Extrapolated static pressure measured at transducer depth (p^*) = 9,396 kPa.

Referring to equations 4-30 and 4-31, the height of freshwater column equivalent to the extrapolated static pressure (h_w) is calculated to 947.59 m above gauge and the equivalent freshwater head (h_{iwf}) to 14.97 m asl.

As a last step, the wellbore storage coefficient is checked for consistency:

The wellbore storage coefficient derived from the type curve analysis is $9 \cdot 10^{-11}$ m^3/Pa. The calculation of the wellbore storage coefficient from the early time data is based on equation 4-27. The input parameters and results are shown in Table 4-2.

For comparison, the theoretical value of the wellbore storage coefficient for a 20 m test zone and a borehole radius of 0.038 m is $6.4 \cdot 10^{-11}$ m^3/Pa if using a test zone compressibility of $7 \cdot 10^{-10}$ 1/Pa.

4.2.7 Uncertainties

The present section describes sources of uncertainty related to the conduction and analysis of pressure recovery tests and how these uncertainties were treated in the analysis. Examples of real test data are given whenever appropriate.

Table 4-2. Calculation of the wellbore storage coefficient from early time data (example).

Calculation of the wellbore storage coefficient				
Parameter	**Units**	**Value**	**SI units**	**Value**
Inputs				
q	L/min	0.157	m^3/s	2.62E–06
dt-start	h	8.30E–05	s	0.30
dt-end	h	3.83E–04	s	1.38
dp-start	kPa	4.76	Pa	4,760
dp-end	kPa	50.02	Pa	50,020
Outputs				
Delta-t			s	1.08
Delta-p			Pa	45,260
Flow Rate			m^3/s	2.62E–06
C			**m^3/Pa**	**6.25E–11**

4.2.7.1 Fast recovery

In many cases the pressure recovered very fast indicating a large pressure loss in the vicinity of the borehole wall. This behavior is consistent with the presence of a large positive skin and could be caused by turbulent flow in fractures near the borehole. In such cases the infinite acting radial flow phase was not achieved. At late times the derivative was sloping downwards indicating a large transmissivity or the presence of a constant pressure boundary. In addition, due to the small pressure differences at late times and the relatively poor resolution of the pressure gauge (approx. 0.5 kPa) the late time derivative becomes numerically unstable, its shape being strongly sensitive to the smoothing factor. Therefore both flow model identification and the derivation of transmissivity become uncertain (see Figure 4-41). In such cases the analysis was mainly based on the results of the preceding constant pressure injection test. The pressure recovery was analyzed to achieve maximum possible consistency with the results of the constant pressure injection test. In addition, in cases of fast recovery, the HORNER straight line analysis is expected to provide more robust results than the derivative type curve method.

4.2.7.2 Ambiguous flow model identification

In several cases, when the transmissivity was relatively low, the tests were stopped in the WBS-IARF transition phase, hence they did not achieve the infinite acting radial flow period. In such cases the derivation of formation transmissivity becomes more uncertain. As presented in Figure 4-42, in such cases the visually most probable type curve match was chosen, which inherently bares a certain degree of subjectivity.

In cases when the test zone transmissivity was very low, the test could only detect the skin zone transmissivity and ended with an upwards sloping derivative indicating the transition to a zone of much lower transmissivity which could also be interpreted as a closed no flow boundary (see Figure 4-43).

In cases were different flow models were matching the data in comparable quality, the simplest model was preferred. For tests where a flow regime could not clearly identified from the test data, a radial flow regime was assumed in the analysis.

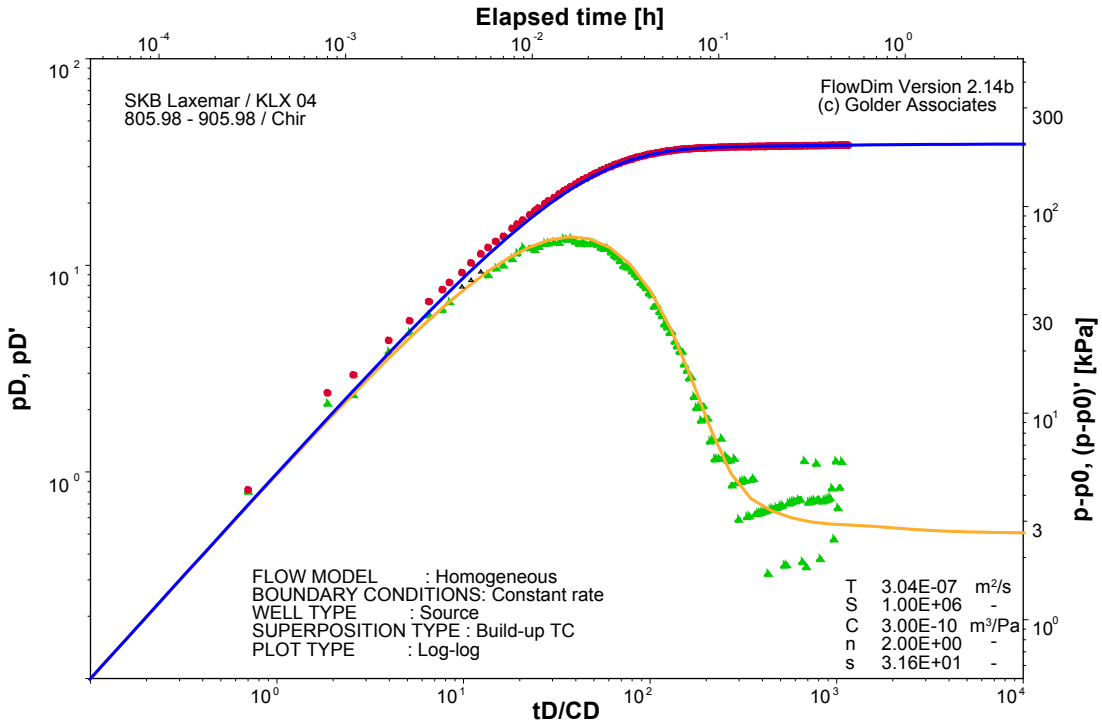

Figure 4-41. *Test 805.98–905.98 m conducted in borehole KLX04; example of fast recovery test indicating large skin; formation transmissivity uncertain.*

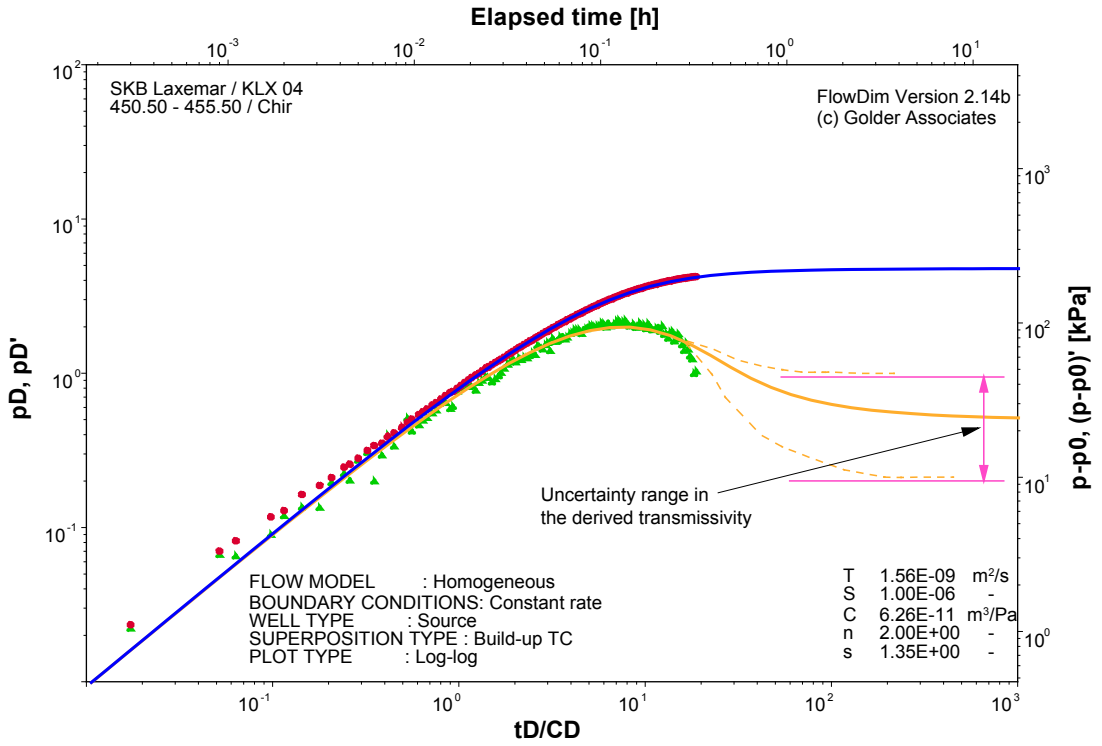

Figure 4-42. *Test 450.50–455.50 m conducted in borehole KLX04; example of uncertain flow model identification and transmissivity calculation due to short test duration.*

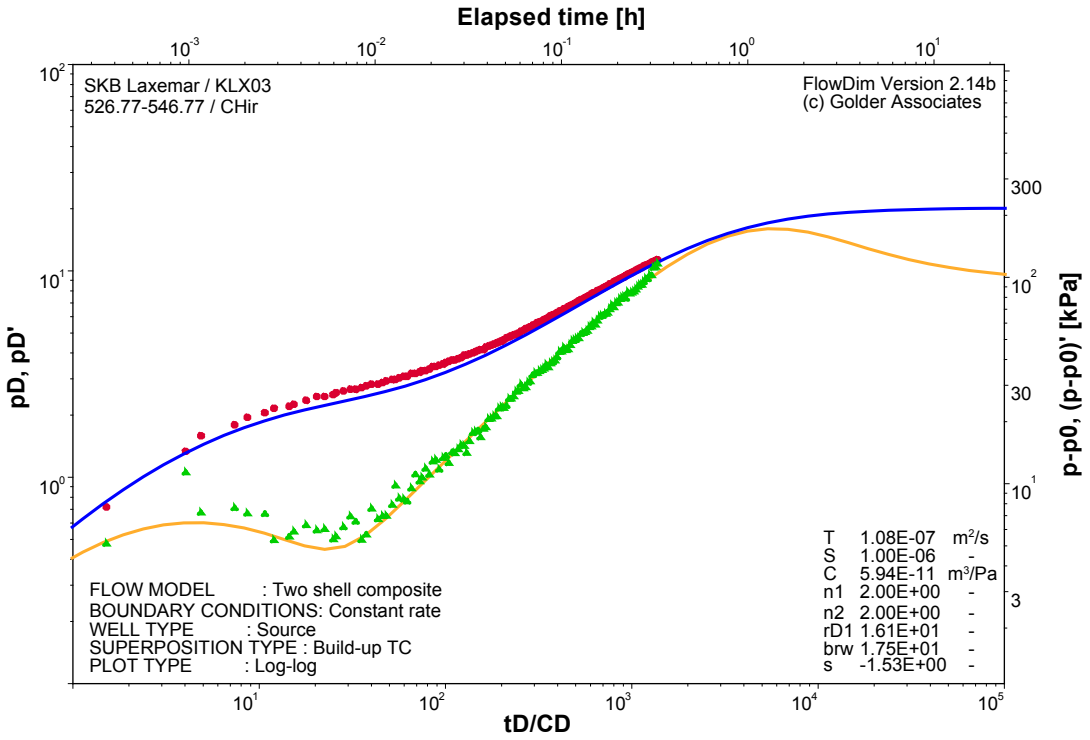

Figure 4-43. *Test 526.77–546.77 m conducted in borehole KLX03; example of closed system behavior; outer zone transmissivity uncertain.*

4.3 Analysis of pulse injection and slug injection tests (the PI and SI phase)

The tests conducted at the Oskarshamn site were always initiated as a constant pressure injection. However, in several cases after a few seconds of injection the rate quickly dropped to zero, indicating a very tight section. In such cases it was decided to close the test valve and measure the pressure recovery. The pressure recovery was analyzed as a pulse injection phase (PI).

During the brief injection phase a small volume (dV) was injected into the test zone (derived from the flowmeter measurements). This injected volume produced a pressure increase of dp. Using a dV/dp approach, the wellbore storage coefficient relevant for the subsequent pressure recovery was calculated. It should be noted though that there is large uncertainty connected with the determination of the wellbore storage coefficient (probably one order of magnitude), which implicitly translates into uncertainty in the derived transmissivity (commented further below).

Pulse tests were analyzed by using the pressure deconvolution method described by /Peres et al. 1989/ with improvements introduced by /Chakrabarty and Enachescu 1997/.

4.3.1 Brief theoretical background (deconvolution type curve analysis)

The type curve analysis method makes use of dimensionless variables, which allow calculating the flow model (i.e. the type curve) independently of the primary formation flow parameters (i.e. transmissivity and storativity) and of the wellbore storage coefficient (C) which controls the pulse or the slug test. For the analysis, the pulse (or slug) test pressure is deconvolved (p_{PR}) using the method published by /Peres et al. 1989/:

$$p_{PR}(t) = \frac{\int_0^t (p_i - p_w(t))dt}{(p_w(t) - p_0)} \qquad (4\text{-}33)$$

where p_i is the static formation pressure or the pressure in the test zone just before the pulse (or slug), p_0 is the initialization pressure of the pulse and $p_w(t)$ is the test zone pressure measured during the pulse. Note that the dimension of the deconvolved pressure (p_{PR}) is seconds.

The dimensionless pressure and dimensionless time are defined as follows:

$$p_D(t_D) = \frac{2\pi T\, p_{PR}(t)}{C \rho g} \tag{4-34}$$

$$t_D = \frac{T}{S}\frac{\Delta t}{r_w^2} \tag{4-35}$$

Since, by definition, dimensionless pressure and time are linear functions of actual deconvolved pressure and time, the logarithm of deconvolved pressure ($\log p_{PR}$) will differ from the logarithm of the dimensionless pressure ($\log p_D$; i.e. the type curve) by a constant amount:

$$\log(p_{PR}) = \log(p_D) - \log\left(\frac{2\pi T}{C \rho g}\right) \tag{4-36}$$

similarly:

$$\log(\Delta t) = \log(t_D) - \log\left(\frac{T}{S}\frac{1}{r_w^2}\right) \tag{4-37}$$

Hence a log-log graph of p_{PR} vs. Δt will have the same shape to the graph of p_D vs. t_D and the curves will be shifted vertically by $\log(2\pi T/C\rho g)$ and horizontally by $\log(T/Sr^2_w)$. Matching the two curves (data and type curve) will provide estimates of Transmissivity (T) and Storativity (S).

Note that the deconvolution process filters out the influence of wellbore storage. Therefore, the pulse (and slug) test data is matched with type curves without wellbore storage, which are in essence similar to the type curves used for the analysis of constant pressure tests. A type curve calculated for a well flowing radially in a confined and homogeneous formation is presented in Figure 4-44.

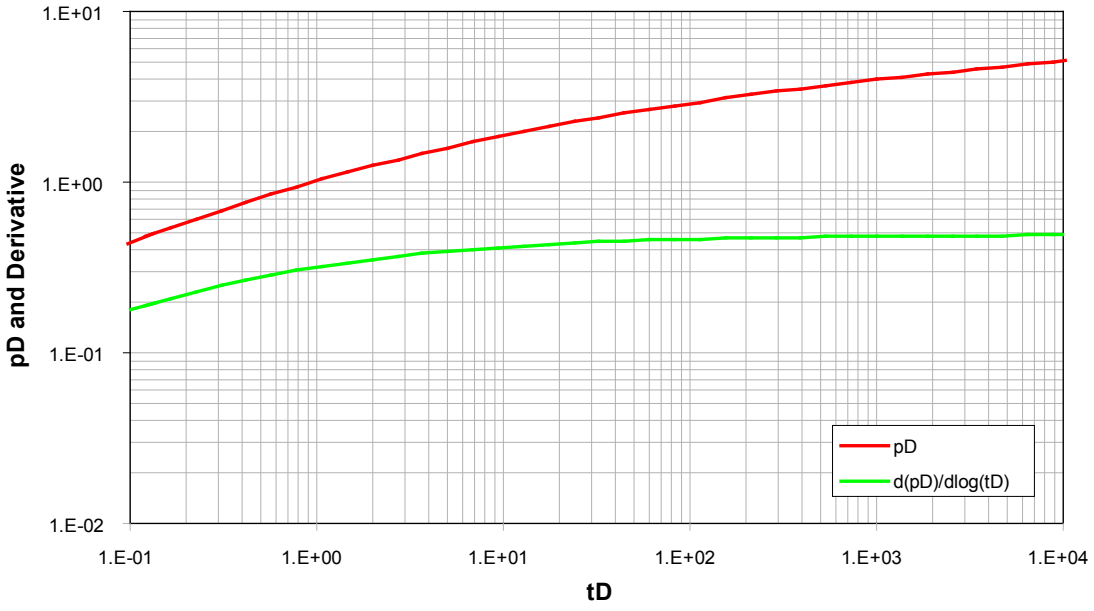

Figure 4-44. *Type curve for a well flowing radially in a confined, homogeneous formation.*

For the analysis of constant pressure tests using the type curve method, further flow models other than the radial homogeneous model have been developed. As a first extension, models are available for flow geometries other than radial (flow dimension = n=2). Flow models are developed for any dimension between linear flow (n=1), radial flow (n=2) and spherical flow (n=3). Figure 4-45 presents type curves for different flow dimensions.

A further flow model extension is the development of type curves for heterogeneous formations, where the transmissivity and/or the storativity of the formation changes at some distance from the borehole. This so called composite flow model provides the both transmissivities in the vicinity of the borehole and further away. Figure 4-46 presents a comparison showing how the type curves change when the transmissivity increases at some distance away from the wellbore.

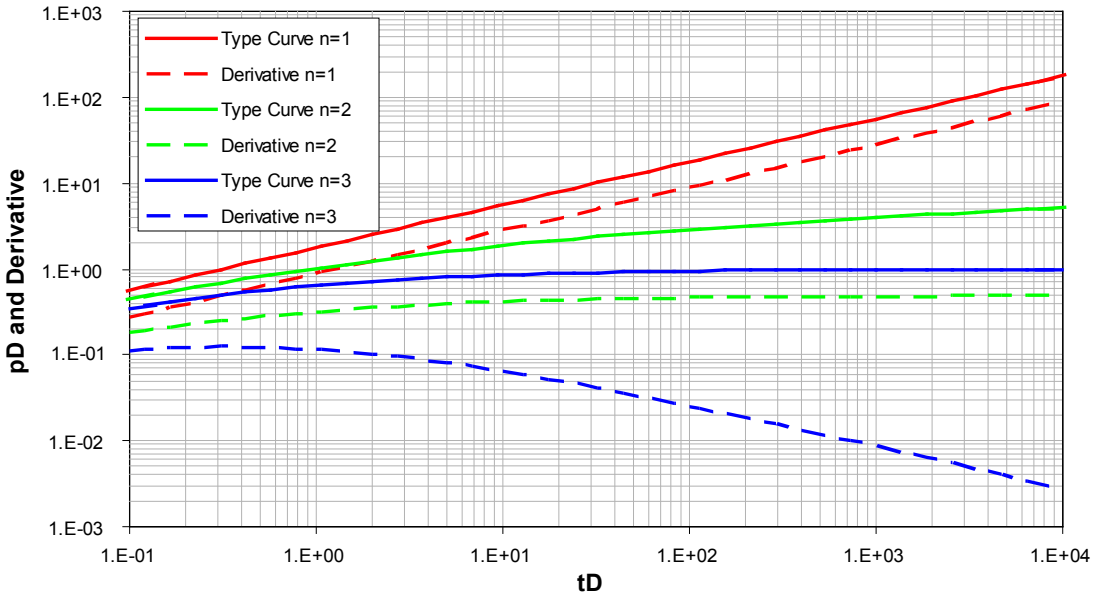

Figure 4-45. *Type curves for flow dimension of 1, 2 and 3.*

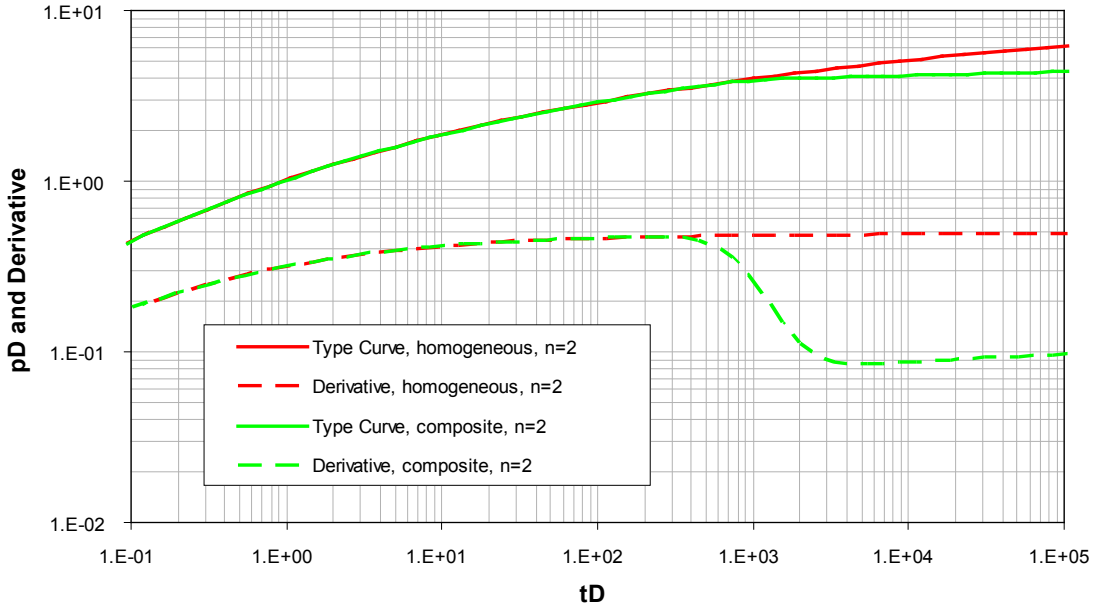

Figure 4-46. *Comparison of type curves for a homogeneous and composite flow model with increasing transmissivity away from the borehole (n=2).*

Composite flow models can be calculated for any given flow dimension, as shown in Figure 4-47.

In addition, type curves accounting for transmissivity change at the wellbore face (described as skin) have been developed. Figure 4-48 presents type curves for radial flow and different skin factors at the wellbore.

Based on the transformation equations presented above and on the type curve describing the appropriate flow model, tests with constant injection pressure can be analyzed for transmissivity, storativity, skin factor, flow dimension and any transmissivity changes away from the borehole (i.e. by using composite flow models). In cases when the early time test data is not available or too noisy due to poor test control, the storativity and the skin factor become correlated, which means that they cannot be solved independently any more. In this case as a result of the analysis

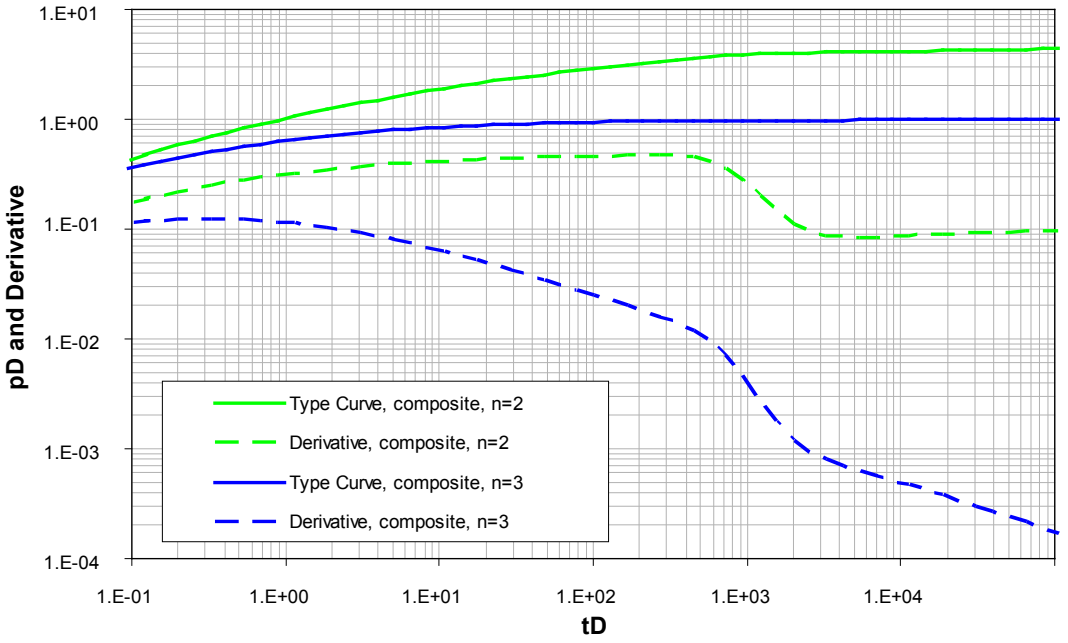

Figure 4-47. *Comparison of composite type curves for radial (n=2) and spherical flow (n=3).*

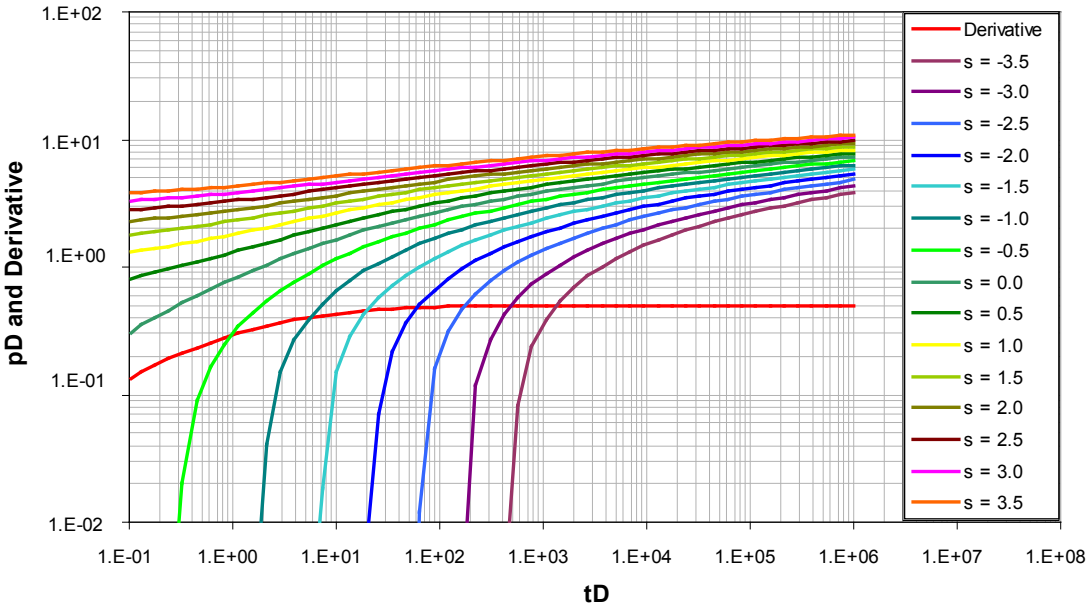

Figure 4-48. *Type curves for radial flow and different skin factors.*

one determines the correlation group $e^{2\xi}/S$. This means that in such cases the skin (ξ) can only be calculated when assuming the storativity (S) as known. In the case of the tests conducted at the Oskarshamn site the storativity was assumed to be 10^{-6} for all tests conducted below the depth of 100 m.

4.3.2 Determination of the flow model

The granite formation at the Oskarshamn site can be described from a hydraulic point of view as a sparsely connected fracture network. The matrix is expected to have extremely low conductivity and storativity, such that hydraulic interaction between fractures and matrix is not expected. Therefore, the tests conducted at Oskarshamn are expected to reveal fracture transmissivities. The derived transmissivities will reflect the properties of fractures intersecting the test zone. Also, the transmissivity may vary with the distance from the borehole to the extent further fractures are intersected. Conceptually, the flow dimension displayed by the tests can vary between linear and spherical. However, as the experience of the tests conducted so far shows, the majority of the tests display radial flow geometry.

The flow models used in analysis of pulse (or slug) tests were derived from the shape of the deconvolved pressure (p_{PR}) derivative calculated with respect to log time (also known as the semi-log derivative) and plotted in log-log coordinates. Due to the fact that the type curves used for pulse test analysis are similar to the ones used for the constant pressure injection tests, the flow model identification follows the same principles and the same patterns presented in Section 4.1.2 apply. In cases were different flow models were matching the data in comparable quality, the simplest model was preferred.

4.3.3 Measuring the wellbore storage coefficient

In the case of pulse and slug tests the wellbore storage coefficient (C) is a direct input in the analysis. From Equation 4-34 it is clear that the magnitude of the wellbore storage coefficient influences linearly the derived transmissivity. Therefore any uncertainties in the derivation of this parameter directly translate into uncertainties in transmissivity.

In the case of slug tests the wellbore storage coefficient can be directly calculated from:

$$C = \frac{\pi r_u^2}{\rho g} \tag{4-38}$$

where r_u is the inner radius of the tubing (pipe string) used for the slug test.

In the case of pulse tests the wellbore storage coefficient is calculated from:

$$C = \frac{\Delta V}{\Delta p} \tag{4-39}$$

where ΔV is the volume of fluid needed to change the test section pressure by Δp. Δp is the pressure used to initialize the pulse and is calculated from the difference between the pressure before the pulse (p_i) and the initial pulse pressure (p_0). The volume needed to initiate this pressure difference must be measured. Because of the fact that the volume involved is typically relatively small, the measurement involves errors. Following example shows the order of magnitude of the volume involved:

Assuming a borehole radius of 0.038 m and a test section length of 20 m, the test section volume (V_i) is $9.1 \cdot 10^{-2}$ m^3. Assuming a test zone compressibility (c_{tz}) of $7 \cdot 10^{-10}$ 1/Pa, the theoretical wellbore storage coefficient can be calculated from:

$$C = V_i c_{tz} \tag{4-40}$$

and is equal to 6.4 10^{-11} m^3/Pa. Assuming the pulse test was initiated with a pressure difference of 200 kPa ($2 \cdot 10^5$ Pa), the volume difference (ΔV) can be calculated from Equation 4-39 to

$1.3 \cdot 10^{-2}$ liters. This is the volume difference to be expected in the case of a pulse test conducted under the conditions described above.

Typically, the volume difference was calculated from integrating the flowmeter readings during the pulse initialization. Alternatively, when the pulse was initiated using an injection vessel with Nitrogen backpressure, the volume was derived from the water level difference in the vessel, before and after the pulse initialization. An additional source of error when applying this method stems from the fact that the volume difference (ΔV) is measured at the surface and the entire water column down to the test section is under compression.

4.3.4 Analysis example – Pulse injection test, 705.81–805.81 m in borehole KLX04

The test 705.81–805.81 was conducted on August 22nd 2004 in borehole KLX04. Figure 4-49 presents a Cartesian plot of the pressure measured in the test section and the injection rate recorded at the surface. Due to the very low transmissivity the test was conducted as pulse injection (PI). Figure 4-50 presents the early test times enlarged to better show the recorded flow rates.

From the data recorded by the flowmeter the volume difference needed to elevate the test section pressure by 230 kPa was $3.2 \cdot 10^{-2}$ L. This results in a wellbore storage coefficient of $1.4 \cdot 10^{-10}$ m^3/Pa. This value compares well to the theoretical value of $3.2 \cdot 10^{-10}$ m^3/Pa calculated based on the test section volume and a test zone compressibility of $7 \cdot 10^{-10}$ 1/Pa.

The analysis of the PI phase starts with the construction of the deconvolution pressure and derivative log-log plot (Figure 4-51). The derivative shows an initial flat portion indicating infinite acting radial flow in the borehole vicinity. At middle and late times the derivative shows an upward trend indicating decreasing transmissivity away from the borehole. The test was analyzed using a radial composite flow model with decreasing transmissivity away from the borehole. The type curve match was performed using non-linear regression.

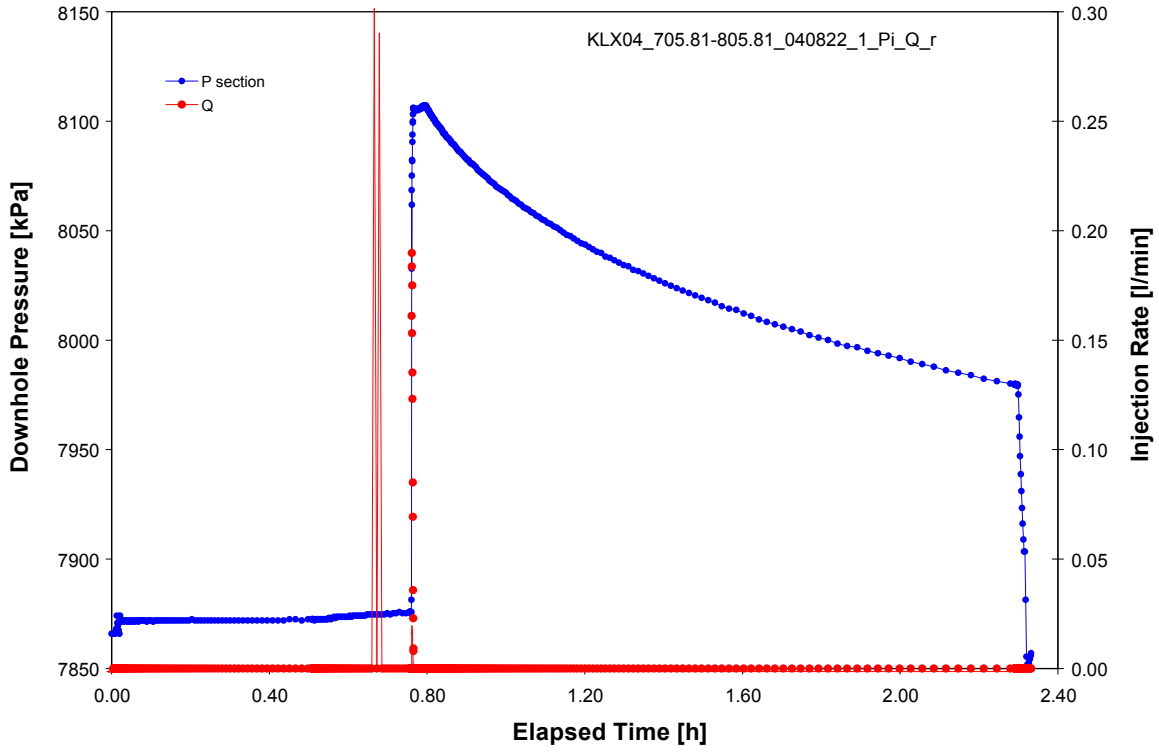

Figure 4-49. *Test 705.81–805.81 m conducted in borehole KLX04; Cartesian plot of test zone pressure and injection rate.*

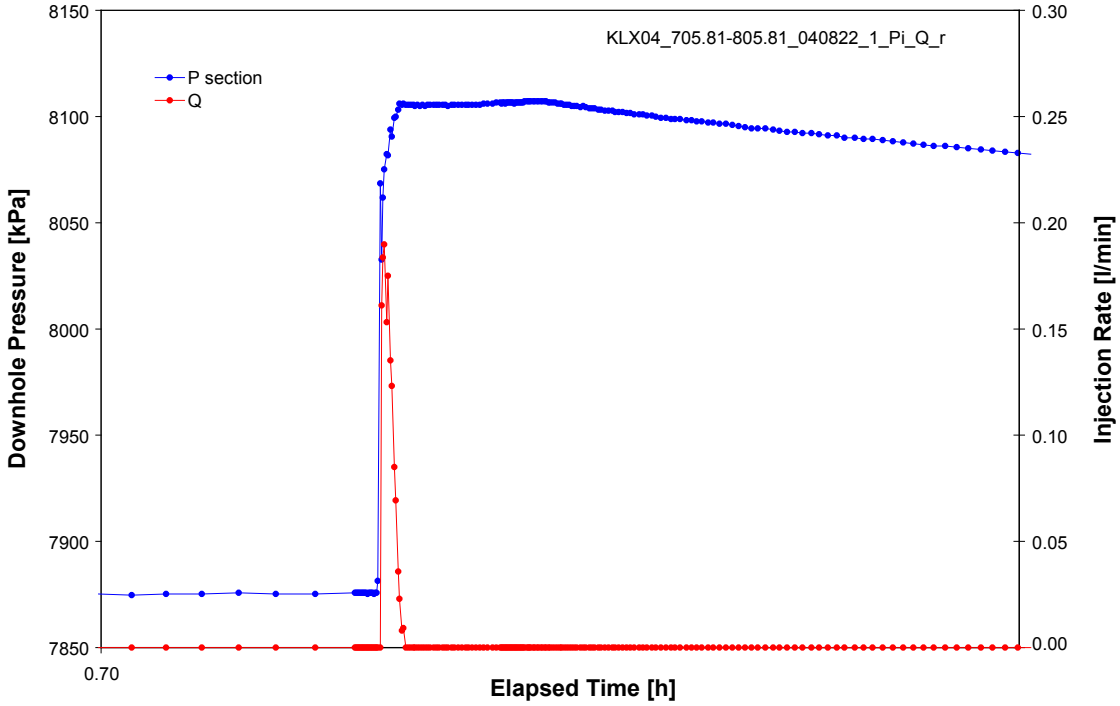

Figure 4-50. *Test 705.81–805.81 m conducted in borehole KLX04; Cartesian plot of test zone pressure and injection rate; early test times enlarged.*

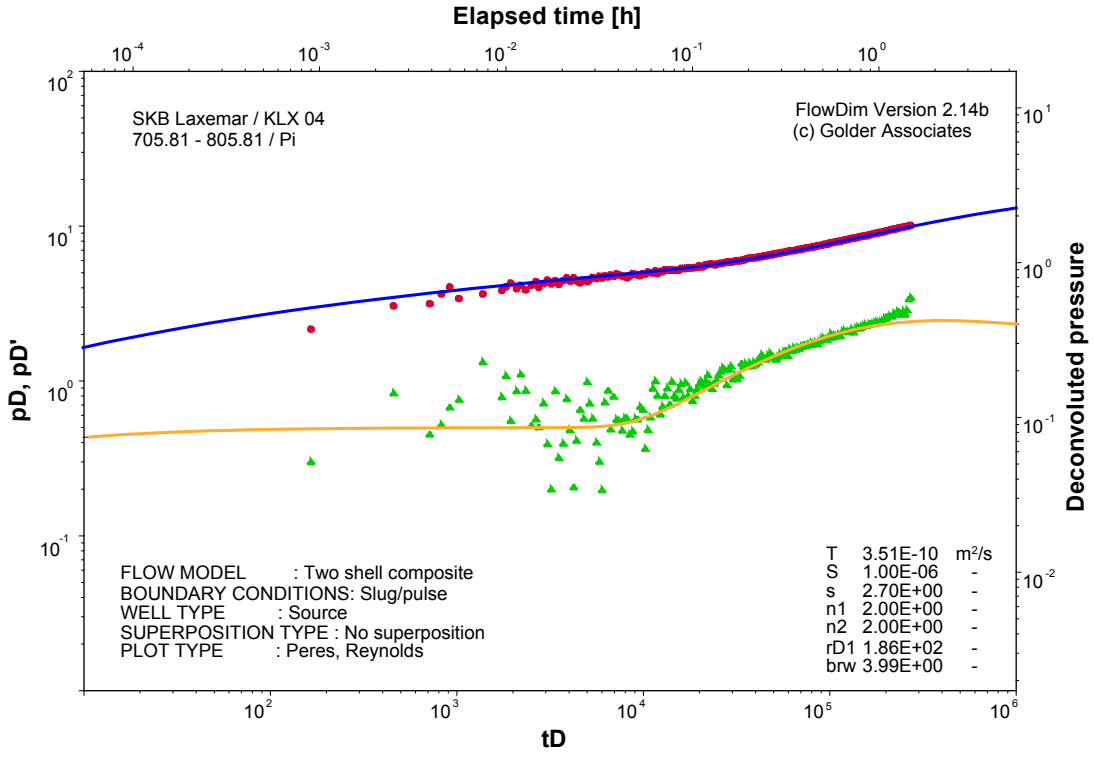

Figure 4-51. *Test 705.81–805.81 m conducted in borehole KLX04; pulse injection test; deconvolution log-log match using a composite flow model.*

The analysis shows that the transmissivity in the borehole vicinity is $3.5 \cdot 10^{-10}$ m^2/s and it decreases by a factor of 4 to $8.8 \cdot 10^{-11}$ m^2/s at approx. 0.5 m. The skin factor was calculated to 2.7 assuming a storativity of 10^{-6}. The wellbore storage coefficient was measured to $1.4 \cdot 10^{-10}$ m^3/Pa.

4.3.5 Uncertainties

The present section describes sources of uncertainty related to the conduction and analysis of pulse injection tests and how these uncertainties were treated in the analysis. Examples of real test data are given whenever appropriate.

4.3.5.1 Determination of the wellbore storage coefficient

As presented in Section 4.3.3, the wellbore storage coefficient used for the analysis of pulse tests is derived from measurements of pressure and volume change. The measurements of volume change are typically subject to relatively large measurement errors. The main source of error rests on the assumption that the entire volume change measured is due to the test zone compressibility. In reality, because the pulse is initiated with a brief (approx. 20 seconds) flowing period, some of the volume change is due to water entering the formation. This volume of water is negligible at low transmissivities (lower 10^{-10} m^2/s) but it becomes increasingly important at higher transmissivities. This means that the errors in volume measurement will generally be positive (i.e. the volume change measured will be higher than the volume change due to test zone compressibility), which leads to calculated wellbore storage coefficients higher than the actual ones.

The wellbore storage coefficient influences linearly the transmissivity derived from pulse test analysis. Hence, using a wellbore storage coefficient higher than the real one will lead to transmissivities which are higher than the actual formation transmissivity. This problem becomes relevant at higher transmissivities.

The consistency of the wellbore storage coefficient used for analysis is controlled against values derived from other sources:

- The theoretical wellbore storage coefficient derived from the theoretical value of the test zone compressibility (described in Section 4.2.3.3); this value can be regarded as a lower limit of the actual wellbore storage coefficient.
- The wellbore storage coefficient derived from the analysis of the CHir phase; this value can be regarded as an upper limit of the actual wellbore storage coefficient.

By deriving confidence limits for the wellbore storage coefficient, the formation transmissivity derived from a pulse test can be constrained.

4.4 Derivation of recommended values and confidence ranges

In most of the cases more than one analysis was conducted on a specific test. Typically both test phases were analyzed (CHi and CHir) and in some cases the CHi or the CHir phase was analyzed using two different flow models. The parameter sets (i.e. transmissivities) derived from the individual analyses of a specific test usually differ. In the case when the differences are small (which is typically the case) the recommended transmissivity value is chosen from the test phase that shows the best data and derivative quality.

In cases when the difference in results of the individual analyses was large (more than half order of magnitude) the test phases were compared and the phase showing the best derivative quality was selected.

The confidence range of the transmissivity was derived using expert judgment. Factors considered were the range of transmissivities derived from the individual analyses of the test as well as additional sources of uncertainty such as noise in the flow rate measurement, numeric effects in the calculation of the derivative or possible errors in the measurement of the wellbore storage coefficient. No statistical calculations were performed to derive the confidence range of transmissivity.

In cases when changing transmissivity with distance from the borehole (composite model) was diagnosed, the inner zone transmissivity (in borehole vicinity) was recommended. This is consistence with SKB's standards.

In cases when the infinite acting radial flow (IARF) phase was not supported by the data the additional uncertainty was accounted for in the estimation of the transmissivity confidence ranges.

While the recommended transmissivity was derived using type curve analysis methods, the confidence range of transmissivity was derived from the comparison of the analysis results of the two phases. In many cases Transmissivity Normalized Plots (TNP) were used to compare the derivatives of the two test phases in a normalized fashion. This way the amount of uncertainty was derived graphically as presented in the following sections.

4.4.1 The use of normalized plots to check consistency between different test phases

The theory of the Transmissivity Normalized Plot (TNP) method is documented in /Enachescu et al. 2004/. The semi-log derivative data of different tests or test phases is normalized with regard to the controlling inner boundary condition and translated to units of radial flow equivalent transmissivity. The result is a Transmissivity Normalized Plot (Figure 4-52) that displays transmissivity versus time in log-log scale. For the case when the test displays infinite acting radial flow (flat derivative), the transmissivity can be derived from the y-axis coordinate of the flat portion of the derivative displayed on the TNP. The inclined grid on the plot represents lines of iso-distance. Using these lines the analyst can estimate the radius of influence of the test as well as distances where formation properties (e.g. transmissivity) change. The lines of iso-distance are calculated assuming a constant and known storativity. The red inclined line represents the borehole wall. The position of the borehole wall on the graph is given by the wellbore storage coefficient. The test derivative (green markers) shows that the test starts with a wellbore storage phase (along the borehole wall) and gradually enters the formation. The test zone transmissivity can be derived from the flat portion of the derivative (Infinite Acting Radial Flow period).

In the following, different tests are presented in order to exemplify cases of consistency and inconsistency between the individual test phases and show how the recommended transmissivity and the transmissivity confidence range are derived by using the TNP method.

4.4.1.1 Consistent test behaviour

Test 304 m to 324 m in borehole KLX02 (Figure 4-53) is an example of consistent test behavior resulting in a clear transmissivity estimation and a relatively narrow transmissivity confidence range. As shown in Figure 4-53, the late time derivatives of both test phases (Chi and CHir) converge in a flat line indicating radial flow. The transmissivity can be derived from the Y-axis coordinate of the flat portion of the derivatives to $3 \cdot 10^{-5}$ m²/s. The width of the transmissivity confidence range is in this case mainly given by the numerical noise in the derivative.

We also see that the near borehole transmissivity is smaller than the transmissivity of the undisturbed formation, which is consistent with a positive skin. Further, we can see a discrepancy between the theoretical wellbore storage (represented by the position of the solid red line in the plot) and the matched wellbore storage coefficient (dotted red line). In this case the matched wellbore storage coefficient is larger than the theoretical value.

4.4.1.2 Consistent test behaviour; unclear radial flow stabilization

Test 304 m to 324 m in borehole KLX02 (Figure 4-54) is an example of consistent test behavior but displaying unclear radial flow stabilization. As shown in Figure 4-54, the two test phases (Chi and CHir) show very consistent behavior, however, the late time derivatives do not show clear stabilization. Moreover, the level of the stabilization is sensitive to the degree of smoothing of the derivative, thus adding to the uncertainty. It is also not clear whether the incipient

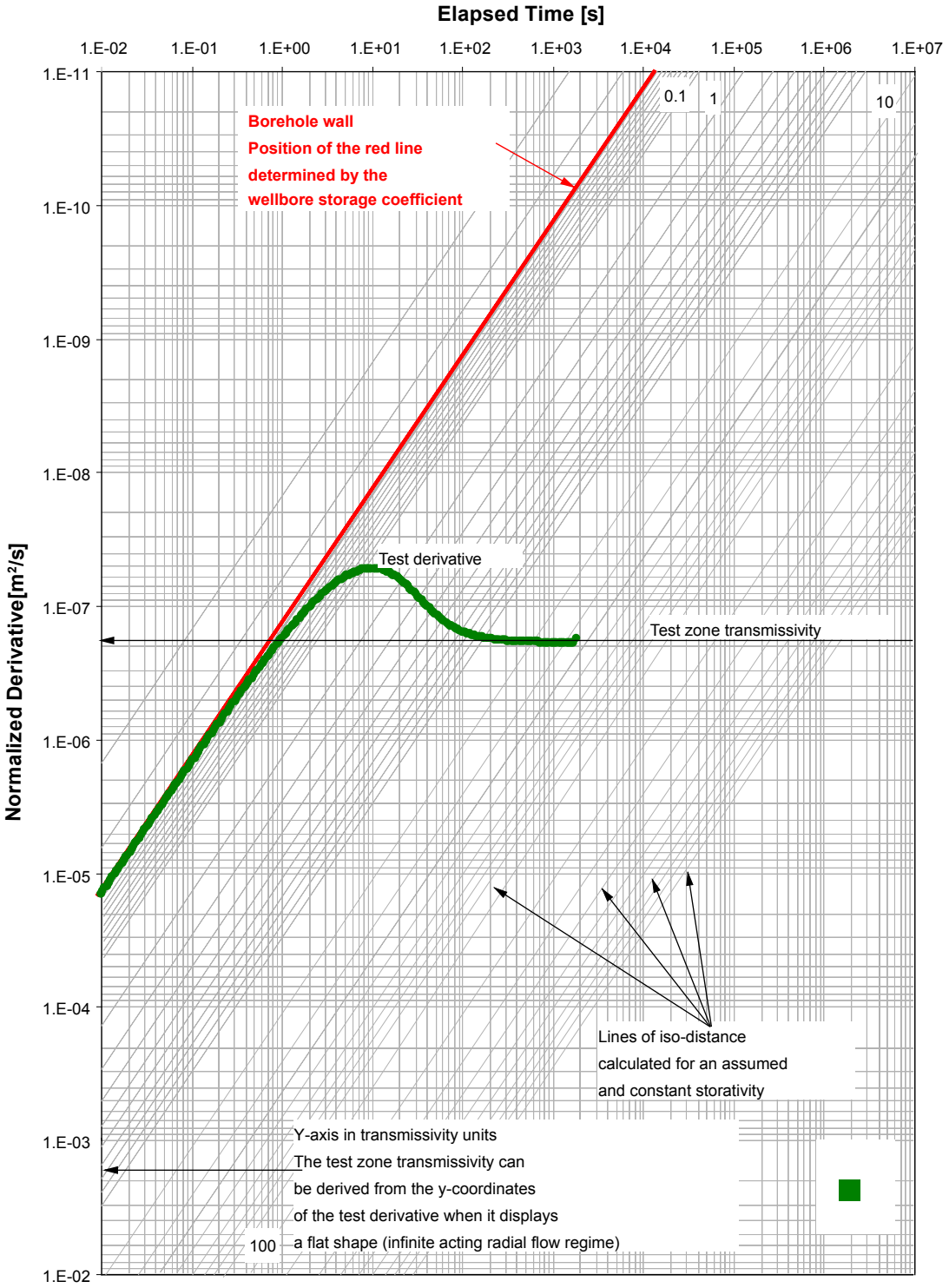

Figure 4-52. *Generic example of a Transmissivity Normalized Plot (TNP).*

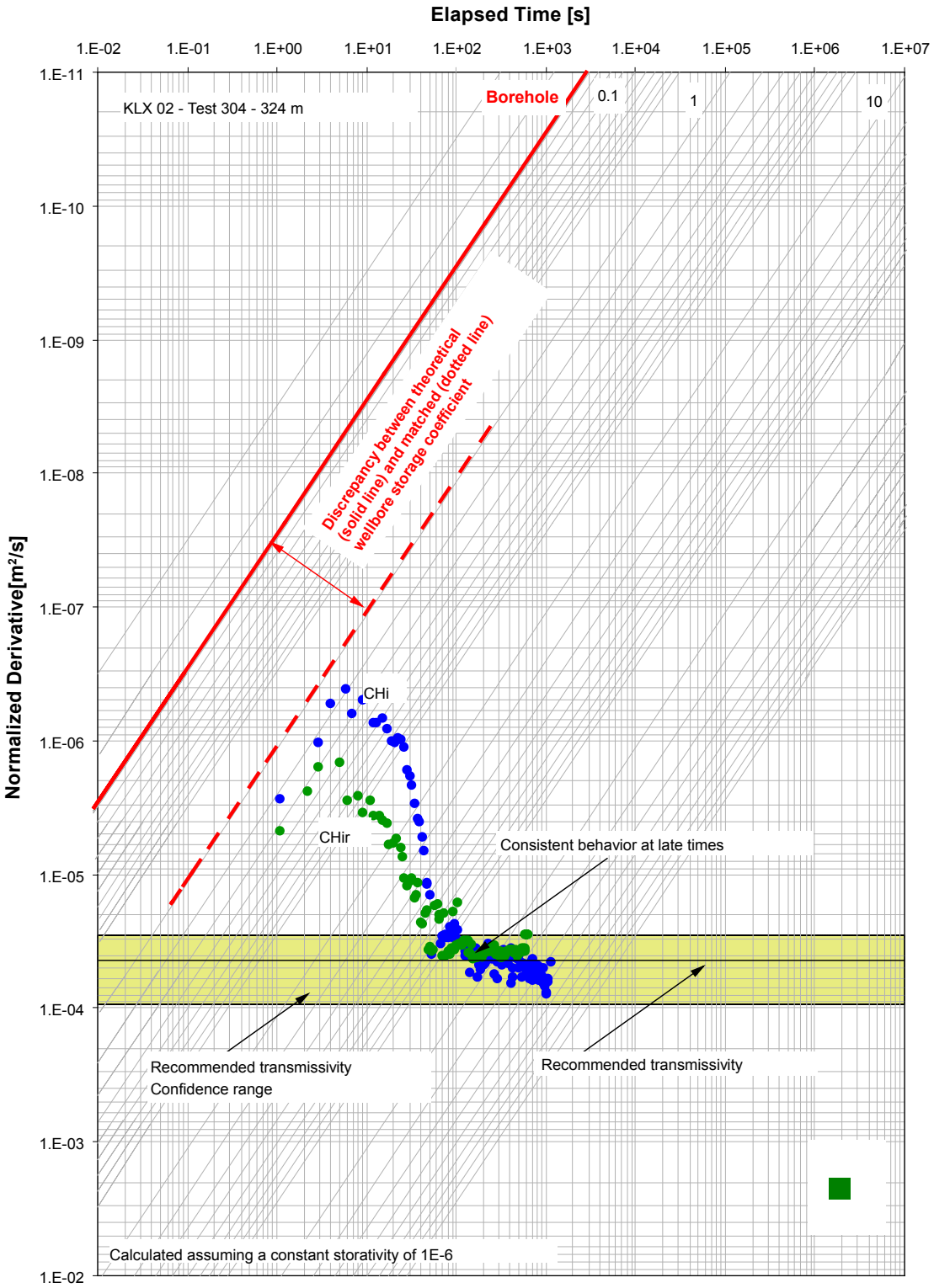

Figure 4-53. *TNP example of consistent test behaviour; Test 304–324 m in borehole KLX02.*

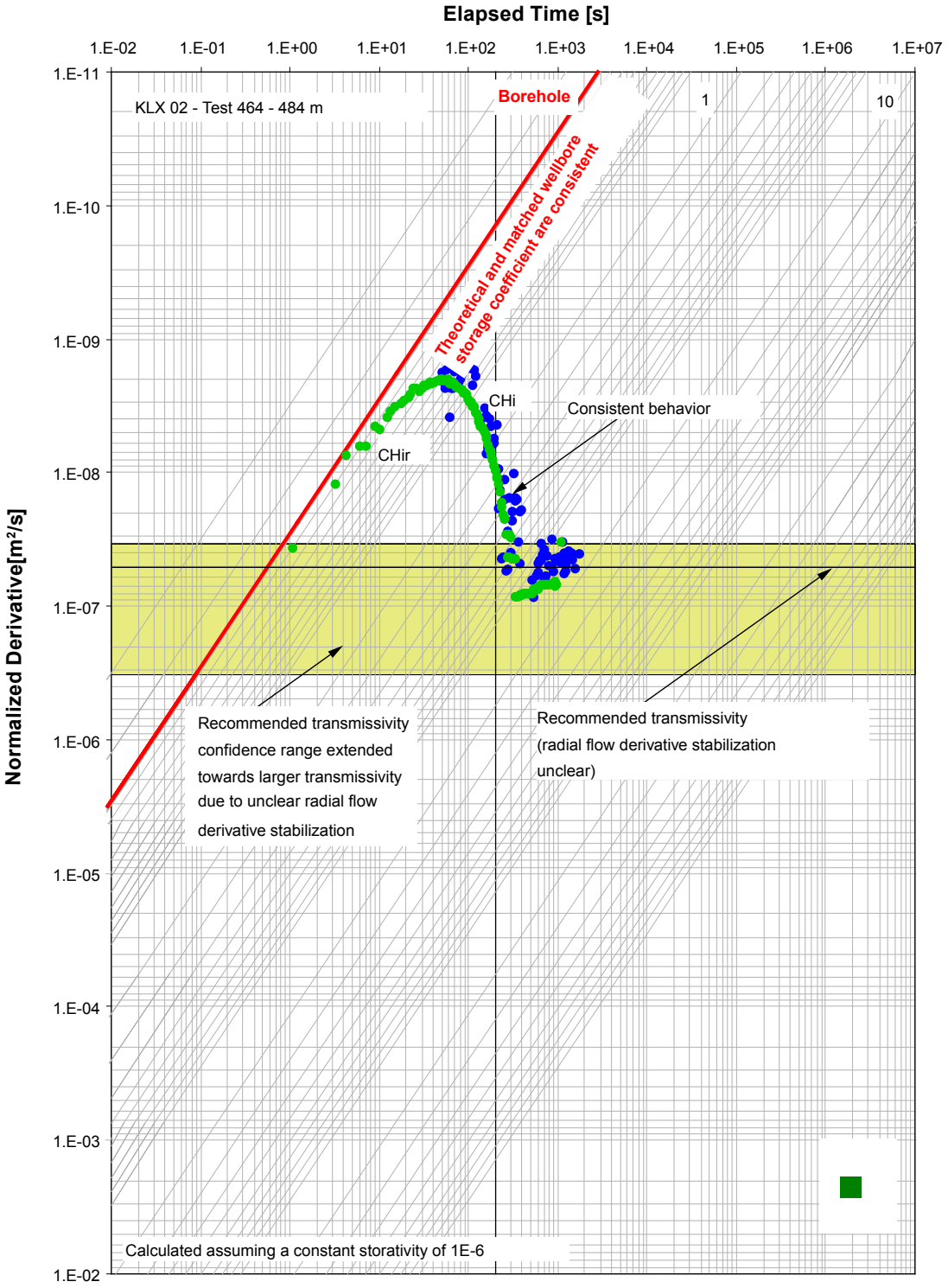

Figure 4-54. *TNP example of consistent test behaviour; unclear radial flow stabilization; Test 464–484 m in borehole KLX02.*

stabilization shown in the plot is real or just a numerical effect. Following from this, the actual test zone transmissivity may be larger than the one suggested by the plot, this being reflected in the transmissivity confidence range extended towards larger values.

We also see that the near borehole transmissivity is smaller than the transmissivity of the undisturbed formation, which is consistent with a positive skin. Further, we can see good consistency between the theoretical wellbore storage (represented by the position of the solid red line in the plot) and the wellbore storage coefficient implied by the data.

4.4.1.3 Inconsistent test behaviour; unclear radial flow stabilization

Test 724 m to 744 m in borehole KLX02 (Figure 4-55) is an example of inconsistent test behavior displaying unclear radial flow stabilization. As shown in Figure 4-55, the two test phases (Chi and CHir) show inconsistent behavior. They both show a downward trend at late times but the two derivatives are shifted in time. The reason for this behavior is unknown. Also, none of the two phases shows a clear radial flow stabilization, thus adding to the uncertainty. In this case, the recommended transmissivity was taken from the late tome CHi data. The transmissivity confidence range was extended towards lower transmissivities due to the unclear radial flow stabilization of the CHir phase.

We also see that the near borehole transmissivity is smaller than the transmissivity of the undisturbed formation, which is consistent with a positive skin. Further, we can see a discrepancy between the theoretical wellbore storage (represented by the position of the solid red line in the plot) and the matched wellbore storage coefficient (dotted red line). The matched wellbore storage coefficient is larger than the theoretical value.

4.4.1.4 Consistent test behaviour; decreasing transmissivity away from the borehole

Test 515 m to 520 m in borehole KLX02 (Figure 4-56) is an example of consistent test behavior displaying decreasing transmissivity away from the borehole (composite flow model). As shown in Figure 4-56, the two test phases (Chi and CHir) show very consistent behavior. The test derivatives show a first stabilization at middle times followed by a unit slope upward trend and the beginning of a second stabilization at late times. The level of the first stabilization was used to derive the recommended transmissivity value. The outer zone transmissivity is indicated in the graph as well. The transmissivity is well constrained, which is reflected in a relatively narrow transmissivity confidence range.

Further, we can see good consistency between the theoretical wellbore storage (represented by the position of the solid red line in the plot) and the wellbore storage coefficient implied by the data.

4.4.2 Other consistency checks

In addition to the analyses described above, the results were validated by checking weather the wellbore storage coefficient and the skin factor fall within certain expected ranges constrained by the test configuration, rock conditions and experience from similar tests.

The wellbore storage coefficient derived from the type curve match was compared with the value derived from the early time CHir data and with the theoretical value derived from laboratory measurements. As presented in Figure 4-34 and Figure 4-35 there was good agreement between the type curve derived wellbore storage and the value derived from the CHir early times. However, both values were typically larger (up to three orders of magnitude) than the theoretical value. This is believed to be caused by turbulent flow in fracture at the interface between borehole and formation. This hypothesis is supported by the publication of /Spivey et al. 2002/.

The skin factors derived from the analysis (especially from the analysis of the CHir phase) were sometimes very large (up to 30), which also suggests the presence of turbulent flow.

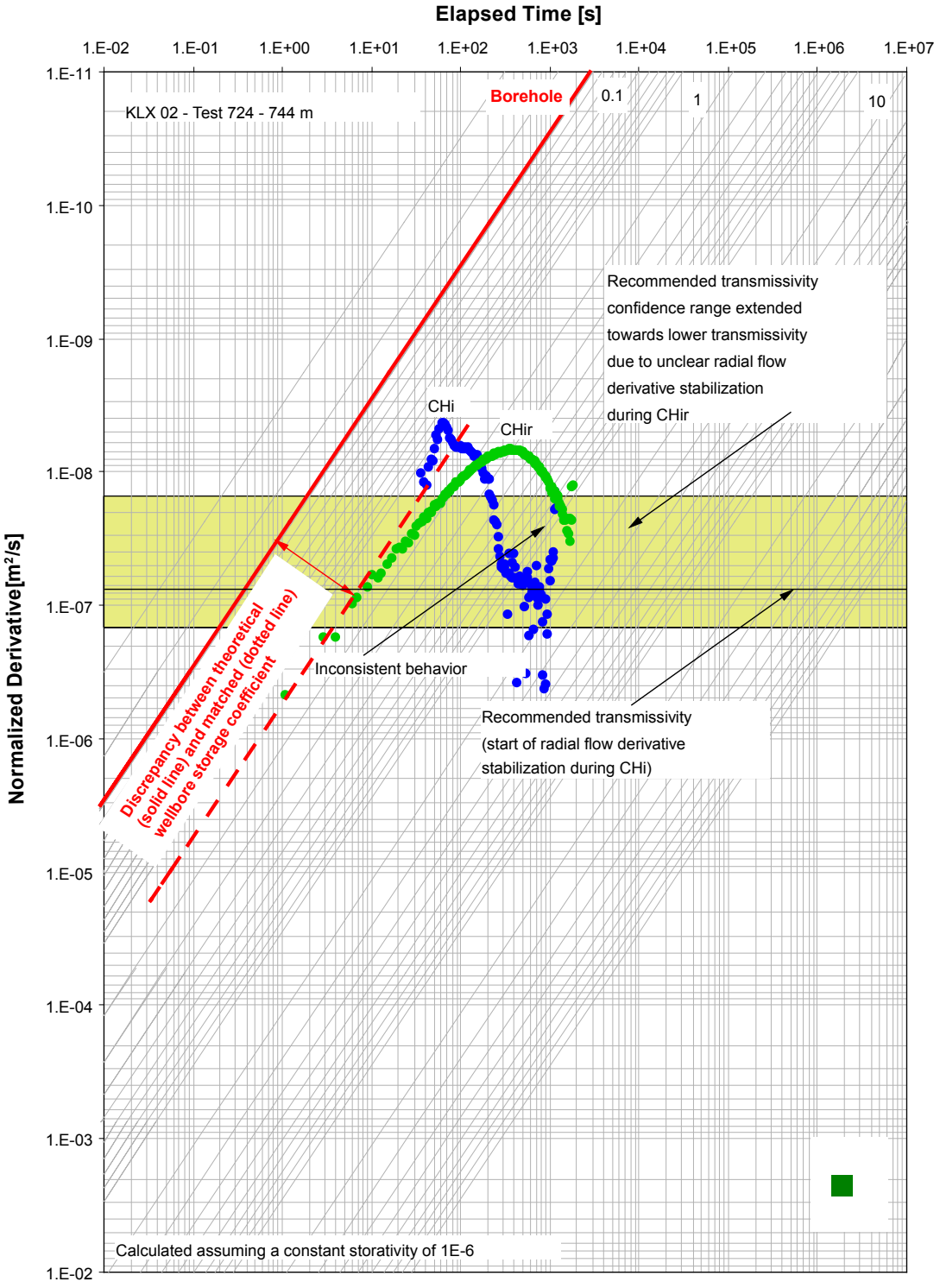

Figure 4-55. *TNP example of inconsistent test behaviour; Test 724–744 m in borehole KLX02.*

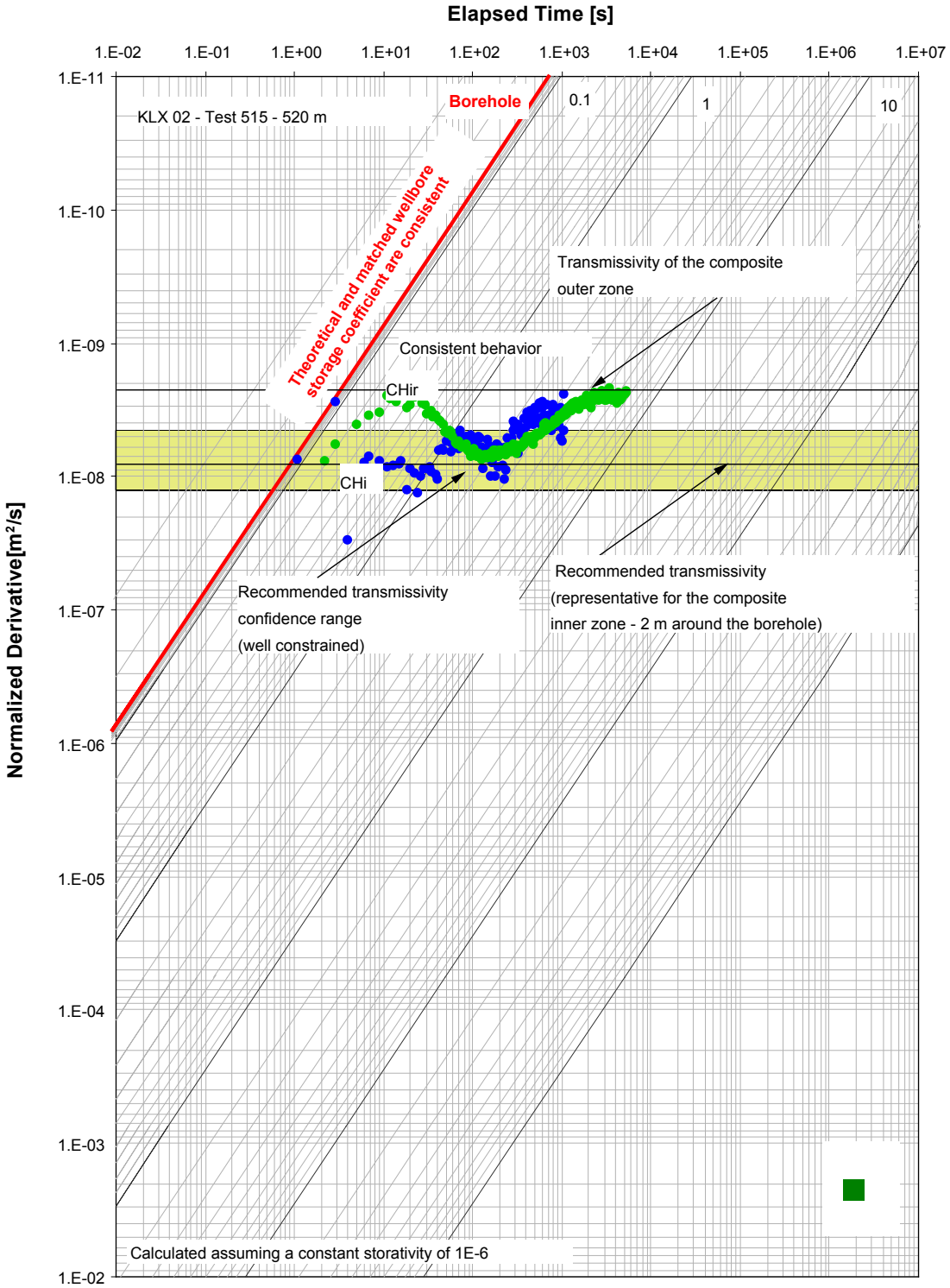

Figure 4-56. *TNP example of consistent test behaviour; decreasing transmissivity away from the borehole; Test 515–520 m in borehole KLX02.*

5 General uncertainties

Two general sources of uncertainty, which are expected to always influence the test response to some degree are considered:

- The packer compliance.
- Background pressure gradients.

In the following, these uncertainties are described.

5.1 Packer compliance (*text by Geosigma*)

5.1.1 General

In conjunction with the construction of equipment for different kind of hydraulic tests, prototypes are manufactured which are tested on the basis of the actual application. In general, tests are made on each component which implies that separate tests are made on the properties of the packers. Since the testing programme is governed by the actual application of the packer, the programme for e.g. a packer designed for piezometric measurements installed in boreholes drilled from a deep tunnel may differ from that for a packer to be used in hydraulic tests in boreholes drilled from the surface.

The types of deformation of packers which may affect the evaluation of hydraulic tests in low-transmissive sections include:

1. Linear-elastic deformation of the packers constitutes one part of the *effective* wellbore storage coefficient (C_{eff}) in an isolated test section. This kind of deformation depends a o on the properties of the rubber used and the relationship between the pressure in the packer and test section, respectively. These deformations are regarded as none time-dependent.

2. Time-dependent deformation of packers is of two kinds:

a) material creeping in e g the rubber at changes of pressure. These effects are reflected by a weakly decreasing pressure in the test section after an instantaneous pressure increase, even if the section is completely tight. Conversely, after an instantaneous pressure decrease, a weakly increasing pressure is obtained in the section. These pressure changes dissipate with time.

b) generated flow caused by the packer inflation. Even after that the packers ”tighten” they continue to expand slightly (“residual expansion”). The resulting decrease of the volume of the test section may in “tight” sections be treated as a fictive flow which affects the flow- as well as the recovery period of the test. The longer packer sealing time the lower this effect.

Both type 1 and 2 are included in the term “packer compliance” used in this report. The performance of the testing of the packers is described in *Geosigma's Methodology report (Appendix 1)*.

3. Other changes of the volume of the test section

a) material generated changes of the packer pressure caused by **temperature variations in the test container.** In hydraulic tests in the upper part of the borehole, apart from the pressure vessel, a major part of the expansion hose to the packers is located in the test container. Large temperature variations in the container may also create large variations of the packer pressure which may, in turn, create small pressure variations in short, “tight” sections. To distinguish such effects, both the packer pressure and the temperature in the test container are measured during the tests.

b) temperature variations in the test section. Since the temperature in “tight” sections may be regarded as stable, this effect may be ignored in most cases.

5.1.2 Linear-elastic deformations

Based on the results of laboratory tests the volume change of two packers was estimated at 0.7 mL/100 kPa pressure changes. This value can be used to calculate the effective compressibility in test sections of different length.

The effective compressibility of a test section depends on the compression of:

- water volume in the test section,
- equipment (packers etc),
- rock.

In the estimation of the effective compressibility below, the rock is assumed as in-compressible. In addition, any volume changes in the cable and the hose in the test section have been ignored. The total change of volume in a test section may thus be calculated as:

$$\Delta V = \Delta V_w + \Delta V_m = \Delta p \cdot V_w \cdot c_w + \Delta V_m \qquad (5\text{-}1)$$

With:
ΔV = total change in volume of water and packers m^3
ΔVw = change of volume of water m^3
ΔVm = change of volume of packers m^3
Vw = volume of water in the test section m^3
Δp = pressure change Pa
cw = compressibility of water Pa^{-1}

The effective compressibility (c_{eff}) of the test section may be calculated as:

$$c_{eff} = \frac{\Delta V}{\Delta p}\frac{1}{V_w} \qquad (5\text{-}2)$$

The effective borehole storage coefficient (C_{eff}) of the test section may be calculated as:

$$C_{eff} = V_w \cdot c_{eff} \qquad (5\text{-}3)$$

The changes of volume in the test section that can be expected for hydraulic tests with a pressure change of 200 kPa in the section together with the estimated effective compressibility and effective borehole storage coefficient of the test section are presented in Table 5-1. The compressibility of water is assumed to $c_w = 4.6 \cdot 10^{-10}$ Pa^{-1} and the rock is assumed to be incompressible in the calculations. Any volume changes of the cable and hose through the section have been ignored. The values on the effective borehole coefficient (C_{eff}) in Table 5-1 can be compared with the corresponding values on this parameter from the test evaluation.

5.1.3 Time-dependent deformations

Material creeping due to instantaneous pressure changes

The laboratory tests exhibited small pressure changes after large pressure disturbances which probably are caused by material creeping. In field tests, the effective compressibility is much higher than in the laboratory tests, why these effects can be ignored by the evaluation of transmissivity from field tests.

Table 5-1. Estimated volume changes in test sections of different length for hydraulic tests with a pressure change of 200 kPa together with the estimated effective borehole storage coefficient. Borehole diameter = 76 mm.

Parameter	Section length (m)		
	5	20	100
Net water volume in test section, Vw (L)	c. 19	c. 78	c. 393
Change of the water volume in the test section at a pressure change of 200 kPa, ΔVw (mL)	c. 1.8	c. 7.2	c. 36
Volume change of 2 packers at a pressure change of 200 kPa, ΔVm (mL)	c. 1.4	c. 1.4	c. 1.4
Volume change of water and 2 packers at a pressure change of 200 kPa, ΔV (mL)	c. 3.2	c. 8.6	c. 37.4
Effective compressibility of test section, ceff (Pa^{-1})	$8.4 \cdot 10^{-10}$	$5.5 \cdot 10^{-10}$	$4.8 \cdot 10^{-10}$
Effective borehole storage coefficient of test section, Ceff (m^3/Pa)	$1.6 \cdot 10^{-11}$	$4.3 \cdot 10^{-11}$	$1.9 \cdot 10^{-10}$

Flow generated by packer sealing

The generated flows from packer sealing by one packer have been measured at different times after start of sealing at two different pressures, i. e. at atmospheric pressure and at 200 kPa, respectively. The calculated packer generated flows are presented for selected test times in Table 5-2 below. The selected times refer to different phases in the current scheme of the performance of hydraulic injection tests of different section lengths. The number of figures of the values in the table is presented without considering the actual measurement accuracy.

The measured packer generated flows at different test times are shown in Figure 5-1 and Figure 5-2, respectively together with the interpolated curve between the measurement points. In the latter diagram, the measured average flow rate value at t=60 min for one packer (0.005 mL/min) was omitted since it is regarded as uncertain. It should also be pointed out that the estimated flow rates below c. 0.1 mL/min are very uncertain.

Table 5-2. Estimated flow generated by two packers at selected times after start of packer sealing (t=0) at atmospheric pressure and an overpressure of 200 kPa in the test section, respectively.

Pressure in test section (kPa)	Flow rate (mL/min)					
	t=30 min	t=45 min	t=50 min	t=70 min	t=75 min	t=105 min
0 (atmospheric pressure)	0.50	0.26	0.18	0.05	0.037	0.0067
200	0.48	0.16	0.08	0.005	0.0039	0.001

The selected times in the figures refer to the following activities in the hydraulic injection tests:

t=0 min start of packer sealing.

t=30 min start of injection period (5 and 20 m tests).

t=45 min start of injection period (100 m tests).

t=50 min stop of injection period/start of recovery period (5 and 20 m tests).

t=70 min stop of recovery period (5 and 20 m tests).

t=75 min stop of injection period/start of recovery period (100 m tests).

t=105 min stop of recovery period (100 m tests).

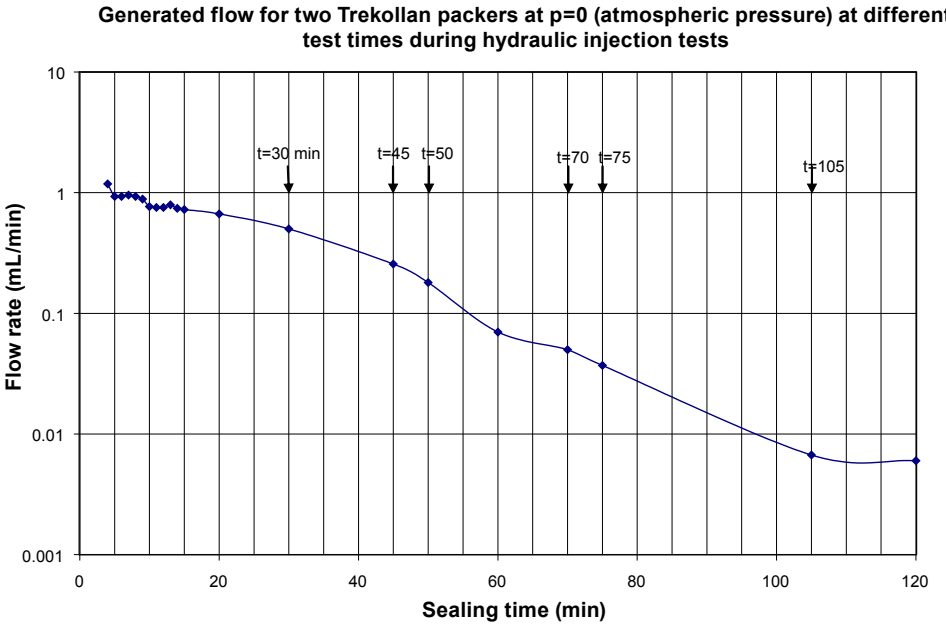

Figure 5-1. *Generated flow of two Trekollan packers at p=0 (atmospheric pressure) at different times during the hydraulic injection tests.*

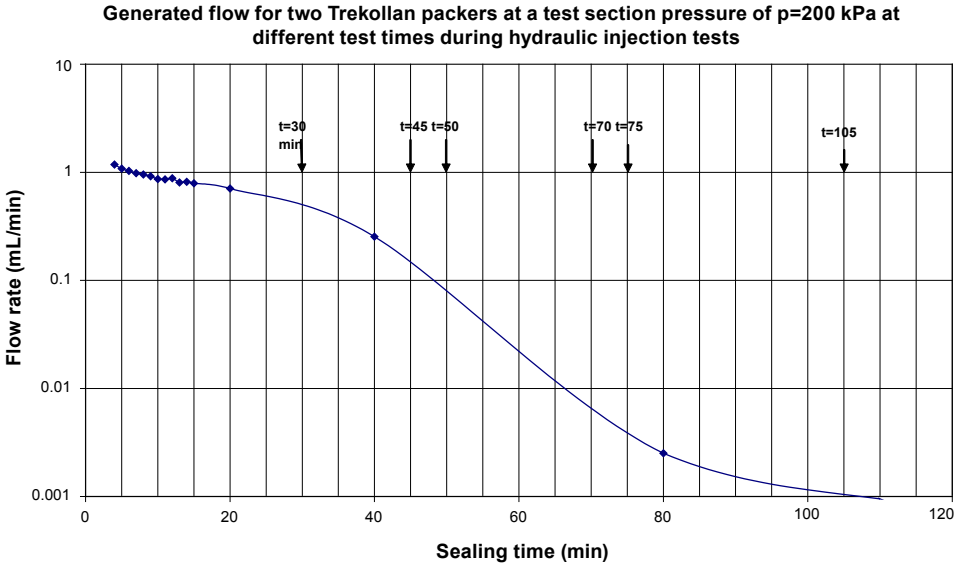

Figure 5-2. *Generated flow of two Trekollan packers at p=200 kPa at different times during the hydraulic injection tests.*

If the estimated packer generated flows in Table 5-2 are assumed as injection tests in the field, the real flow into the formation at the end of the injection period (t=50 min) is c. 0.08 mL/min higher than the actually measured flow by the flow meter at the surface in 5 m and 20 m test sections. This value can be compared with the lower standard measurement limit for flow rate of 1 mL/min for the PSS system. The effect of the generated flow will disappear if sufficient time is allowed between start of packer sealing and the start of subsequent hydraulic tests.

5.2 Effects of packer compliance on testing

5.2.1 Flow generated by the packers

Consistency checks of C_{eff} and the flow generated by the packers may be made from pressure changes measured during the packer sealing period of tests conducted very tight sections (below the measurement limit). The results can be compared with the corresponding estimations from the laboratory tests described above. However, no independent estimations of C_{eff} and the generated flow can be made from the field tests.

Below, some examples of such estimations of the flow generated by the packers from tests in very low-transmissivity test sections at Oskarshamn exhibiting the highest pressure increases after the application of the pressure pulse during the recovery period due to packer compliance. These sections are considered to be tight, i. ew. the flow into the rock is assumed to be extremely small and thus negligible in relation to the flow generated by the packers. The estimations of the packer generated flow were made from the pressure increase in the test section during the first 10 mins of the recovery period after the pressure pulse due to the generated flow together with the estimated value of C_{eff} from the laboratory tests described above according to Equation 5-4:

$$C_{eff} \frac{dp_{packer}}{dt} = Q_{packer} \qquad (5\text{-}4)$$

Qpacker = packer generated flow (m^3/s)
Ceff = effective borehole storage coefficient of test section (m^3/Pa)
dppacker / dt = pressure increase in test section per time unit (Pa/s)

5.2.1.1 Test examples

Example 1: Test 805.98–825.98 m in borehole KLX04

The packer sealing time was 30 min. Figure 5-3 shows the pressure history of the test. The test was stopped after packer inflation due to the steep rise in pressure, indicating very low transmissivity.

dp/dt = 48 Pa/s
C_{eff} = $4.3 \cdot 10^{-11}$ m^3/Pa (from lab. measurements)
Q_{packer} = 0.12 mL/min

Example 2: Test 826.02–846.02 m in borehole KLX04

The packer sealing time was 30 min. Figure 5-4 shows the pressure history of the test. The pressure build-up deviates before (test phase 3) and after the application of the pressure pulse (test phase 5).

dp/dt = 16 Pa/s
C_{eff} = $4.3\ 10^{-11}$ m^3/Pa (from lab. measurements)
Q_{packer} = 0.04 mL/min

Example 3: Test 846.05–866.05 m in borehole KLX04

The packer sealing time was 30 min. Figure 5-5 shows the pressure history of the test. The test was stopped after packer inflation due to the steep rise in pressure, indicating very low transmissivity.

dp/dt = 22 Pa/s
C_{eff} = $4.3\ 10^{-11}$ m^3/Pa (from lab. measurements)
Q_{packer} = 0.06 mL/min

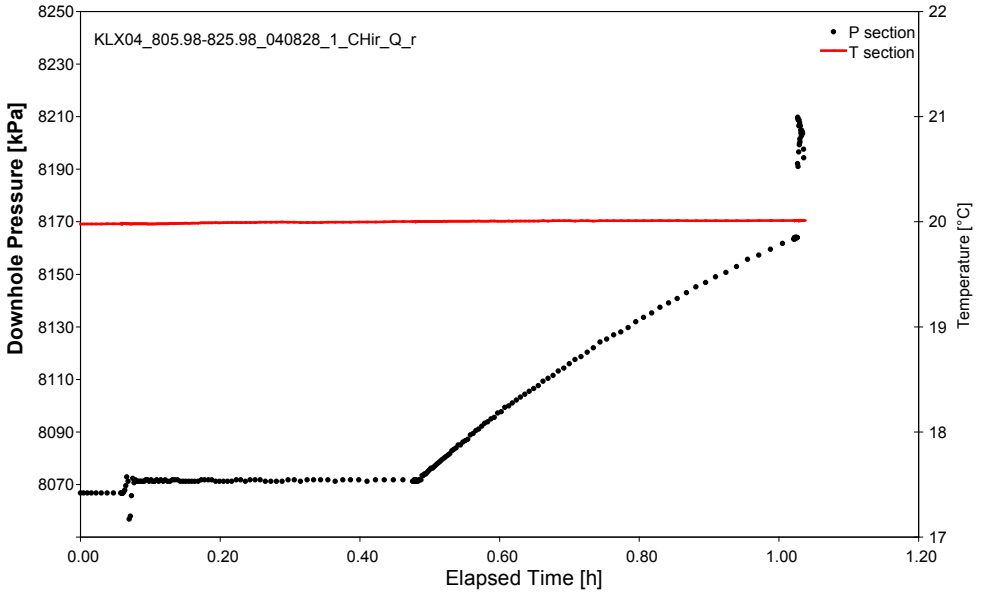

Figure 5-3. *Pressure history during test 805.98–825.98 in borehole KLX04.*

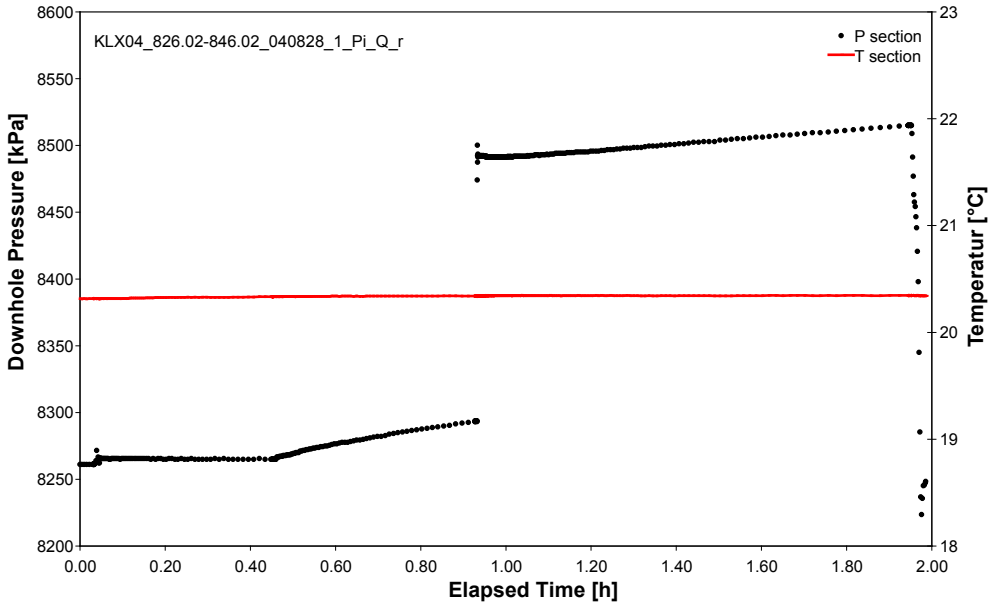

Figure 5-4. *Pressure history during test 826.02–846.02 in borehole KLX04.*

5.2.1.2 Comparison of results from the laboratory measurements

The results from the estimations of flow generated by the two packers in selected, ”tight” 20 m sections at sealing times of approx. 30 min were compared with the corresponding flows estimated from the laboratory tests. The results from the selected sections are presented in Table 5-3.

The agreement between the field- and laboratory tests is not so good and may be caused by small amounts of water entering the formation. An additional cause may be the fact that the lab tests were performed at pressures lower that the test pressure.

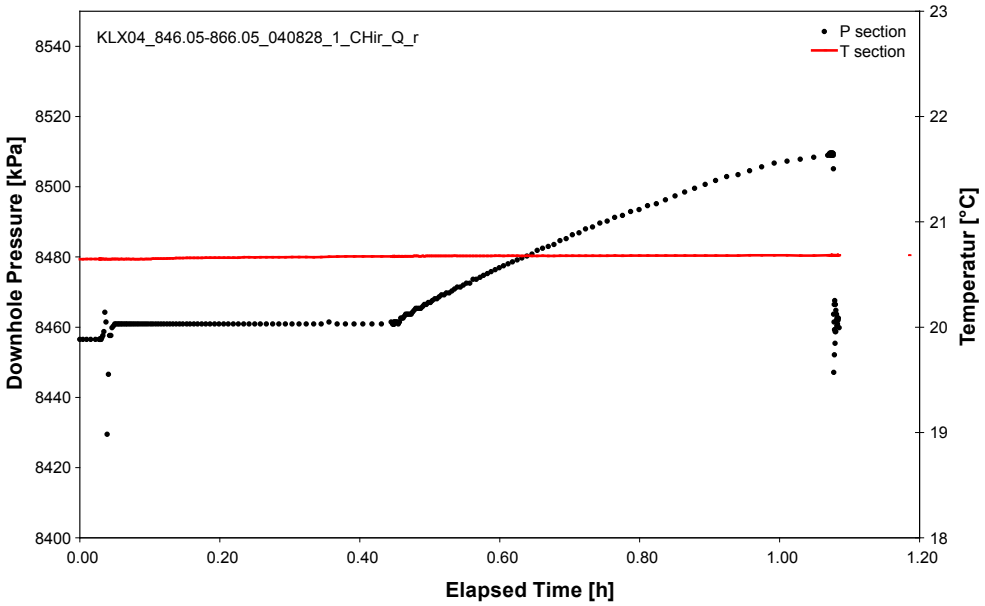

Figure 5-5. *Pressure history during test 846.05–866.05 in borehole KLX04.*

Table 5-3. Comparison of the estimated packer generated flow from field tests and laboratory measurements.

Borehole section	Test type	Packer sealing time (mins)	Packer generated flow (mL/min)	
			Field tests	Laboratory tests
KLX04:805.98–825.98	Test stopped after packer inflation	30	0.12	0.4
KLX04:826.02–846.02	Pulse	30	0.04	0.4
KLX04:846.05–866.05	Test stopped after packer inflation	30	0.06	0.4

5.2.1.3 Estimation of transmissivity of tight sections

Based on the analysis experience of the past tests, in cases when the test pressure response resembles the cases discussed above, the test zone transmissivity must be below 10^{-11} m^2/s. This value is based on the observation that test zones of higher transmissivity do not display a strong pressure build-up caused by packer inflation and because of this pulse tests (at a minimum) or constant pressure injection tests can be conducted.

In cases of tight pressure response the transmissivity value of 10^{-11} m^2/s was reported as maximum transmissivity (T_{max}).

5.2.2 Numeric simulation of packer compliance effects

The present section describes the influence of packer compliance (as described by laboratory measurements) on the response of pulse injection tests. The simulation results were organized in an Excel spreadsheet (SIMS_PackerCompliance.xls). The spreadsheet allows the user to compare three simulations with different parameter sets (L, T, S) at the choice of the user. More detailed description of the spreadsheet is given further below. The main question asked in this section is: "How good is our ability to derive the formation transmissivity correctly by using pulse test deconvolution analysis, while neglecting the packer compliance?"

Simulations

The simulations were calculated using nSIGHTS. The simulated sequence was:

- Packer inflation (at time = 0).
- Pressure measurement with test valve open (duration 30 min).
- Pressure measurement with test valve closed (duration 20 min).
- Pulse injection with pressure difference of 200 kPa measured from the last pressure of the previous phase (duration 40 min).

The test sequence described above roughly resembles the current testing procedure in Oskarshamn when pulse tests were conducted.

The simulations were conducted for an array of parameters as listed below:

- Transmissivity (T) = 10^{-8}, 10^{-9}, 10^{-10}, 10^{-11}, 10^{-12} and 10^{-13} m^2/s.
- Storativity (S) = 10^{-5}, 10^{-6} and 10^{-7}.
- Section length (L) = 5, 20 and 100 m.

The wellbore storage coefficient was calculated from the actual interval volume and a test zone compressibility of $2 \cdot 10^{-9}$ 1/Pa (this is how L influences the simulations).

All simulations were started at an initial formation pressure of 5,000 kPa.

During the simulation, the interval volume decreases at a rate described by the packer compliance measurements from the laboratory.

Presentation of results

Figure 5-6 presents a snapshot from the spreadsheet showing three simulations conducted for a section length of 20 m, a storativity of 10^{-6} and transmissivities of 10^{-9}, 10^{-10} and 10^{-11} m^2/s, respectively.

The upper graph compares the simulations in Cartesian coordinates together with the packer displacement rate.

The lower graph shows the normalized deconvolution derivative of the simulated pulse tests (dots) together with the ideal response derived from the type curve derivative (solid line). The data in the yellow area would not be available in the case of a real test, because it corresponds to sample rates lower than 1 reading/second. Generally, the difference between the simulated response (the dots) and the ideal type curve (the solid line) is a measure for the error introduced by packer compliance. Note that the Y-axis is plotted in transmissivity units (m^2/s), such that vertical differences between the dots and the corresponding solid line can be directly quantified in terms of transmissivity error.

Summary:

- Packer compliance (i.e. decreasing interval volume during the test) in the magnitude described by the laboratory measurements influences the ability of deriving the formation transmissivity correctly when the true formation transmissivity is 10^{-11} m^2/s or lower. In this case, a transmissivity lower than the correct one would be derived.
- Larger formation storativity (10^{-5}) improves the situation at transmissivities in the range 10^{-11} m^2/s.
- A lower wellbore storage coefficient (i.e. smaller section length) improves the situation at transmissivities in the range 10^{-11} m^2/s.

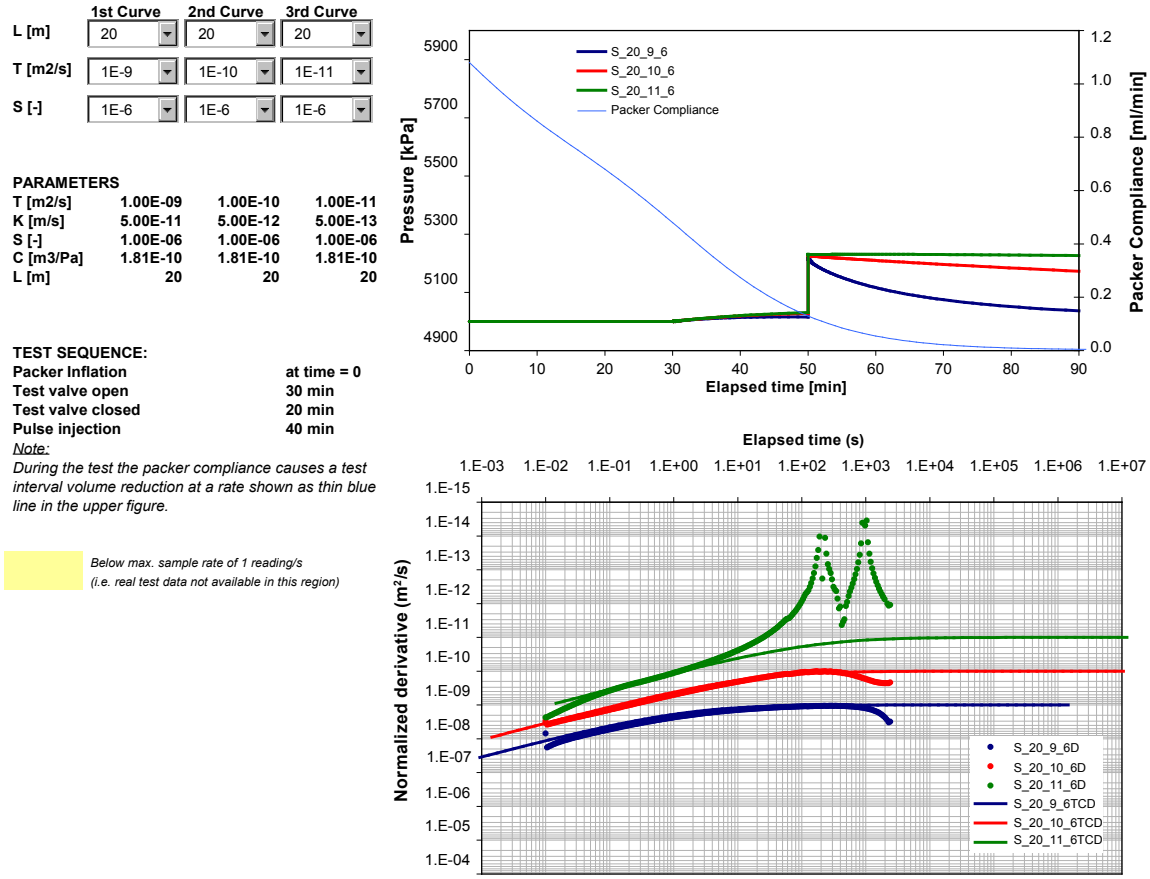

Figure 5-6. *Presentation of simulation results.*

- The situation would change considerably in case the actual packer compliance under downhole conditions is different than the one measured under surface conditions. Generally, it can be expected that under downhole conditions the effect of packer compliance would decrease. Also as addressed by Geosigma, the effect of packer aging was not considered. It can be expected that the magnitude of the compliance would decrease with the age of the packer (i.e. number of inflations).

5.3 Background pressure gradients

Hydraulic test responses can be affected by pressure gradients present in the formation. As presented for example in equation 4-4, background pressure gradients not accounted for in the analysis may lead to erroneous transmissivity results. Theoretically, the magnitude of the error depends on the relative size of the pressure disturbance induced by the background gradient compared to the magnitude of the pressure disturbance induced by the test itself. Factors inducing background pressure gradients, that may adversely influence test results are:

- Tidal effects.
- Precipitation.
- Barometric pressure changes.
- Sea level fluctuations.
- Earth quakes.
- Drilling and other activities in surrounding boreholes.
- Re-establishment of section pressure to formation pressure after packer sealing (i.e. the pressure history of the tested section).

The influence of such factors can in general be neglected in the evaluation of short-time injection tests. The observed magnitude of the disturbances listed above is documented with examples in the Methodology report of Geosigma (Forsmark site).

Tidal effects were observed during cross-hole pumping tests conducted in shallow percussion boreholes at the Oskarshamn site. No tidal disturbances could be identified during the injection tests conducted with the PSS. Further, no influences of precipitation, barometric pressure changes, sea level fluctuations or earth quakes were identified. There was no drilling activity in the vicinity of the boreholes tested.

The pressure history of the tested section is often a factor influencing the test response. Once the test section is drilled through, the formation is open to the pressure imposed by the water level in the borehole. This borehole pressure is not always equal to the static formation pressure, and it created a pressure disturbance in the formation around the borehole. Based on the head calculations from the hydraulic tests, head differences along one borehole of up to 8 m (80 kPa) were observed. In most of the cases the pressure history influence dissipates quickly after packer inflation. Figure 5-7 shows the case of test 704–804 in borehole KLX02. We see that after inflating the packers and closing the test valve the pressure in the test section decreased by 84 kPa within 20 minutes and was nearly stable before starting the CHi phase. Therefore it can be assumed that the influence of pressure gradients caused by the pressure history of the test section was low.

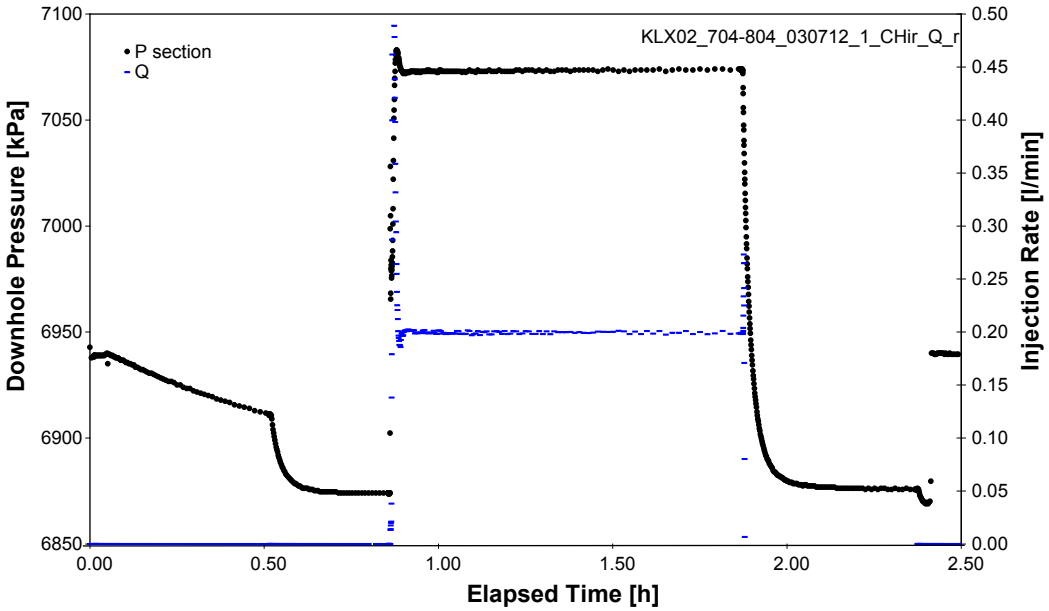

Figure 5-7. *Test 704–804 in borehole KLX02; influence of pressure history.*

6 Test statistics

Statistics of the results of all injection tests performed at the Oskarshamn site in the boreholes KLX02, KSH01A, KSH03A, KAV04A and KLX04 is shown in Table 6-1 together with a description of the definition of the columns. The information in the table is based on the primary data evaluation reports of the respective boreholes.

Comments on the meaning of the columns are given below:

6.1 Column 1 – Total number of sections

Initially planned number of sections according to the activity plan. Depending on transmissivity thresholds preliminarily defined in the program, not all sections listed in the activity plan were actually tested.

6.2 Column 2 – Number of sections tested

Number of test sections actually tested in the respective borehole.

6.3 Column 3 – Number of sections < 1 mL/min (flow rate could NOT be extrapolated)

Injection tests were performed and the measured flow rate dropped below 1 mL/min during the first two minutes of the test (CHi phase NOT analysable; see Figure 6-1).

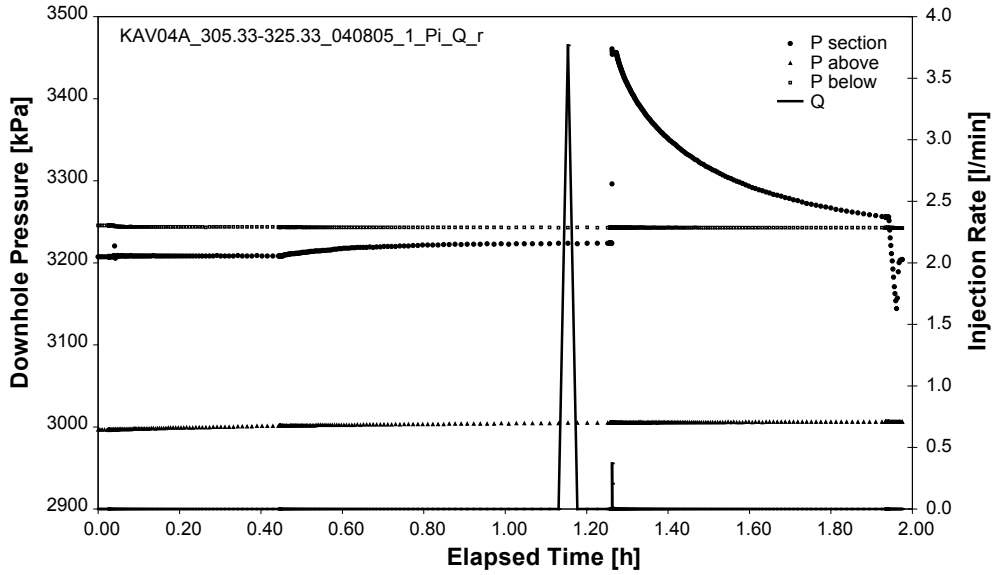

Figure 6-1. *Example of test with flow rate dropping below 1 mL/min; flow rate could NOT be extrapolated.*

6.4 Column 4 – Number of sections < 1 mL/min (flow rate could be extrapolated)

Injection tests were performed and the measured flow rate dropped below 1 mL/min after a longer period of time (CHi phase analysable; see Figure 6-2)

6.5 Column 5 – No test performed due to packer compliance

No test performed due to prolonged packer expansion in very tight sections (Figure 6-3).

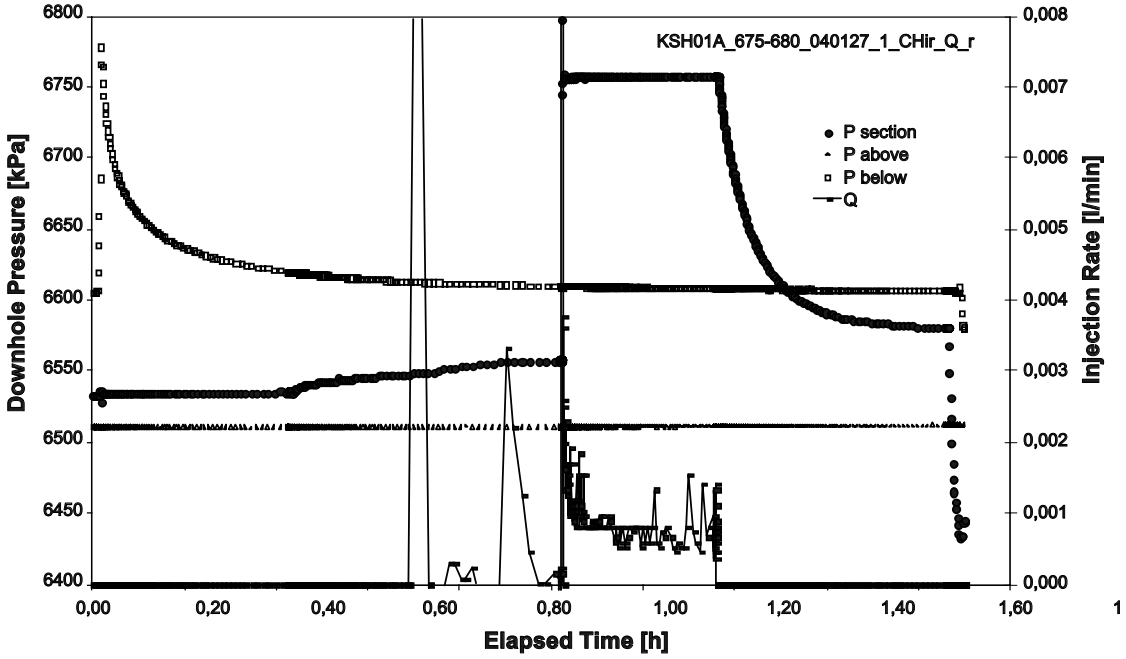

Figure 6-2. *Example of test with flow rate dropping below 1 mL/min; flow rate could be extrapolated.*

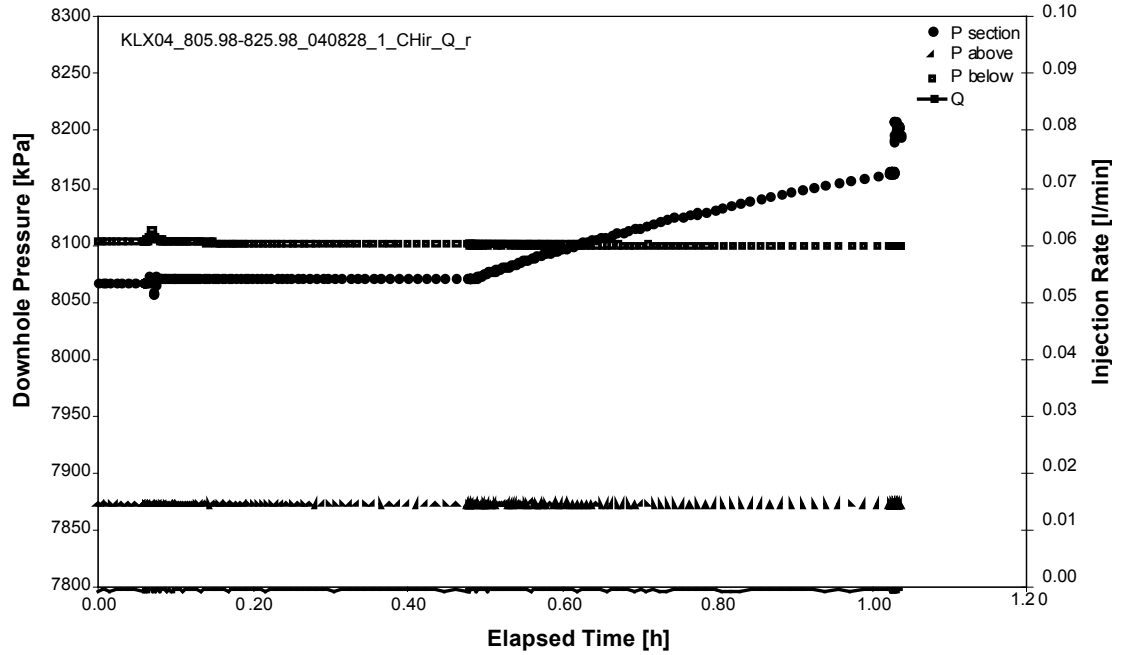

Figure 6-3. *No test performed due to packer compliance (example).*

6.6 Column 6 – Number of pulse tests

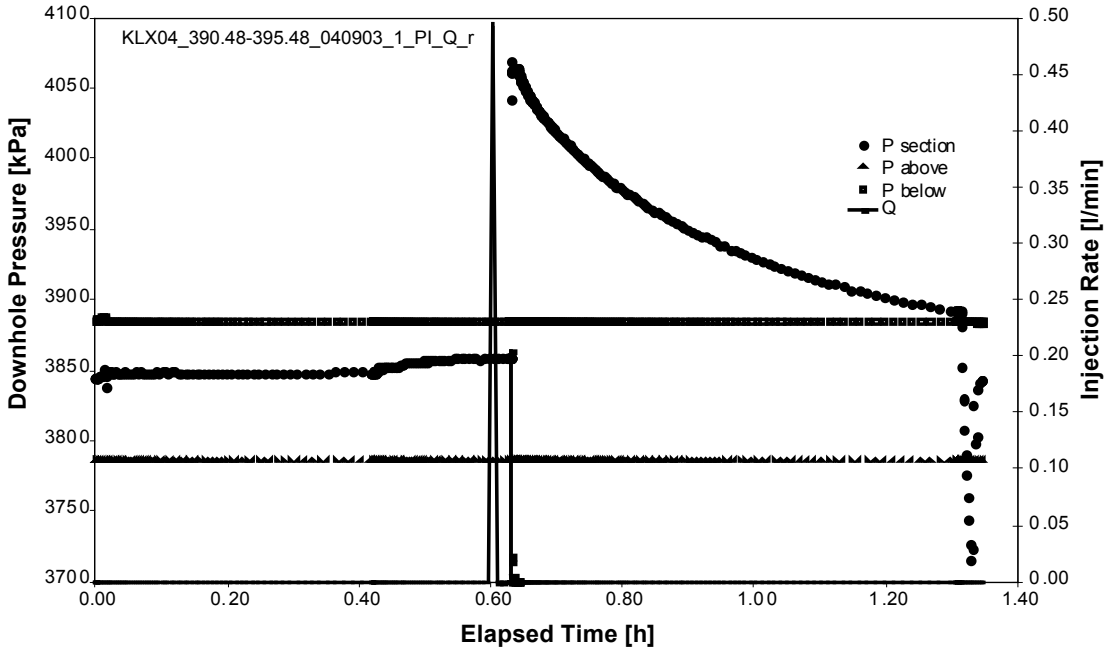

Figure 6-4. *Example of pulse test.*

6.7 Column 7 – Ambiguous interpretation

Tests with no clear flow model identification due to:

1. test time too short (see Figure 6-5).
2. poor gauge resolution (see Figure 6-6).
3. poor CHi control; too much noise in the flow rate (see Figure 6-7).

6.8 Column 8 – Inconsistency between CHi and CHir phase and between different sections

Different flow models used for interpretations of the CHi and CHir phase of the same section and/or different transmissivities derived (differing by more than 30% of a log cycle).

Flow rate and/or transmissivity of one section is higher than the one of the corresponding longer section (e.g. $T_{105–110\ m} > T_{100–120\ m}$).

6.9 Column 9 – Gauge resolution problem

Due to the gauge resolution (Figure 6-8), the shape of the derivative of the CHir phase (Figure 6-9) depends very much on the smoothing factor.

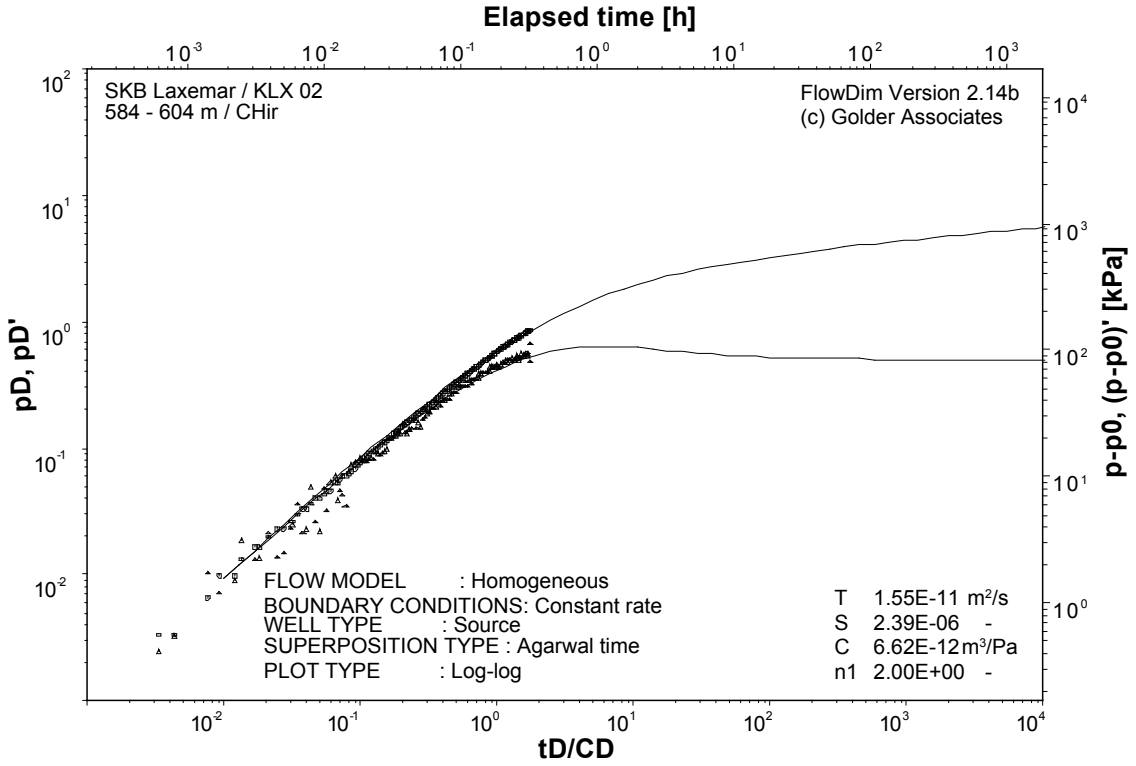

Figure 6-5. *Test time too short (example).*

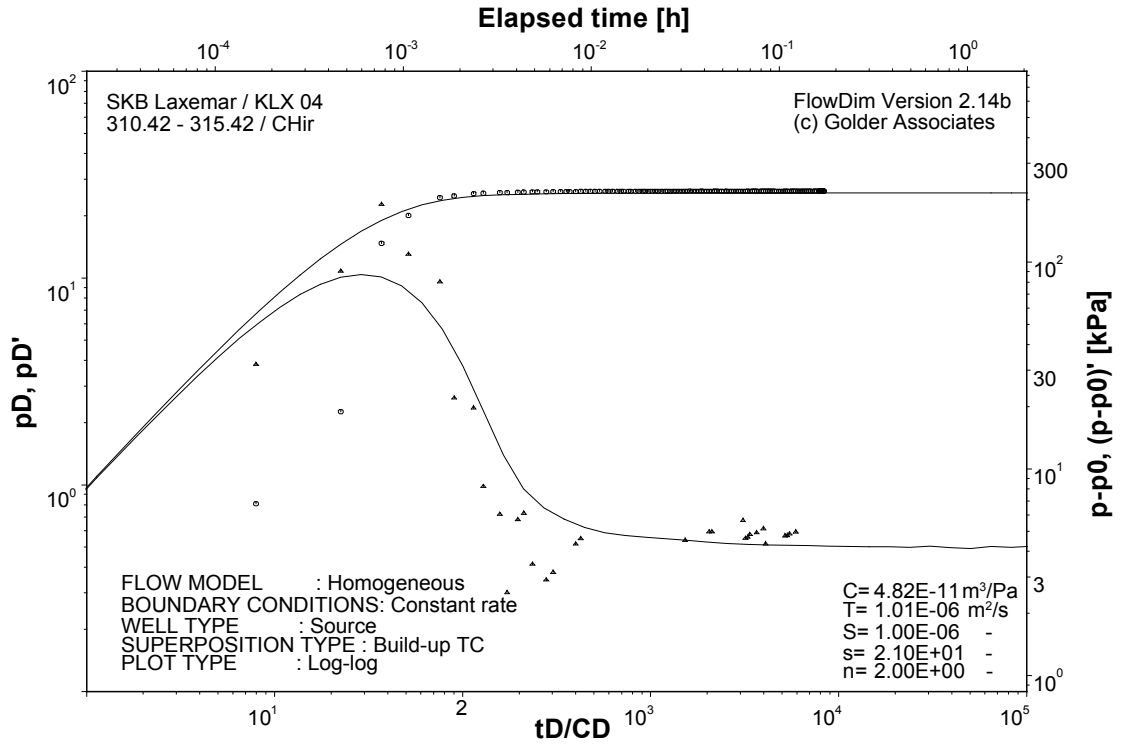

Figure 6-6. *Poor gauge resolution (example).*

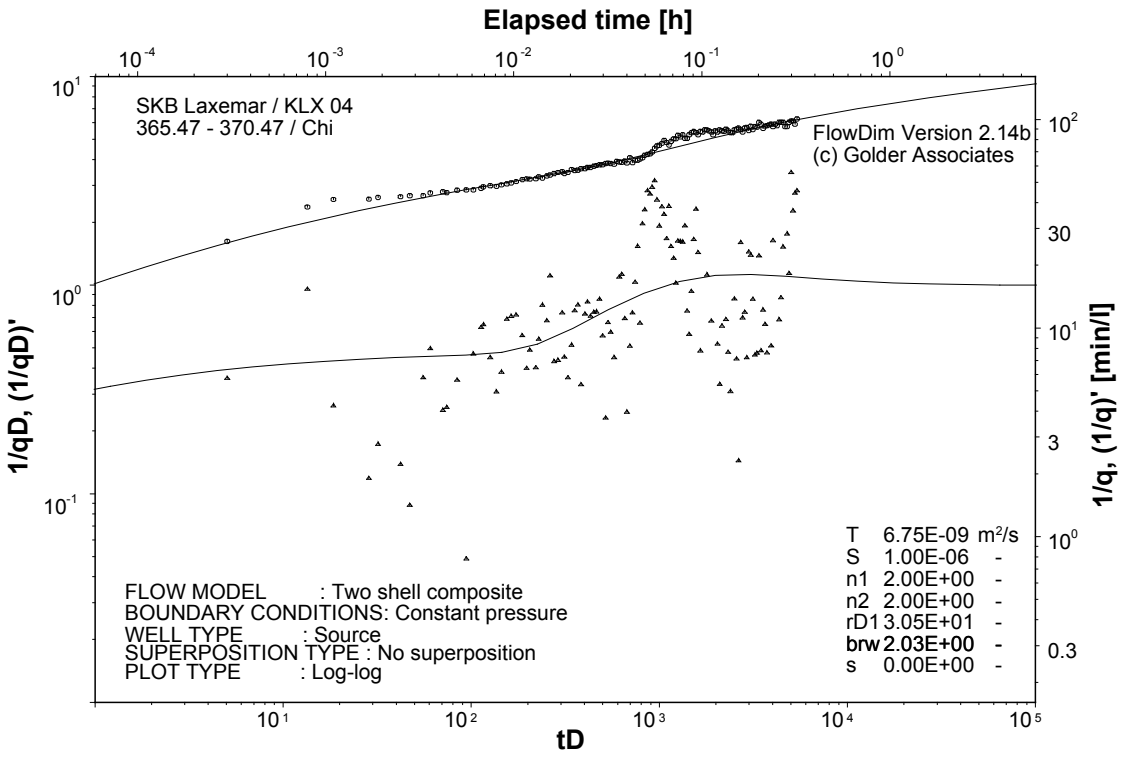

Figure 6-7. *Poor rate control (example).*

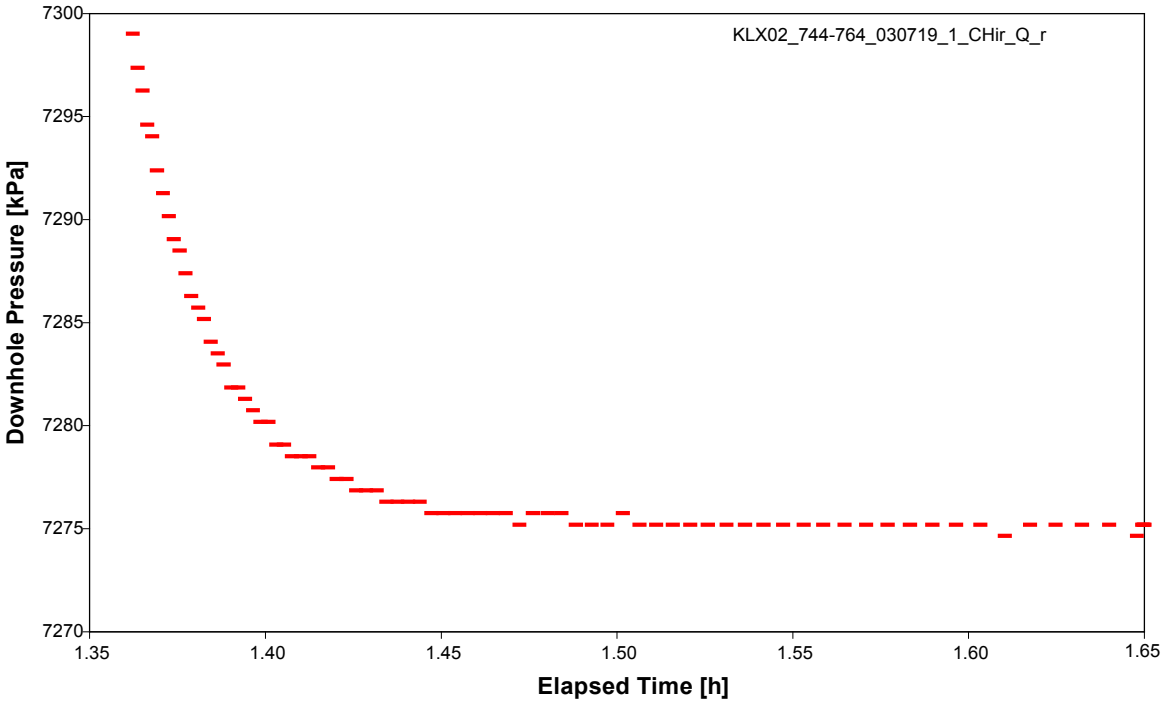

Figure 6-8. *Example of poor gauge resolution.*

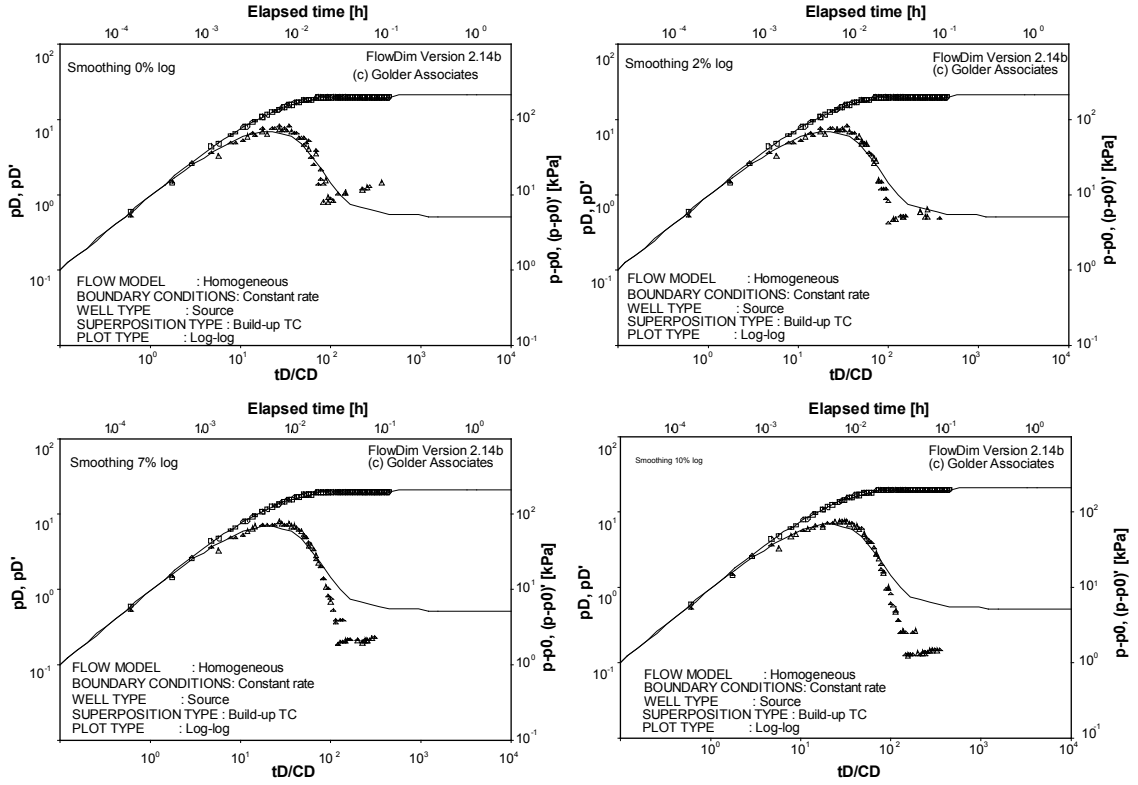

Figure 6-9. *Influence of smoothing factor on the shape of the derivative.*

6.10 Column 10 – Fast recovery

Tests showing fast recovery during the CHir phase (subjective judgement; see Figure 6-10).

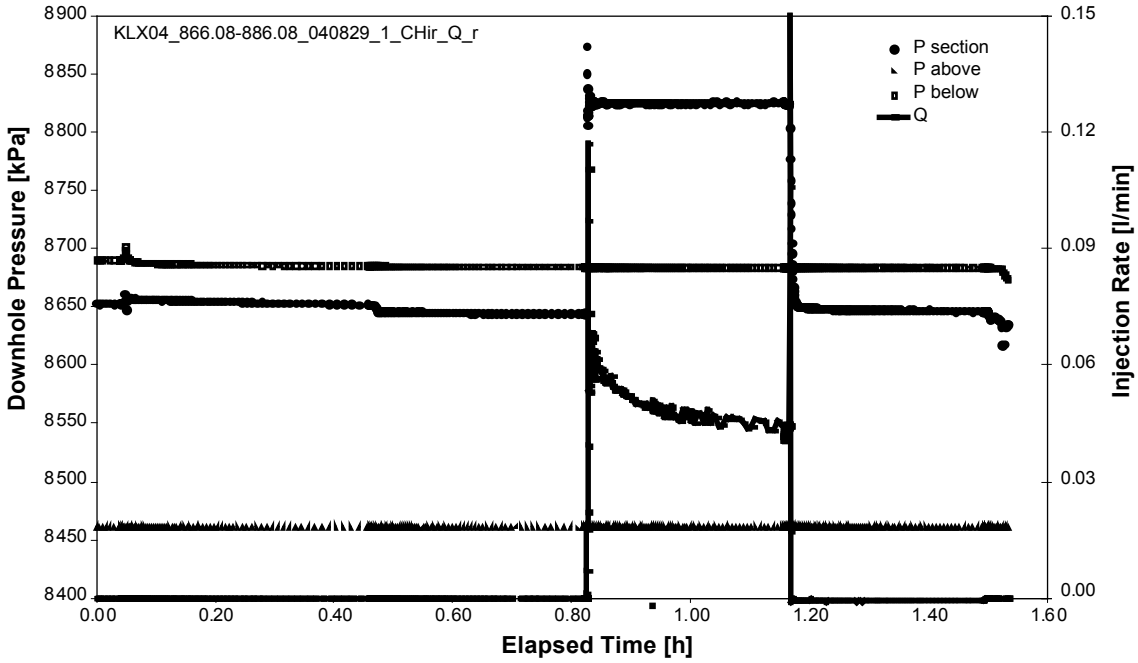

Figure 6-10. *Example of CHir fast recovery.*

6.11 Column 11 – No formation flow

The CHir phase was dominated by WBS effects and the beginning of the formation flow was covered by those effects.

6.12 Column 12 – Not analysable

Test phases that were stated in the report as “not analysable”. Typically flow rate bml, poor CHi control, very tight section, gauge resolution problems.

6.13 Column 13 – Clearly analysable

Both test phases ran as planned. No problems with the analysis. The analysis of both phases show good consistency (same flow model and $T_{CHi} \cong T_{CHir}$). In case of a pulse injection; a very good match with the type curve and only a small degree of uncertainty.

It should be born in mind that the individual number of tests in the table is subjective and should only be used in a statistical sense. In addition, some of the columns may represent similar information which thus causes some redundancy in the table. For example, tests exhibiting fast recovery may also lead to inconsistent tests and resolution problems of the pressure gauge. Such tests are scored in all of these columns (and possibly also in further columns). The table below (Table 6-1) presents the results of the test classification performed in accordance to the criteria described above:

Table 6-1. Compilation of results from constant head injection tests at the Oskarshamn site.

A	B	C	D	E	F	G	H	I	J	K	L	M	N	O	P	Q	R	S
Borehole Seclength	Total no of sections according to AP[1]	No of sections tested[2]	No of sections < 1 mL/min[3] (flow rate could NOT be extrapolated)	No of sections < 1 mL/min[4] (flow rate could be extrapolated)	No of sections not tested due to prolonged packer compliance[5]	No of pulse tests[6]	Ambiguous interpretation[7]		Inconsistency between[8]		Gauge resolution problem[9]		Fast recovery[10]	No formation flow[11]		Not analysable[12]		Clearly analysable[13]
							CHi	Chir	Chi and CHir	Sections	CHi	CHir	Chir	CHi	CHir	CHi	CHir	Chi and Chir Pi
KLX02																		
100 m	9	8	1	0	0	0	2	3	1	–	0	3	0	0	3	2	0	4
20 m	45*	36	8	0	0	5	11	20	17	5	0	15	4	0	14	5	1	10
5 m	80*	36	6	1	14	6	4	12	9	3	0	11	3	0	6	19 26	14 15	3
Total:	134*	80	15	1	14	11	17	35	27	8	0	29	7	0	23			17
KSH01A																		
100 m	9	9	0	1	0	0	3	4	7	–	0	0	0	0	2	0	0	2
20 m	45*	45	0	0	0	0	13	25	25	18	0	17	0	0	18	0	0	9
5 m	80*	81	11	17	22	0	19	35	31	9	0	8	0	0	35	29 29	28 28	13
Total:	134*	135	11	18	22	0	35	64	63	27	0	25	0	0	55			24
KSH03A																		
100 m	9	9	0	0	3	0	2	1	2	–	0	1	0	0	0	3	3	3
20 m	45*	0	0	0	0	0	0	0	0	0	0	0	0	0	0	0	0	0
Total:	54*	9	0	0	3	0	2	1	2	0	0	1	0	0	0	3	3	3
KAV04A																		
100 m	9	9	1	0	0	1	0	2	6	–	0	1	1	0	1	0	0	2
20 m	45*	42	5	0	0	5	6	19	21	5	0	18	9	0	8	0	0	14
5m	80*	0	–	–	–	–	–	–	–	–	–	–	–	–	–	–	–	–
Total:	134*	51	6	0	0	6	6	21	27	5	0	19	10	0	9	0	0	16
KLX04																		
100 m	9	9	1	0	0	1	0	2	4	–	0	3	1	0	0	0	0	3
20 m	45*	39	3	0	3	3	5	23	22	5	0	14	13	0	7	3	3	10
5 m	80*	69	9	4	11	9	13	35	30	5	0	25	22	0	13	11 14	14 17	9
Total:	134*	117	13	4	14	13	18	60	56	10	0	42	36	0	20			22

* Maximum number of tests.

7 Comparison of analysis methodology between Golder and Geosigma

Below, a summary of the test analysis methodologies used by Golder and Geosigma in selected main items together with a comparison and conclusions is presented. Any differences and their implications, with emphasis on the results presented to the Sicada data base, are discussed.

7.1 Software used

7.1.1 Geosigma

The test analysis software Aqtesolv, extended for constant pressure tests, was used for test analysis. The software contains a suite of analytical solutions (models) of different types of tests (constant rate, constant pressure, slug- and pressure pulse tests) and flow characteristics. Both manual analysis and automatic simulation by non-linear regression technique can be performed. The software simulates the response in real time according to a certain analytical model for a given set of hydraulic parameters and compares with the observed response. The associated derivatives may be calculated according to the algorithms by /Bourdet et al. 1989/ and/or /Spane and Wurstner 1993/.

7.1.2 Golder

The Golder in-house test analysis program FlowDim V2.14b was used for the analysis. FlowDim allows the analysis of constant rate, constant pressure, slug and pulse tests both in source and observation boreholes. The program uses manual and automated (non-linear regression) type curve and derivative analysis. The flow models available include homogeneous, two-zone composite and dual porosity for any flow dimension between 1 and 3. FlowDim uses one step superposition for the analysis of constant rate and recovery tests and deconvolution as well as RAMEY analysis for the analysis of slug and pulse tests. The program has been widely used in the frame on radioactive waste projects since 1994.

7.1.3 Comparison and conclusions

Both software programs used implement state of art test analysis methods and have been validated in the frame of past testing projects. It can be assumed that both analysis programs produce compatible results.

7.2 Models used for transient analysis of the injection period of the injection tests

7.2.1 Geosigma

Models based on /Hurst et al. 1969/ for radial flow and /Hantush 1959/ for pseudo-spherical (leaky) flow in an equivalent porous medium were used. Both models include the inverse flow rate derivative and skin according to the effective wellbore radius concept. The models by /Ozkan and Ragavan 1991ab/ were used for linear flow in single fractures.

The evaluation of the hydraulic parameters are made on the time interval representing the rock conditions close to the borehole (inner region) or outside the skin zone if such a zone is present. In some cases the properties of an outer zone with different transmissivity were also calculated.

The presence of apparent outer hydraulic boundaries (no-flow and constant pressure) was only evaluated qualitatively.

The storativity was estimated from a regression relationship between T and S /Rhén et al. 1997/ from borehole KFM05A and onward. For previous boreholes the storativity was assumed at $1 \cdot 10^{-6}$ independently of the transmissivity.

7.2.2 Golder

Golder uses a generic two-zone composite fractional dimension model in the analysis. According to the observed behaviour, the model was configured in most cases to a flow dimension of two (radial flow). Linear and spherical flow can be simulated as well as changes of flow dimension at some distance from the borehole. All models account for borehole effects (i.e. wellbore storage and skin).

In cases when only one parameter zone was seen by the tests, a homogeneous (one zone) flow model was used. Constant pressure boundaries were modelled as an increase of transmissivity in the outer composite zone, no flow boundaries were modelled as a decrease of transmissivity in the outer composite zone.

The storativity was assumed known and constant at 10^{-3} (above 100 m depth) and 10^{-6} (below 100 m depth). The evaluation of the hydraulic parameters are made on the time interval representing the rock conditions close to the borehole (inner zone) or outside the skin zone if such a zone is present. If seen by the test, the properties of an outer zone were also calculated.

7.2.3 Comparison and conclusions

Although the two analysis approaches use a slightly different flow model philosophy, the differences are in terms of nomenclature and not in the description of the flow phenomena actually occurring. Each of the flow models used in one of the approaches can be translated in the other model system, respectively.

The two analysis approaches use different assumptions for storativity, which leads to incompatible calculation of skin factors and distances.

7.3 Models used for transient analysis of the recovery period of the injection tests

7.3.1 Geosigma

The models by /Dougherty and Babu 1984/ for radial flow and /Hantush 1955/ for pseudo-spherical (leaky) flow in an equivalent porous medium were used by the evaluation of the recovery period. Both models include the pressure derivative together with skin according to the effective wellbore radius concept and wellbore storage represented by a fictive standpipe connected to the test section. The models by /Ozkan and Ragavan 1991ab/ and /Gringarten and Ramey 1974/ were used for linear flow in single fractures.

The evaluation of the hydraulic parameters is made on the time interval representing the rock conditions close to the borehole (inner region) outside the zone affected by skin and wellbore storage. In some cases the properties of an outer zone with different transmissivity were also calculated. The presence of apparent outer hydraulic boundaries (no-flow and constant pressure) was only evaluated qualitatively.

The analysis of the recovery period was made on the pressure recovery plotted versus the Agarwal equivalent time using the multi-rate approach, i. e superposition of the flow rates during the injection period /Agarwal 1980/. The wellbore storage coefficient C was determined

from the recovery period by type curve matching as well as from the initial straight line with slope 1:1. C was only determined for tests with a well-defined slope of 1:1 in the beginning of the recovery period.

The storativity was estimated from a regression relationship between T and S according to /Rhén et al. 1997/ from borehole KFM05A and onward. For previous boreholes the storativity was assumed at $1 \cdot 10^{-6}$ independently of the transmissivity.

7.3.2 Golder

Golder uses a generic two-zone composite fractional dimension model in the analysis. According to the observed behaviour, the model was configured in most cases to a flow dimension of two (radial flow). Linear and spherical flow can be simulated as well as changes of flow dimension at some distance from the borehole. All models account for borehole effects (i.e. wellbore storage and skin).

In cases when only one parameter zone was seen by the tests, a homogeneous (one zone) flow model was used. Constant pressure boundaries were modelled as an increase of transmissivity in the outer composite zone, no flow boundaries were modelled as a decrease of transmissivity in the outer composite zone.

The pressure recovery was analysed using Bourdet superposition /Bourdet 1984/.

The storativity was assumed known and constant at 10^{-3} (above 100 m depth) and 10^{-6} (below 100 m depth). The evaluation of the hydraulic parameters are made on the time interval representing the rock conditions close to the borehole (inner zone) or outside the skin zone if such a zone is present. If seen by the test, the properties of an outer zone were also calculated.

7.3.3 Comparison and conclusions

Although the two analysis approaches use a slightly different flow model philosophy, the differences are in terms of nomenclature and not in the description of the flow phenomena actually occurring. Each of the flow models used in one of the approaches can be translated in the other model system, respectively.

The two analysis approaches use different assumptions for storativity, which leads to incompatible calculation of skin factors and distances.

7.4 Steady-state analysis

7.4.1 Geosigma

The steady-state transmissivity was calculated according to /Moye 1967/ for all tests for comparison.

7.4.2 Golder

The steady-state transmissivity was calculated according to /Moye 1967/ for all tests for comparison.

7.4.3 Comparison and conclusions

Both analysis approaches use the same steady-state analysis.

7.5 Assumed conceptualisation of the rock

7.5.1 Geosigma

The rock at Forsmark is assumed to be represented by a network of sparsely connected fractures forming an equivalent fractured porous medium or alternatively, by single fractures in a very low-conductive rock matrix with no hydraulic interaction between the fractures and rock matrix. A certain interval with pseudo-radial flow may be identified in most of the tests. Apparent pseudo-spherical (leaky) flow, reflected by a higher flow dimension, may represent intersection by fractures of higher transmissivity or flow in a wide, well-connected fracture zone. Apparent no-flow boundaries may reflect flow in fractures of limited extent.

7.5.2 Golder

The granite formation at the Oskarshamn site can be described from a hydraulic point of view as a sparsely connected fracture network. The matrix is expected to have extremely low conductivity and storativity, such that hydraulic interaction between fractures and matrix is not expected. Therefore, the tests conducted at Oskarshamn are expected to reveal fracture transmissivities. The derived transmissivities will reflect the properties of fractures intersecting the test zone. Also, the transmissivity may vary with the distance from the borehole to the extent further fractures are intersected. Conceptually, the flow dimension displayed by the tests can vary between linear and spherical. However, as the experience of the tests conducted so far shows, the majority of the tests display radial flow geometry.

7.5.3 Comparison and conclusions

The assumed conceptualization of the rock is compatible for both analysis approaches.

7.6 Determination of the flow model

7.6.1 Geosigma

From qualitative analysis of the semi-log derivative in log-log diagrams the dominating flow regimes during the tests were determined, e.g. pseudo-radial, pseudo-spherical (leaky) and pseudo-linear flow. The models for analysis were selected accordingly. Increases or decreases in the derivative may be assumed to be due to the presence of hydraulic features with higher and lower transmissivity, respectively away from the borehole. In addition, apparent outer boundary effects, e.g. no-flow boundaries and constant pressure boundaries were identified.

7.6.2 Golder

From the qualitative analysis of the semi-log derivative plotted in log-log coordinates. The characteristic flow regimes were determined using the shape of the derivative. Typical flow regimes considered were:

- wellbore storage,
- skin-dominated transition period,
- infinite acting flow of a given flow dimension (typically radial),
- transition to a second composite zone with increase or decrease of transmissivity (also interpreted as constant pressure or no-flow boundaries).

7.6.3 Comparison and conclusions

Both analysis approaches use the semi-log derivative for flow model identification. Differences are only in nomenclature and caused by the different flow model philosophy used (see above).

7.7 Flow rates below the measurement limit

7.7.1 Geosigma

For all injection tests with a final flow rate below 1 mL/min a test-specific lower measurement limit was estimated based on the observed background level of flow rate before and after the injection period. The test-specific lower measurement limit, which ranges from c. 0.3–0.6 mL/min, does not account for the flow generated by the packers (packer compliance). The latter flow is assumed to constitute between c. 0.1–0.2 mL/min.

In some boreholes at Forsmark pressure pulse tests were performed in such sections.

7.7.2 Golder

In cases when the flow rate was below measurement limit from the beginning of the test pulse tests were performed. In cases when the flow rate fell below measurement limit during the CHi phase, the analysis was conducted using the normal derivative type curve matching procedure. However, the early test data was emphasized in the analysis, which accounts for the fact that the late time data may not be as accurate due to the measurement limit.

7.7.3 Comparison and conclusions

Both analysis approaches recognise the need of additional measures in case the injection rate falls below measurement limits. While Geosigma re-defines the measurement limits on an individual case basis, Golder bases their strategy on the conduction of alternative test types (i.e. pulse tests). Both methods successfully push the detectable transmissivity limit down by approx. one order of magnitude.

7.8 Determination of the static formation pressure and freshwater head

7.8.1 Geosigma

The static formation pressure and freshwater head using the Horner method was only determined in borehole KSH02 at Simpevarp. In boreholes at Forsmark, no determination of the static formation pressure and freshwater head according to the Horner method was made. The static pressure may be estimated from the initial pressure in the tests section immediately before the injection period.

7.8.2 Golder

The static formation pressure and equivalent freshwater head was determined from the pressure recovery phases with the HORNER extrapolation method by using the HORNER straight line or the type curve, depending on whether the infinite acting radial flow period was reached at the late times of the test.

7.8.3 Comparison and conclusions

Both analysis approaches use the same method for determining the static formation pressure.

7.9 Analysis of pressure pulse tests

7.9.1 Geosigma

The standard model by /Dougherty and Babu 1984/ assuming radial flow was used for analysis of all the pressure pulse tests performed at Forsmark. No determination of flow regimes during the tests was made for these tests.

The effective borehole storage used in the analyses was determined from laboratory measurements of the total compressibility of the test system (PSS) used.

A new simple method was derived for estimation of the transmissivity accounting for the estimated packer compliance effects in very low-conductive test sections.

7.9.2 Golder

Pulse tests were analysed using both the RAMEY method as well as the pressure deconvolution method /Peres et al. 1989, Enachescu et al. 1997/. The flow model determination was made using the pressure deconvolution method. All flow models available in FlowDim can also be used for pulse test analysis. The wellbore storage coefficient was directly measured in the field using the dV/dp method (see description in the text).

7.9.3 Comparison and conclusions

The pressure deconvolution method used by Golder allows flow model identification for pulse tests, which is an advantage in cases of very low transmissivity. Further, the method allows the use of a large variety of flow models for analysis. It should be emphasised that this difference will not typically influence the recommended transmissivity.

The wellbore storage coefficient used by the two analysis approaches was derived differently. While Geosigma bases their analysis on values derived in the laboratory, Golder measures the wellbore storage coefficient in situ for each test. None of the methods is completely accurate; however, discrepancies should be expected in the results (i.e. transmissivity) due to the different inputs.

7.10 Derivation and use of the wellbore storage coefficient

7.10.1 Geosigma

The wellbore storage coefficient C was determined from the simulation of the transient test responses during the recovery period of the injection tests by type curve matching and from the initial straight line of slope 1:1, respectively. Consistent values on C were generally obtained with the two methods but only values from the latter method were reported. C was only reported for tests with a reasonable well-defined slope of 1:1 in the beginning of the recovery period. In fact, calculated C-values in sections of higher transmissivity than c. $1 \cdot 10^{-8}$ m^2/s are considered as increasingly uncertain due to lack of a well-defined line of slope 1:1.

For comparison, the borehole storage coefficients, based on the estimated (total) effective compressibilities from laboratory tests for corresponding section lengths, were calculated as described in Section 5.1.2. In addition, the net values on C based on borehole geometry (volume of test section) and the compressibility of water are also shown for comparison. The estimated

C-values from the injection test responses were generally in good agreement (or only slightly higher) with the C-values from the laboratory tests and the net values of C for test sections with a transmissivity less than c. $1 \cdot 10^{-8}$ m^2/s. Some test sections with significantly deviating (high) C-values were however observed. Some of these values may be real due to e.g cavities or presence of gas in the water in the borehole sections whereas others, particularly for transmissivities above $1 \cdot 10^{-8}$ m^2/s, may be non-representative for the test (poorly defined due to lack of character from WBS).

In the analysis of the pressure pulse tests, the estimated wellbore storage coefficient from the laboratory tests was used. C was not estimated from the pulse test responses.

7.10.2 Golder

The theoretical value of the wellbore storage coefficient was used just as a reference for comparison with the values derived from testing. The theoretical value was calculated as the product of total compressibility and volume of the test section. The total compressibility is calculated as the sum of the compressibilities of the individual system components: (a) water compressibility = $5 \cdot 10^{-10}$ 1/Pa (from physik), (b) rock compressibility 10^{-10} 1/Pa (estimated) and (c) packer compressibility on average $5 \cdot 10^{-11}$ 1/Pa (from laboratory measurements). The sum of these three components is approximately $7 \cdot 10^{-10}$ 1/Pa with the largest component being the water. If the packer compressibility is accepted to be small (in the order of $5 \cdot 10^{-11}$ 1/Pa) it follows that the value of the total compressibility is not controlled by the packers but by the water. So the influence of the packer compresibility can basically be neglected. Based on the above, a total compressibility of $7 \cdot 10^{-10}$ 1/Pa is approx. the minimum to be expected if considering that water allone is $5 \cdot 10^{-10}$ 1/Pa. The theoretical value of the wellbore storage coefficient was not used for the analysis of pulse tests (see additional comments below). In conclusion, the theoretical compressibility (or wellbore storage coefficient) does not influence the analysis results.

The wellbore storage coefficient derived from the recovery phases (CHir) is a result of the analysis. Two methods were used to derive it. The first method was type curve matching and the second method was to calculate the wellbore storage coefficient from the linear portion of the pressure recovery at early times. In effect, both methods are the same, and if discarding the subjectivity inherent to the analysis they should give the same C-values. A correlation analysis of the C-values derived using the two methods shows very good agreement. However, the C-values derived using these two methods are often much larger than the theoretical C-value. This has been frequently observed but the reason for this is not clear. Up to this point, the only plausible explanation for this phenomenon was found in Spivey's paper on turbulent flow (2002). This does not necesarrily mean that turbulent flow exists, this hypothesis is just the only plausible explanation currently available.

The wellbore storage coefficient used for the analysis of pulse tests is a result of direct measurements. The C-value is calculated as $\Delta V/\Delta p$ where ΔV is measured as the the volume of water needed to elevate the pressure in the test section by Δp (usually 200 kPa). The measured values are more consistent showing discrepancies of maximum one order of magnitude to the theoretical values. Considering how the volume difference (and hence the C-value) is measured, the derived C-value should be regarded as an upper bound for the true C-value of the system. The reason for this assessment is twofold: (1) the volume difference is measured using the entire column of water in the test tubing and (2) it cannot be excluded that small volumes of water flow into the formation, so the volume difference may also have a formation flow component.

Because of the above, the C-value can be bounded between the theoretical value and the measured value during the pulse. The C-value matched from the CHir phase is often larger, but it may not reflect the actual storage conditions in the test section (perhaps due to turbulent flow).

7.10.3 Comparison and conclusions

The theoretical value of the wellbore storage coefficient was determined in different ways by Geosigma and Golder. Geosigma determined slightly different values on the effective (total) compressibility for test sections in 100 m, 20 m and 5 m, respectively from laboratory tests ($4.8 \cdot 10^{-10}$, $5.5 \cdot 10^{-10}$ and $8.4 \cdot 10^{-10}$ 1/Pa, respectively).

Golder estimated the total (effective) compressibility of the test system as c. $7 \cdot 10^{-10}$ 1/Pa with the largest component being the compressibility of water, independently of the section length. The theoretical value of the wellbore storage coefficient was calculated as the product of total (effective) compressibility and volume of the test section by both Geosigma and Golder.

For the actual test section lengths, the differences in the theoretical values of C used by Geosigma and Golder are considered of minor importance since these values were only used as reference values in the analysis of the injection tests.

In the analysis of pressure pulse tests, Geosigma always used the estimated theoretical values on C while Golder estimated C from each test. The actual C-value is assumed to be bounded between the theoretical value and the measured value. Both approaches are uncertain which may affect the estimated transmissivities from the pressure pulse tests.

7.11 Derivation of recommended values and confidence ranges

7.11.1 Geosigma

In general, both the injection-and recovery period of the injection tests were evaluated by transient methods. The hydraulic parameters from the period exhibiting the most well-defined period with pseudo-radial flow, or other flow regime, were selected as the representative ones. The parameters from the inner region were selected if more than one region was evaluated. In most cases the parameters from the injection period were selected as the representative. If no transient evaluation could be made, the steady-state transmissivity was selected.

No confidence interval for the estimated parameters was reported for the tests at Forsmark. The approximate 95% statistical confidence range for each estimated parameter is calculated by the software from the regression analysis. In addition, there are several other uncertainties which may affect the confidence range of the estimated parameters.

7.11.2 Golder

In most of the cases more than one analysis was conducted on a specific test. Typically both test phases were analyzed (CHi and CHir) and in some cases the CHi or the CHir phase was analyzed using two different flow models. The parameter sets (i.e. transmissivities) derived from the individual analyses of a specific test usually differ. In the case when the differences are small (which is typically the case) the recommended transmissivity value is chosen from the test phase that shows the best data and derivative quality.

In cases when the difference in results of the individual analyses was large (more than half order of magnitude) the test phases were compared and the phase showing the best derivative quality was selected.

The confidence range of the transmissivity was derived using expert judgment. Factors considered were the range of transmissivities derived from the individual analyses of the test as well as additional sources of uncertainty such as noise in the flow rate measurement, numeric effects in the calculation of the derivative or possible errors in the measurement of the wellbore storage coefficient. No statistical calculations were performed to derive the confidence range of transmissivity.

In cases when changing transmissivity with distance from the borehole (composite model) was diagnosed, the inner zone transmissivity (in borehole vicinity) was recommended.

In cases when the infinite acting radial flow (IARF) phase was not supported by the data the additional uncertainty was accounted for in the estimation of the transmissivity confidence ranges.

While the recommended transmissivity was derived using type curve analysis methods, the confidence range of transmissivity was derived from the comparison of the analysis results of the two phases. In many cases Transmissivity Normalized Plots (TNP) were used to compare the derivatives of the two test phases in a normalized fashion. This way the amount of uncertainty was derived graphically as presented in the report.

7.11.3 Comparison and conclusions

Both approaches use “best data quality” test phases for the derivation of the recommended transmissivity. In both cases the transmissivity confidence range is derived using “expert judgement”; however Geosigma does not report these values.

Golder uses the TNP method to identify compatibility (or incompatibility) between the individual test phases and translates this information into transmissivity confidence ranges.

8 Conclusions and recommendations

The following main conclusions may be drawn from the performance and evaluation of the injection tests at Oskarshamn:

Injection period:

- In cases when the rate control functioned well at early times, the injection period is best suited to describe the near-borehole formation.
- Generally speaking, rate data has more noise than pressure data (i.e. CHir phase). Therefore, the flow model identification for portions of the formation further away from the borehole can be better conducted using the CHir data.
- The average stabilization time to get a constant pressure was 20–30 s for most tests using the automatic flow regulation system. Lower times (0–10 s) was achieved in low-transmissivity tests using the pressure vessel directly
- Tests exhibiting radial flow regime during the injection period dominate in relation to other flow regimes.
- In general, it was possible to identify the radial flow regime during the injection period for most of the tests on which the transient evaluation can be made.
- Tests with flow rates below 1 mL/min during the injection phase were conducted as pulse injection in most of the cases.

Recovery period:

- The beginning of the recovery period is frequently disturbed by WBS decreasing the analyzable part of the data curve (in general less than one log cycle of time).
- The recovery data is of better quality (less noise) and therefore better suited to describe the formation further away from the borehole.
- In many cases the CHir phase showed fast recovery. This phenomenon may be caused by turbulent flow in fractures. Fast recovery was in most of the cases correlated with the presence of high skin factors (up to 30) and high wellbore storage coefficients derived from the type curve analysis. These observations are consistent with literature results.

Pulse tests:

- Pulse tests are considered to provide correct results in the low transmissivity range (10^{-11} m^2/s to 10^{-9} m^2/s).
- Tests strongly affected by packer compliance were skipped and marked as not analyzable. These tests are considered to have transmissivities lower than 10^{-11} m^2/s.
- The transient decline of the flow rate generated by the packers was estimated from field tests in tight sections and from laboratory tests. Numeric simulations showed that packer compliance in the order of magnitude derived from laboratory measurements does not impede the correctness of pulse test results if the transmissivity is larger than 10^{-11} m^2/s.
- The effective compressibility and effective wellbore storage coefficient was estimated from field measurements.

Representative test results:

- The representative hydraulic parameters of the test were selected from the test phase with best data quality and clear flow model identification. In most cases this was the recovery period.

Background pressure gradients may affect both injection tests and pressure pulse tests if the transient evaluation is made on very small pressure changes during the tests. Such pressure gradients include:

Effect	Influence on injection tests
Tidal effects	Low
Effects of precipitation	Low
Barometric pressure changes	Low
Sea level fluctuations	Low
Remote earth quakes	Not Observed
Drilling and other external activities in surrounding boreholes	Not Observed
Re-establishment of the formation pressure in the test section after packer sealing	Low; dissipates at start of test

Recommendations:

The following recommendations were discussed, agreed on and implemented in the course of the tests conducted at Oskarshamn during 2005:

- Conduct step injection tests to assess whether turbulent flow and rate dependent skin occurs.
- Use a high resolution memory pressure gauge in the test section to assess the importance of poor gauge resolution on the analysis of CHir phases.
- Conduct long lasting test phases (e.g. slug injection tests) over night to profit of the test time and increase the radius of investigation in selected test sections.

9 References

Agarwal R G, 1980. A new method to account for producing time effects when drawdown type curves are used to analyze pressure build-up and other test data. Soc. Pet. Eng. Paper 9289.

Bourdet D, Ayoub J A, Pirard Y M, 1989. Use of Pressure Derivative in Well-Test Interpretation. SPEFE (June 1989). Pp 293–302. Trans., AIME, 287.

Chakrabarty C, Enachescu C, 1997. Using the Devolution Approach for Slug Test Analysis: Theory and Application. – Ground Water Sept.–Oct. 1997, pp 797–806.

Dougherty D E, Babu D K, 1984. Flow to a partially penetrating well in a double-porosity reservoir. Water Resour. Res., 20 (8), 1116–1122.

Gringarten A C, Ramey H J, 1974. Unsteady state pressure distributions created by a well with a single horizontal fracture, partial penetration or restricted entry. Soc. Petrol. Engrs. J., pp 413–426.

Gringarten A C, 1986. Computer-aided well-test analysis. – SPE Paper 14099.

Hantush M S, 1955. Non-steady radial flow in an infinite leaky aquifer. Am. Geophys. Union Trans., v. 36, no 1, pp 95–100.

Hantush M S, 1959. Non-steady flow to flowing wells in leaky aquifer. Jour. Geophys. Research, v. 64, no 8, pp 1043–1052.

Horne R N, 1990. Modern well test analysis. – Petroway, Inc., Palo Alto, Calif.

Horner D R, 1951. Pressure build-up in wells. – Third World Pet. Congress, E.J. Brill, Leiden II, pp 503–521.

Hurst W, Clark J D, Brauer E B, 1969. The skin effect in producing wells. J. Pet. Tech., Nov.1969, pp 1483–1489.

Jacob C E, Lohman S W, 1952. Nonsteady flow to a well of constant drawdown in an extensive aquifer. – Transactions, American Geophysical Union, Volume 33, No 4, pp 559–569.

Moye D G, 1967. Diamond drilling for foundation exploration Civil Eng. Trans., Inst. Eng. Australia, Apr. 1967, pp 95–100.

Ozkan E, Raghavan R, 1991a. New solutions for well test analysis; Part 1, Analytical considerations. SPE Formation Evaluation vol 6, no 3, pp 359–368.

Ozkan E, Raghavan R, 1991b. New solutions for well test analysis; Part 2, Computational considerations and applications. SPE Formation Evaluation vol 6, no 3, pp 369–378.

Peres A M M, Onur M, Reynolds A C, 1989. A new analysis procedure for determining aquifer properties from slug test data. – Water Resour. Res. v. 25, no. 7, pp 1,591–1,602.

Pickens J F, Grisak G E, Avis J D, Belanger D W, Thury M, 1987. Analysis and Interpretation of Borehole Hydraulic Tests in Deep boreholes: Principles, Model Development, and Applications. – Water Resources Research, Vol. 23, No. 7, pp 1,341–1,375.

Ramey H J Jr, Agarwal R G, Martin R G I, 1975. Analysis of “Slug Test” or DST flow Period data. – J. Can. Pet. Tec., September 1975.

Roberts R M, 2002. Moderately Fractured Rock Experiment: Well Test Analysis Using nSIGHTS. Report No: 06819-REP-01300-10062-R00. 194 pages. Ontario Power Generation.

Roberts R M, Beauheim R L, Avis J D, 2002. Quantifying parameter uncertainty in well-test analysis in proceedings of Bridging the gap between measurement and modeling in heterogeneous media, IAHR Int. Groundwater Symposium, March, 2002, Berkeley, CA.

SKB, 2001a. Site investigations: Investigation methods and general execution programme. SKB TR-01-29, Svensk Kärnbränslehantering AB.

SKB, 2001b. Geoveteskapligt program för platsundersökning vid Simpevarp. SKB R-01-44, Svensk Kärnbränslehantering AB.

SKB, 2002. Execution programme for the initial site investigations at Simpevarp. SKB P-02-06, Svensk Kärnbränslehantering AB.

SKB, 2006. Preliminary site description. Laxemar subarea – version 1.2. SKB R-06-10, Svensk Kärnbränslehantering AB.

Spane F A, Wurstner S K, 1993. DERIV: A computer program for calculating pressure derivatives for use in hydraulic test analysis. Ground Water, vol. 31, no. 5, pp 814–822.

Spivey J P, Brown K G, Sawyer W K, Frantz J H, 2002. Estimating Non Darcy Flow Coefficient from Buildup Test Data with Wellbore Storage. – Society of Petroleum Engineers, SPE 77484.

10 Nomenclature

Symbol	Description	Units
T	Transmissivity	m^2/s
p	Pressure	Pa
Δp	Pressure difference (e.g. pressure difference used to conduct a constant pressure test)	Pa
ρ	Density (freshwater density = 1,000 kg/m³)	kg/m^3
g	Gravitational acceleration (9.81 m/s²)	m/s^2
M	Slope of the semi-log straight line:	
	$d(1/q)/dlog(t)$ for constant pressure tests	s/m^3
	$dp/dlog(t)$ for constant rate tests	Pa
	$dp/dlog(t_{HORNER})$ for pressure recovery tests	Pa
q	Flow rate	m^3/s
q_D	Dimensionless flow rate	–
t	Time	s
Δt	Elapsed time	s
S	Storativity(= $\phi c, h\rho g$)	–
r_w	Wellbore radius	m
n	Flow dimension	–
ϕ	Porosity	–
c_t	Total compressibility (formation + fluid)	1/Pa
t_D	Dimensionless time	–
p_D	Dimensionless pressure	–
ξ	Skin factor (also denoted as s)	–
T_M	Transmissivity calculated after /Moye 1967/	m^2/s
Q_p	Flow in test section immediately before stop of flow	m^3/s
dp_p	Maximal change in pressure during the perturbation phase	Pa
Q/s	Specific capacity	m^2/s
$p_{D\,BU}$	Dimensionless pressure calculated for pressure recovery (i.e. build-up) tests	–
C	Wellbore storage coefficient	m^3/Pa
C_D	Dimensionless wellbore storage coefficient	–
C_De^{2s}	Type curve parameter (correlation group) for constant rate and pressure recovery tests	–
$(C_De^{2s})_M$	The parameter of the type curve used in the match	–
PM	Pressure Match	Pa
TM	Time Match	s
t_p	Production/injection time; used for superposition analysis and HORNER analysis of pressure recovery tests	S
t_{pD}	Dimensionless production/injection time	–
t_{HORNER}	HORNER time	–
c_w	Water compressibility	1/Pa
c_{tz}	Test zone compressibility (also noted as ceff)	1/Pa
V_i	Test zone volume	m^3
p^*	Static formation pressure	Pa
Gd	Gauge depth, corrected for borehole inclination	mbRP
RP_{elev}	Elevation of the reference point, typically top of casing (TOC)	m.a.s.l.
p_{atm}	Atmospheric pressure	Pa
h_w	The height of freshwater column equivalent to the extrapolated static pressure	m above transducer
h_{iwf}	The equivalent freshwater head	m.a.s.l.
p_{RP}	Deconvolved pressure /Peres 1989/	s
p_i	Initial pressure before the pulse (slug)	Pa
p_0	Pressure at t = 0 of the pulse (slug)	Pa
pw	Pressure during the pulse (slug)	Pa
r_u	Tubing (pipe string) radius	m
C_{eff}	Effective wellbore storage coefficient	m^3/Pa
Q_{packer}	Flow generated by packer compliance	m^3/s